



T.C.

ALTINBAŞ UNIVERSITY

Graduate School of Science and Engineering

Electrical and Computer Engineering

**EFFICIENT UNCONSTRAINED IRIS  
RECOGNITION SYSTEM BASED ON CCT-LIKE  
MASK FILTER BANK**

Hala Nafie Fathee

PhD Thesis

Supervisor

Prof. Dr. Osman N. UCAN

Istanbul, (2019)

**EFFICIENT UNCONSTRAINED IRIS RECOGNITION SYSTEM BASED  
ON CCT-LIKE MASK FILTER BANK**

By

**Hala Nafie Fathee**

Electrical and Computer Engineering

Submitted to the Graduate School of Science and Engineering

in partial fulfillment of the requirements for the degree of

Doctor of Philosophy

ALTINBAŞ UNIVERSITY

2019

This is to certify that we have read this thesis and that in our opinion it is fully adequate, in scope and quality, as a thesis for the degree of Doctor of Philosophy.

*J. M. Abdul-Jabbar*

Prof. Dr. Jassim M. Abdul-Jabbar

Co-Supervisor

Prof. Dr. Osman Nuri UCAN

Supervisor

Examining Committee Members (first name belongs to the chairperson of the jury and the second name belongs to supervisor)

Prof. Dr. Osman Nuri UCAN	School of Engineering and Natural Science, Altinbas University	_____
Prof. Dr. Oguz BAYAT	School of Engineering and Natural Sciences, Altinbas University	_____
Asst. Prof. Dr. Oguz ATA	School of Engineering and Natural Sciences, Altinbas University	_____
Prof. Dr. Hasan Huseyin BALIK	Air Force Academy, National Defense University	_____
Asst. Prof. Dr. Adil Deniz DURU	Faculty of Sport Sciences, Marmara University	_____

I certify that this thesis satisfies all the requirements as a thesis for the degree of Doctor of Philosophy.

Asst. Prof. Dr. Cagatay AYDIN

Head of Department

Prof. Dr. Oguz BAYAT

Director

Approval Date of Graduate School of  
Science and Engineering: \_\_\_\_/\_\_\_\_/\_\_\_\_

I hereby declare that all information in this document has been obtained and presented in accordance with academic rules and ethical conduct. I also declare that, as required by these rules and conduct, I have fully cited and referenced all material and results that are not original to this work.

Hala Nafie Fathee

## **DEDICATION**

I dedicate this project to God Almighty my creator, my strong pillar, my source of inspiration, wisdom, knowledge and understanding. I dedicate my dissertation work to my family and many friends. A special feeling of gratitude to my loving parents whose words of encouragement and push for tenacity ring in my ears. My sister, brothers and son (Aubyda) have never left my side and are very special, and to the spirit of my daughter (Amina).

## **ACKNOWLEDGEMENTS**

I am grateful to everyone who has helped me in my struggle to achieve my dream of becoming a Ph. D. I would like to sincerely thank my thesis advisers, Prof Osman N. UCAN and Prof. Jassim M. Abdul-Jabbar, for his guidance and support throughout this study and especially for his confidence in me. I would like to acknowledge and thank Prof. Oguz BAYAT and thanks goes to the members of the staff of electrical and computer engineering department for their continued support.



## **ABSTRACT**

### **EFFICIENT UNCONSTRAINED IRIS RECOGNITION SYSTEM BASED ON CCT-LIKE MASK FILTER BANK**

Fathee, Hala Nafie,

PhD, Electrical and Computer Engineering, Altınbaş University,

Supervisor: Prof. Dr. Osman N. UCAN

Co-Supervisor: Prof. Dr. Jassim M. Abdul-Jabbar

Date: August, 2019

Pages: 124

Iris recognition systems has been getting increasing attention from researchers in both academic and industrial prospective. Picking the iris image using Near-Infrared camera makes the segmentation and feature extraction steps relatively easy task. On the other hand, in unconstrained environments the iris recognition systems becomes very important and widely considered. Recently, there are many published papers aim to develop new algorithms that can segment and recognize human iris templates in visible wavelength environments. The main problem of less constrained environments is that high error rate due to increasing number of noise sources in eye images, which leads to severe degradation in the segmentation process. As a result, the iris segmentation process has become a major issue in iris recognition, since most of the traditional iris segmentation techniques fail under such challenging conditions. In this thesis, we address both the segmentation and feature extraction steps of the iris recognition systems. Firstly, a new segmentation algorithm is proposed to handle iris images acquired in visible wavelength environments. The proposed segmentation algorithm decreases the degradation and noise by

starting to search from the most easily distinguishable region of the iris, which is the pupil. After that, the iris is localized accurately using a fast circular Hough transform. In addition, the methods which are most convenient are used to isolate the upper and lower eyelids and eyelashes from the iris region. Secondly, a new proposed recognition system is proposed. The proposed system has encouraging performance in terms of high recognition rates and a reduced number of elements of the feature vector. This reflects reliable and rapid recognition properties. In addition, some promising characteristics of the system are apparent since it can efficiently be realized with lower computation complexity. The proposed iris recognition method is a modified version of the classical iris recognition method, which usually consists of four steps: segmentation, normalization, feature extraction and coding, and matching.

**Keywords:** iris recognition, iris segmentation, circular Hough transform, biometrics, feature extraction.



# TABLE OF CONTENTS

	<u>Pages</u>
<b>ABSTRACT</b> .....	<b>vii</b>
<b>LIST OF TABLES</b> .....	<b>xii</b>
<b>LIST OF FIGURES</b> .....	<b>xiv</b>
<b>LIST OF ABBREVIATIONS</b> .....	<b>xix</b>
<b>1. INTRODUCTION</b> .....	<b>1</b>
1.1 BIOMETRICS.....	1
1.2 IDENTIFICATION VS. VERIFICATION.....	2
1.3 PHYSIOLOGICAL AND BEHAVIORAL BIOMETRICS .....	4
1.4 WHAT DOES BIOMETRICS MEAN?.....	4
1.5 ADVANTAGES OF BIOMETRICS .....	5
1.6 TYPES OF BIOMETRICS .....	8
1.6.1 Fingerprint Biometric .....	8
1.6.2 Face Biometric .....	9
1.7 IRIS RECOGNITION SYSTEMS.....	10
1.7.1 Human Eye Anatomy .....	10
1.7.2 Iris Recognition .....	11
1.7.3 UNCONSTRAINED.....	12
1.8 Iris recognition steps:- .....	14
Unconstrained Iris Recognition.....	24
1.9 IRIS IMAGE DATABASES.....	24
1.9.1 CASIA Database .....	25
1.9.1.1 CASIA version 1 .....	25
1.9.1.2 CASIA version 2 .....	26

1.9.1.3 CASIA version 3 .....	27
1.9.1.4 CASIA version 4 .....	29
1.9.2 UBIRIS Database .....	31
1.9.3 UPOL Database.....	33
1.9.4 MMU Database .....	34
1.9.5 ICE Database.....	35
1.9.6 BATH Database .....	35
<b>2. RELATED WORK.....</b>	<b>37</b>
2.1 REVIEW OF THE SEGMENTATION METHODS.....	37
2.2 REVIEW OF THE IRIS RECOGNITION SYSTEMS .....	50
<b>3. PUPIL-BASED IRIS SEGMENTATION ALGORITHM FOR VISIBLE WAVELENGTH IMAGES.....</b>	<b>61</b>
3.1 INTRODUCTION.....	61
3.2 BACKGROUND ON IRIS SEGMENTATION .....	63
3.3 OUR PROPOSED SEGMENTATION ALGORITHM.....	65
3.3.1 Determining the Candidate Pupil Region.....	66
3.3.2 Localizing the Pupil Boundaries .....	70
3.3.3 Localizing the Iris Boundaries .....	71
3.3.4 Removing the Upper and Lower eyelashes and eyelids.....	72
3.3.5 Removing the Upper eyelashes and eyelids.....	73
3.3.6 Removing the Lower eyelashes and eyelids .....	73
3.4 RESULTS AND DISCUSSION.....	74
3.5 REVIEW OF THE CHAPTER .....	79
<b>4. THE NEW PROPOSED IRIS RECOGNITION SYSTEM BASED ON CCT-LIKE MASK FILTER BANK .....</b>	<b>81</b>
4.1 FEATURE VECTOR EXTRACTION AND CODING STEP.....	83
4.2 RESULTS AND DISCUSSION .....	94
4.3 CHAPTER CONCLUSIONS.....	95

**5. CONCLUSION..... 97**  
**REFERENCES..... 98**



## LIST OF TABLES

	<u>Pages</u>
Table 1.1: The advantages and disadvantages of different biometrics .....	8
Table 2.1: Upui remote database frontal look eyes matching results [83].....	42
Table 2.2: Comparative results [84].....	43
Table 2.3: Performance between LCV and BLCV on NICE.II [87] .....	45
Table 2.4: Segmentation results for decreased number of training samples [90].....	46
Table 2.5: Simulation results [91].....	47
Table 2.6: Comparison between the performances obtained by the method proposed in this paper with respect to three state-of-art strategies [93].....	48
Table 2.7: Segmentation accuracy of Bazrafkan, S., and Corcoran, P algorithm [94] .....	49
Table 2.8: Results of algorithm given from [97] by tested it on CASIA database .....	51
Table 2.9: Comparison of available Iris Recognition Algorithms [105] .....	54
Table 2.10: Efficiency comparison on CASIA database for popular algorithms [108].....	56
Table 2.11: Visual Segmentation Results of the Images in the CASIA V4, MMU2, and UBIRIS V1 Databases [113].....	60
Table 3.1: Performance comparison between the proposed iris segmentation algorithm and the other five algorithms .....	77
Table 4.1: Some samples of UBIRIS V1 images before standard normalization.....	90

Table 4.2: Some samples of UBIRIS V1 images after standard normalization..... 90

Table 4.3: Decimal values corresponding to 10-bit implementation of the normalized values ... 91

Table 4.4: Final 72-bit-length feature vectors of UBIRIS V1 images of Table (4.3)..... 92

Table 4.5: Comparison of the proposed methods with some known methods ..... 95



# LIST OF FIGURES

	<u>Pages</u>
Figure 1.1: Biometric systems .....	2
Figure 1.2: A biometric system to show the enrollment and the identification steps [4] .....	3
Figure 1.3: Flexible to reveal smartcard [10].....	7
Figure 1.4: Samples device and images of human fingerprint.....	9
Figure 1.5: An example of how the face template can be extracted [13] .....	9
Figure 1.6: Human eye anatomy [15] .....	10
Figure 1.7: Human iris anatomy [17].....	11
Figure 1.8: The steps of the iris recognition system .....	12
Figure 1.9: shows samples .....	13
Figure 1.10: The general steps of iris segmentation .....	15
Figure 1.11: iris image after determine two boundaries .....	16
Figure 1.12: steps of canny edge detector.....	17
Figure 1.13: (a) Upper and Lower Search Regions of the Iris Image. (b) Upper and Lower Eyelids Detection .....	19
Figure 1.14: Detecting the noise in the original image.....	20
Figure 1.15: Iris image after removing the noise .....	20

Figure 1.16: Shows the original image and normalize the iris image.....	21
Figure 1.17: Shows convert the original image to normalizing image .....	22
Figure 1.18: Two samples images form CASIA V1 database [57] .....	26
Figure 1.19: Three samples iris images from CASIA V2 Device1 [57].....	26
Figure 1.20: Three samples iris images from CASIA V2 Device2 [57].....	27
Figure 1.21: OKI Device that used to pick CASIA V1, V2, V3 [63].....	27
Figure 1.22: CASIA IRIS LAMP [63].....	28
Figure 1.23: CASIA IRIS INTERVAL [63].....	28
Figure 1.24: CASIA IRIS TWINS [63] .....	28
Figure 1.25: CASIA-Iris-Interval image sample [66].....	29
Figure 1.26: CASIA -Iris-Lamp image sample [66].....	30
Figure 1.27: CASIA-Iris-Twins image sample [66] .....	30
Figure 1.28: CASIA-Iris- Distance image sample [66] .....	30
Figure 1.29: CASIA-Iris-Thousand image sample [67] .....	31
Figure 1.30: Some samples of UBIRIS V1 sessao_1[68].....	32
Figure 1.31: Some samples of UBIRIS V1 sessao_2[68].....	32
Figure 1.32: Two samples of UBIRIS V2 sessao_1[68].....	33

Figure 1.33: Two samples of UBIRIS V2 sessao_2[68].....	33
Figure 1.34: Samples of UPOL dataset [74].....	34
Figure 1.35: Some samples of MMU iris database [76].....	34
Figure 1.36: Samples of ICE database [24].....	36
Figure 1.37: Some examples of BATH iris database [61].....	36
Figure 1.38: The used camera for Bath iris database.....	36
Figure 2.1: Template generation (VHDL) system block diagram [77] .....	38
Figure 2.2: Stopping function for the GACs [78]. (a) Original iris image .....	39
Figure 2.3: Block diagram of the iris segmentation procedure [79].....	40
Figure 2.4: Block diagram of iris segmentation method [80].....	40
Figure 2.5: The proposed quality assessment method [81].....	41
Figure 2.6: Segmentation results [82] a) iris image with pupil deformation. b) Iris image with off-axes view.....	42
Figure 2.7: Hierarchical face-eye detection [85] .....	44
Figure 2.8: Stages of eye image extraction in NIR face videos [86].....	44
Figure 2.9: Example of the split between tp, fp, tn and fn for an iris image segmentation [89] ..	46
Figure 2.10: The proposed system for iris segmentation [92] .....	47
Figure 2.11: The DFCN architecture [95] .....	50



Figure 2.12: Overview of proposed algorithm [99] .....	51
Figure 2.13: Division of an iris edge image into non-overlapping blocks [100], [101] .....	52
Figure 2.14: The Proposed video-based non cooperative iris recognition system [102].....	52
Figure 2.15: The block diagram of the designed system [103].....	53
Figure 2.16: Combining multiple sources of evidence using DS theory [107] .....	55
Figure 2.17: Block diagram to evaluate the quality of iris segmentation [25] .....	57
Figure 2.18: Block diagram for the process of weights assign with PSO [111].....	58
Figure 2.19: ROC Curve of DAML Optimized [112] .....	59
Figure 3.1: Parts of the human iris [29] .....	62
Figure 3.2: The main steps of the proposed iris segmentation algorithm.....	68
Figure 3.3: The main steps of the proposed iris segmentation algorithm.....	69
Figure 3.4: Eliminating the non-pupil dark regions in the proposed iris segmentation algorithm	71
Figure 3.5: Iris localization steps of three selected images from the UBIRIS v1 database.....	72
Figure 3.6: Removing the upper and lower eyelids and eyelashes from the iris region using images from the UBIRIS v1 database .....	74
Figure 3.7: Sample selected images before and after applying the proposed segmentation algorithm from the UBIRIS v1 database [31].....	75

Figure 3.8: Sample images before and after applying the proposed segmentation algorithm steps .....	76
Figure 3.9: Sample images from falsely segmented iris images after applying the proposed segmentation algorithm.....	78
Figure 3.10: Sample images from falsely segmented iris images after applying the proposed segmentation algorithm.....	78
Figure 3.11: Sample images from falsely segmented iris images after applying the proposed segmentation algorithm.....	79
Figure 4.1: Iris image after segmentation step.....	83
Figure 4.2: Block diagram of the proposed system .....	84
Figure 4.3: Flow chart for constructing features from iris images .....	87
Figure 4.4: Block diagram of a reduced system .....	88
Figure 4.5: Flow chart for reduced-length bit-coding and feature vector creation.....	89
Figure 4.6: Flow chart of the HD matching algorithm .....	92
Figure 4.7: inter-class and intra-class distributions .....	94

## LIST OF ABBREVIATIONS

CASIA	:	Chinese Academy of Sciences' Institution of Automation
2D	:	Tow Dimension
XOR	:	Exclusive OR.
HD	:	Hamming Distance
FAR	:	False Accept Rate
FFR	:	False Reject Rate
NIR	:	Near Infrared lightening
JPEG	:	Joint Photographic Experts Group
UBIRIS	:	University of Beira Iris
UPOL	:	University Palackeho Olomouc
MMU	:	Mean Multimedia University
ICE	:	Iris Challenge Evaluation
BATH	:	University of Bath
CHT	:	Circular Hough Transform
CCT	:	Circular Contourlet Transform
LHT	:	Linear Hough Transform
SVM	:	Support Vector Machine

# 1. INTRODUCTION

In this chapter, we introduce the related topics and definitions to our thesis main work. First, the biometrics are reviewed and explained including the types, properties, problems and categories. After that, the iris recognition systems (constrained and unconstrained) are described in Section 2. Section 3 summarizes the image databases that used to test the performance of iris recognition system.

## 1.1 BIOMETRICS

Biometric systems are used increasingly to recognize individuals and regulate access to physical spaces, information, services, and to other rights or benefits, including the ability to cross international borders. The motivations for using biometrics are diverse and often overlap. They include improving the convenience and efficiency of routine access transactions, reducing fraud, and enhancing public safety and national security [1].

In modern terminology, biometrics is required where statistical methods try meet biological data. The main purpose of biometrics is to confirm the identity of individuals from intrinsic traits. Accurate identification is fundamental to many investigating and security services, such as, information security, physical security, national security, contracts, financial transactions, criminal justice, public services and more. The need is increasing for a wide range and frequent identity verifications. For example, air passenger numbers are anticipated to double in the next 20 years along with a single identity fraud is also increasing year on year, while two older systems of identification, such as manual passport checks and computer passwords, are therefore under considerable questions [2]. Figure 1.1 shows some biometric examples.

Biometrical authentication (or simply biometrics) is the process of making sure that the person be the exact claiming one. Authentication of identity of the user can be done in three ways:

- 1) Something that person knows (password),
- 2) Some code the person own (key, special card),
- 3) Some property that the person has (fingerprints, footprint).

Biometrics may be based on anatomic uniqueness behavior of a person, that's why it can be used for person identification. A unique characteristic can be used to prevent unauthorized access to the system with the help of some automated method of biometric control. Such control can be achieved by checking some unique physiological features or some behavior characteristics that identifies the person [3].



**Figure 1.1:** Biometric systems

## **1.2 IDENTIFICATION VS. VERIFICATION**

There are two categories of Biometric Systems. They are identification and verification. Identification is known as the process that compares a present person to a biometric pattern or database. Verification is a process that validates a person's ID by comparing his/her biometric data with already captured biometric data that is stored in a system. Identification is more complex than the verification process. Identification may generate a one to many matches, where verification generates a one to one match. For example, a person uses biometrics at an airport. During the verification process the passenger would provide a smart card, (already programmed with his/her biometric data). When it is time for the passenger to be scanned, authorization would be verified against both the person and the smart card. This process is extremely straightforward and more easy to use. The identification process is more complicated. For example, take this same passenger, but this time he/she does not have a smart card. Figure 1.2 shows the steps of the verification process.

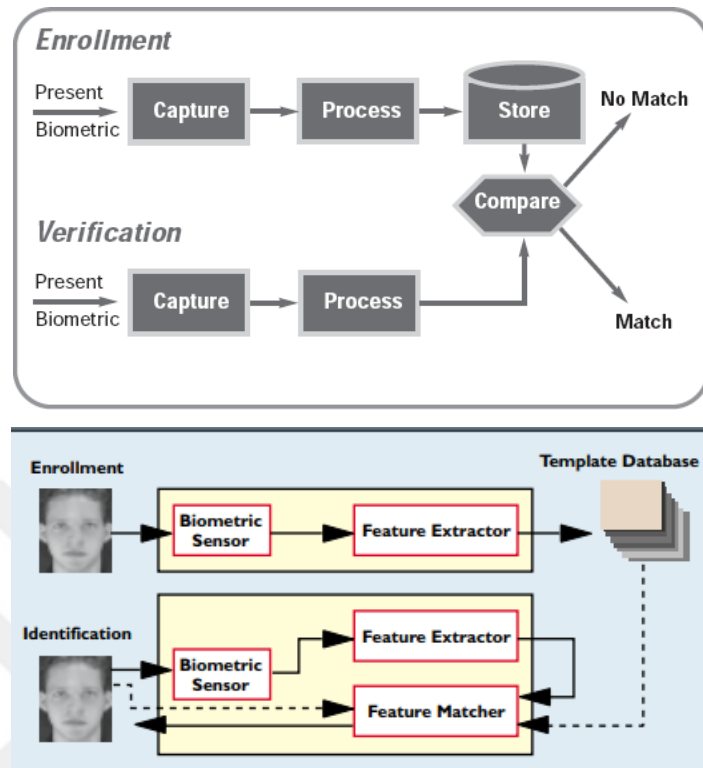


**Figure 1.2:** A biometric system to show the enrollment and the identification steps [4]

To decide what biological measures can represent biometrics? It is quite simple and obvious to say that any characteristic can serve as biometrics if it has the following desirable properties:

- 1) Universality- something that each person has
- 2) Uniqueness- some characteristics that separate this person from others, remembering that not all characters are suitable for biometrics.
- 3) Permanence- biometric measurement for each person should be constant with time.
- 4) Measurability (collectability) - easy to measure, no too much demandable time and costs.
- 5) Performance- the method is speedy, accurate and robust.
- 6) Acceptability- how people accept biometrics testing.
- 7) Circumvention- how difficult it is to fool the system.

### **1.3 PHYSIOLOGICAL AND BEHAVIORAL BIOMETRICS**

Biometric identifying characteristics can be divided into two big groups: 1) Physiological 2) Behavioral. Though behavior biometrics is less expensive and less dangerous for the user, physiological characteristics offer highly exact identification of a person. Nevertheless, the two groups provide high level of identification than classical passwords and cards.

#### **1. Physiological Group of Biometrics:**

Physiological systems are considered to be more reliable as individual features of a person used by these systems, do not change by influence of psych-emotional state. Physiological systems of identification deal with statistical characteristics of a person: such as fingerprints, hand geometry, face recognition, iris recognition, DNA, palm print, etc. [5].

#### **2. Behavioral Group of Biometrics:**

Behavioral characteristics deal with some characteristics representing the behavior of a person, such as signature, gait, typing patterns. Note that most biometric traits are a mix of physical and behavioral characteristics.

It should be also noted that biometric authentication can be defined as those technologies that measure and analyze human physical and behavioral characteristics for authentication.

### **1.4 WHAT DOES BIOMETRICS MEAN?**

The term biometrics is initially derived from the Greek words bio meaning life and metric meaning to measure. Biometrics is a technological and scientific authentication method used in information assurance (IA). It is based on biology. Human biological information such as DNA or fingerprints is used in biometric identification to authenticate secure entry, data or access. It should be noted that several linked components are included for effective functionality of a biometric system. The biometric system can connect an event to a single person, whereas other ID forms, such as a personal identification number (PIN), may be used by anyone.

A biometric system includes the following components and features:

1- A sensor that acquires data which may be obtained from human behavioral or physical characteristics, such as a fingerprint or retinal scan. An acquisition device, such as a microphone or scanner, is needed to capture the data. The sensor changes such data into a useful digital format via some software.

2- A biometric template developed via the biometric system's signal processing algorithms. Data is usually coded and encrypted for security purposes. The resulting coded templates are compared to the biometric system's data storage using a matching algorithm.

3- A decision process uses the matching results to decide [6].

4- Biometrics consist of the measurement and statistical analysis of a unique physical and behavioral characteristics of people. It is mainly applied in identification and access control. In biometric authentication, every person can be accurately identified by his or her intrinsic physical or behavioral characteristics.

## **1.5 ADVANTAGES OF BIOMETRICS**

Day by day, biometric technology is becoming more popular with its applications all around the world. Biometric solutions are highly accepted by many government agencies, multinational organizations, institutions, banks, and hospitals just to name a few industries. The applications are growing rapidly in most life sectors including finance, banking, workforce, borders and most rapidly in applications of national identity. People and governments become more faith with modern biometric technologies rather than traditional security systems. Such uprising of biometric technologies is because of their special following advantages:

### **1. Security**

There are millions of hacking incidents happening every year and our money constantly may be lost. So it is needed to use passwords with numbers, alphabets, symbols, etc. Biometric technology brings different types of solutions which are nearly impossible to hack unlike passwords. This is a great help for us, specifically for business owners who are fighting with security problems for a long time [7].



## **2. Accuracy**

Traditional security systems mess up regularly costing us a big amount of time, money and resources. The most common security systems are passwords; personal identification numbers (PINs) and smart cards that are not always accurate. However, biometric works with your physical traits such as fingerprints, palm vein, retina amongst others that will always serve you accurately anywhere, anytime [7] [8].

## **3. Accountability**

Continuously, we are suffering from the highly-risky-problem of using our password or security number by other persons to hack our personal information. In case of biometric security, it needs our direct interactions to login or pass the security system which guarantees 100% accountability for all activities [7].

## **4. Convenient**

There are many handy tools to note down or to memorize every required password. None of these tools is convenient and can never ever beat the convenience of biometric solutions. Credentials are with us forever, so we don't need to memorize or note down anything [7].

## **5. Scalability**

Biometrics are highly scalable solutions for all types of applications. Because of their scalability, biometric technologies are widely used in government projects, banking security systems, workforce management, etc. [9]

## **6. ROI**

Biometric solutions can provide best ROI compared to other security systems. The tracking of thousands of employees of a large company can be kept with just one biometric device/ software. On the other hand, huge resources are needed to be managed in order to accomplish the same job with more time and money [7].

## 7. Flexibility

Biometric systems are the most flexible security solution. A person has his own security credentials with him. Therefore, he does not need to bother about memorizing complex password containing alphabets, numbers and symbols [7]. Figure 1.3 shows an example of smartcard.



**Figure 1.3:** Flexible to reveal smartcard [10]

## 8. Trustable

It is noted that the young generations trust biometric solutions more than other solutions. Biometric secure systems have already been used in banks to enhance the security and for reliable accessibility for their customers [7].

## 9. Save Time

Traditional security solutions have many layers of hassles and interrogations, which become annoying and unbearable. On the other hand, biometric solutions are highly time conserving, that is we just need to put our finger on a device or look at a retina device to pass the system [7].

## 10. Save Money

Accurate government services can be provided to the people with less cost via creating a national biometric database. Corporations are also adopting biometric systems for accurate information while saving both time and money. Any company can easily track its employees by adopting inexpensive biometric system [7]. Biometric security systems are called long-term commercial security solutions. Efficient, effective, and versatile, biometric security systems will keep business secure while saving you time, money, and resources. [11].

## 1.6 TYPES OF BIOMETRICS

In our human life, we can find many physiological and behavioral biometrics that already used to simplify our life. Physiological biometrics includes fingerprint, iris, face, palm vein recognition, where behavioral biometrics includes signature and voice recognition. For each biometric, there is different properties and flaws, Table 1.1 show the power and weaknesses of each one. In next paragraphs, we summarize the common types of biometrics:

**Table 1.1:** The advantages and disadvantages of different biometrics

Biometric	Uniqueness	Permanence	Collectability	Performance	circumvention
Face	L	M	H	L	H
Fingerprint	H	H	M	H	H
Keystroke dynamics	L	L	M	L	M
Iris	H	H	M	H	L
Retina	H	M	L	H	L
Signature	L	L	H	L	H
Voice	L	L	M	L	H
Hand geometry	M	M	H	M	M
Hand vein	M	M	M	M	L
DNA	H	H	L	H	L

### 1.6.1 Fingerprint Biometric

Fingerprint recognition system is a biometric that is taken using a scanner for photograph of human fingertips. This photograph can record most of the characteristics of our fingers such as whorls, patterns of ridges, arches, minutiae and loops. The fingerprint is considered as one of the oldest biometrics since it is used from a long time. It is selected since it is very stable, reliable and secure biometric. For decades, many governments and law enforcement agencies are depending on this biometric to identify criminals. Nowadays, this biometric becomes more common and can be

found in many places such as banking systems, workforce management, electronic doors ... etc [12]. Figure 1.4 shows sample images of the human fingerprint and the devices that can read it.



**Figure 1.4:** Samples device and images of human fingerprint

### 1.6.2 Face Biometric

The face is another popular biometric that has been used in many applications. It is a technique to record human face images using a good resolution camera and the analyses the facial characteristics that can be any feature on face such as distance between eyes, nose size, mouth characteristics, and other face edges. These measurements are broken into facial planes and retained in a database, further used for comparison. After that a template is created and stored on a database for each person [12].

There are many features for the face biometric such as it considers as a passive biometrics since it does not require any person cooperation. Moreover, it is highly complex technology and largely software based, Figure 1.5 shows face recognition stages . The most good advantage is that picking the biometric by “hands-free” and a user’s identity is confirmed by simply staring at the screen. The main weakness of face biometric is that it is more suited for authentication than verification.

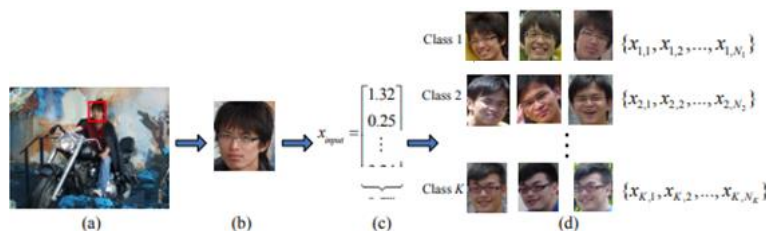


**Figure 1.5:** An example of how the face template can be extracted [13]

## 1.7 IRIS RECOGNITION SYSTEMS

In this section, we describe the features and anatomy of the human eye, after that, an introduction to the iris recognition systems and its main steps are viewed. At the end of this section, the unconstrained iris recognition system is defined.

### 1.7.1 Human Eye Anatomy

The eye structure consists of iris, cornea, pupil, lens and sclera. The eye system works like digital camera. The important parts that we should dealing with when the iris recognition system works are iris and pupil. The human iris has many colors like brown, blue, green etc. The responsibility of the iris is to control the amount of illumination enters to the eye and reaches the retina part. The pupil is the black ring in the middle of iris that adjust the light. If the pupil is small, this means that there is small amount of illumination enters. Figure 1.6 describes the parts and regions of human eye. [14]

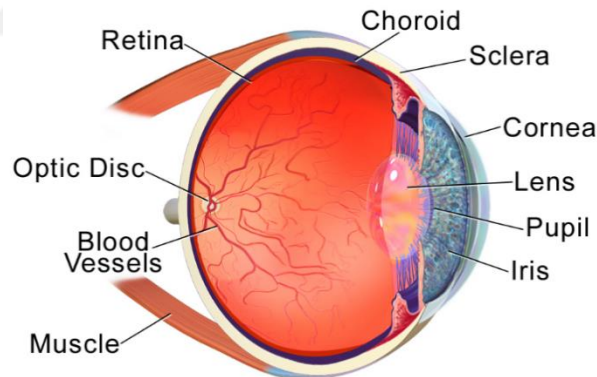


**Figure 1.6:** Human eye anatomy [15]

Iris has a single model for each person that encloses the pupil part. It stays with a person during all his life without any changing and affecting. The iris description system has significantly numerous accuracy and reliability than the other biometric techniques; therefore, it is utilized to detect the identity of humans [16]. The iris internally structure has a complex structure, to represent the characteristics of iris images that need challenges study to discover a new technique for finding iris characteristics. Figure 1.7 describes the parts and regions of human iris.

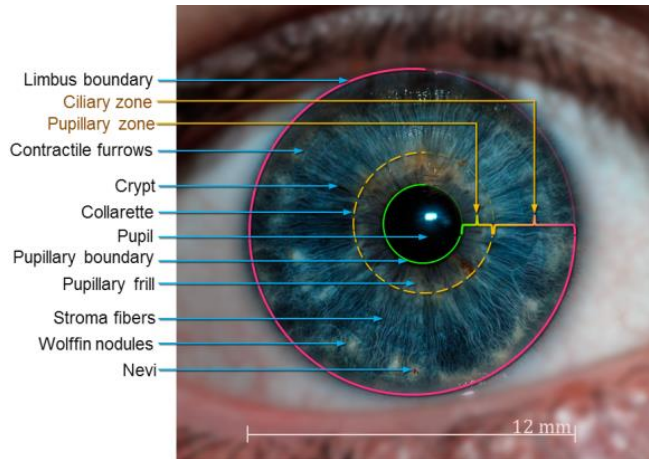


**Figure 1.7:** Human iris anatomy [17]

In addition to authenticity (reliability) and accurately for iris recognition, it possesses a safety and more security to use from other biometrics. [18].

### 1.7.2 Iris Recognition

Recently, because of the highest precision and protection, the iris recognition system obtained more attention in different fields by utilizing industrial, security, borders, ATM banking systems and medical domains, etc. Iris recognition is a biometric system that handles the human iris images for authentication and identification purposes. The stability of the iris enables the researchers to develop iris recognition techniques that able to extract the iris texture from iris image under different conditions [19]. The iris recognition systems have many features: accurate, reliable, uniquely, and stable along with human life. Therefore, it considered as a more robust system than the other biometric techniques [20].

Iris recognition system performs great significant functions in several mission-critical utilization like control, Identification card, border passage, and miss children ID, etc. The iris pattern is randomly organized and sporadically formed in the internal structure. Therefore, the human iris is uniquely even for the twin which makes it an ideal option to detect the similarity among two-persons [21].

In iris recognition systems, the iris images are captured using the near-infrared imaging systems. This is because Near-infrared illumination can work within multi iris surfaces, and detects the intricate textile specifics, which are existing even in dim-colour iris [22].

Iris recognition is becoming a common field of study in the earlier decade. It represents a significant purpose to recognize and identify individually given an enormous database. Two difficulties are faced while improving iris recognition scheme, first the dynamic size for iris area, which is caused by matching directly to become infeasible. The second, the different angles of the head during the iris capturing which causes the capturing of the iris image with adding noises and un-circular shapes. Despite of these challenges, there are many automated iris recognition systems which have been developed over last years using different approaches. Iris identity recognition systems are mostly used in real time to authenticate an individual. Therefore, a rather quick processing speed is needed in order to fulfil the real time requirement [23].

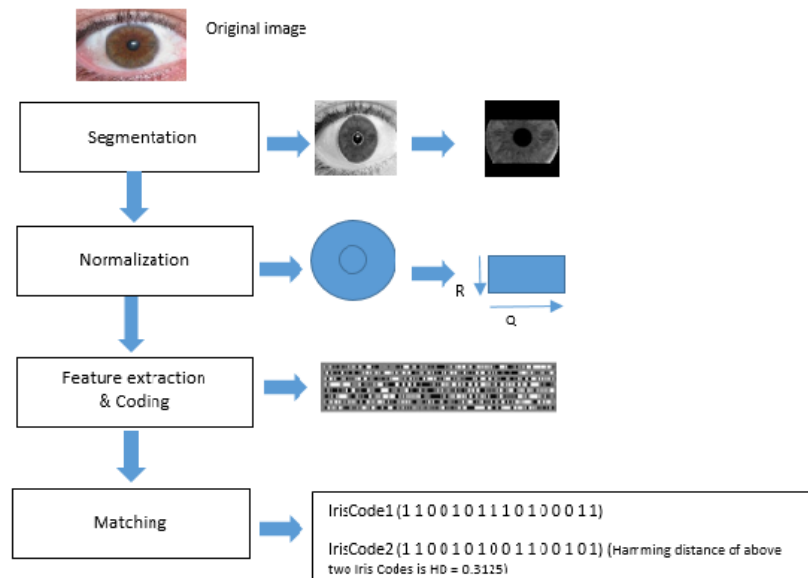


**Figure 1.8:** The steps of the iris recognition system

### 1.7.3 UNCONSTRAINED

Constrained iris images was taken by including near infrared conditions that NIR is lighting origin for detecting the iris textile easily and a constant closing space for all images between the camera and iris. Therefore, the precision of the ideal iris recognition is reduced the significant. Recently, the proposed unconstrained iris is an improvement that is taking different datasets in un-ideal environments. However, the unconstrained iris recognition can be taking the human iris images in different positions from the camera devise. Un-ideal iris images are used the visible wavelength

lighting origin instead of the NIR lighting. Unconstrained can obtain iris images from a mobile or digital camera because they are used visible wavelength lighting also [24].

Unconstrained is considered the new biometric protection sets, demanding which the biometric schemes perform under unconstrained conditions by developing difficult circumstances. It needs challenges algorithms to reach the best accuracy and high performance [25].

Recently, researchers interesting have concentrated on iris recognition system that has condition images like disgraced during an off-axis image, blur the image, lighting variations, occlusion image, and noise image. If the iris images are taking in a limited cooperative at either a distance position or taking image while moving that is unconstrained iris images has become very challenging to recognize. Furthermore, there are various effects on the iris image. Like brightness difference, inadequate focus, putting lenses and putting glass that becomes very meaningful. The performance has affected by the efficiency and the correctness the localization level to get the best results in iris recognition [26]. Using the visible spectrum to take iris textile (texture) introduce more challenges to gain the textile characteristics from iris images.

Unconstrained iris has unideal conditions like take images in a movement and a distance that need lots of effort to detect the iris. Iris images that capture in the ideal case is easy to detect rather than that taking in non-ideal cases. Hence, unconstrained increase and supply the dataset high quality for iris images that make the researches more powerful to solve the problems [27]. Figure 1.9 shows samples of iris image that difficult to perform segmentation.

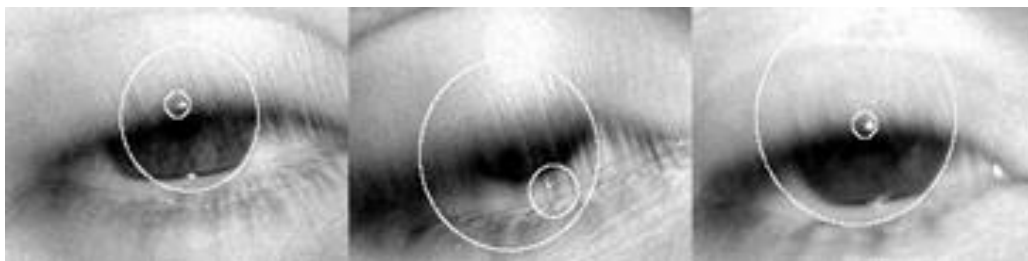


**Figure 1.9:** shows samples



## 1.8 IRIS RECOGNITION STEPS

### First Step: Segmentation

In general, image segmentation expression indicates the partition of an image into a group of meaningful parts of it. Forests of a satellite image, crops and urban areas, and eye iris are examples on such important regions in images [28]. In other words, the goal of image segmentation is to bunch pixels into salient image regions, i.e., regions corresponding to individual surfaces, objects, or natural parts of objects. There are many applications for image segmentation; such as feature extraction, compression of image, editing of image and database look-up of image [29]. In iris recognition systems the segmentation of the iris is very important since it determines the region that will be handled on next steps. Therefore, iris segmentation is considered as one of the most significant steps in iris recognition systems.

In iris recognition operation, the initial step is to separate the area of iris as shown in figure 1.8. The iris area can be isolated by two rings, the first ring is for the pupil (inside iris boundary) and the second one is for the sclera (outside iris boundary) [30], after that the noise regions should be removed from the segmented region.

The main steps are started by localizing the candidate region of iris or directly localize it using a certain method. After that we should omit the unimportant parts, like the pupil, the slice outside the iris, eyelids, eyelashes and skin [31]. The iris area is usually enclosed by the top-down limitations (i.e, eyelids and eyelashes). Segmentation of iris steps can generally be shown as in Figure 1.10.

The Detection of inner boundary circle and outer boundary circle can simply be accomplished using Canny edge detection [32] followed by a Hough Transform method. Hough Transform is a standard computer vision algorithm that can be used to determine the simple geometric objects existing in an image; such as lines and circles [33].

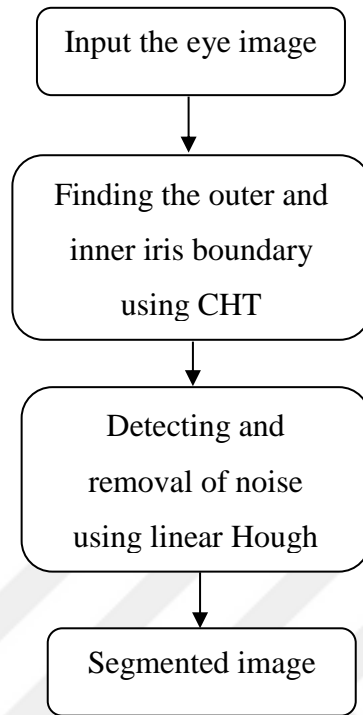


**Figure 1.10:** The general steps of iris segmentation

### **Determining iris region.**

Determining a suitable iris area is the first significant source of inaccuracy in iris segmentation. Iris detection errors belongs to the high local contrast which reflects some non-iris regions. These non-iris regions (the sources segmentation errors) may include eyebrow, eyelashes, frame of glasses and white regions that are caused by the luminance on skin behind eye region. Thus, to avoid such segmentation errors, unimportant non-iris areas must be perfectly excluded before starting the segmentation step. In that sense, in order to avoid the errors as well as to reduce the time of processing of segmentation step, the iris image must be segmented correctly into three areas; skin, iris and sclera areas [34].

In some work, iris recognition is called localization instead of determining iris recognition. The iris is localized and the unimportant parts (e.g. eyelid, pupil, etc.) are removed from the original image. Localization the iris is an annular portion between the pupil (inner boundary) and the sclera (outer boundary). Both inner and outer boundaries of a typical iris can be approximated by two circles [35]. These boundaries have been determined as shown in Figure 1.11. The resulting zone in Figure 3 can be used characterize and processes each eye iris [36].

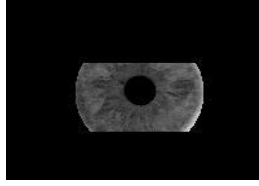


**Figure 1.11:** iris image after determine two boundaries

### **Detecting Edges of the Image.**

Detection of edges can be accomplished by many algorithms. In this work, the popular canny detection technique has been utilized. It is the more effective one for detecting edges. This technique is used to find fast and slow variances for gray scale in all images. This technique has best capacity to detect and find pixels in gray scale for digital image processing [37]. Canny edge detection has been used to detect iris circle and pupil circle from the iris database images. Approximate-to-exact results have been obtained for the detection of iris and pupil circles from the iris images [38].

In the next stage, after accomplishing the detection of the two circles, it is needed to save six values; namely, both radiuses of the two rings with the x-axis and y-axis coordinate values of two centers. To find an edge map by canny detection, horizontal gradient inputs is only required [39]. Other task for Canny detection is the marking out the inner circle to separate the iris image from the pupil [36]. Canny detection is considered as one of the techniques applied in shape recognition and is used, in addition, to find a wide-range edges by applying a multi-operation steps in image processing. Figure 1.12 shows the edge detection steps via canny detection technique. These steps are as follows:

1. Smoothing of the iris image by de-noising or de-blurring.
2. Finding strength and orientation of edges.
3. Thin edges across the image are achieved using directional non-maximum suppression.
4. Performing hysteric-threshold to result in corrected edges over all images.

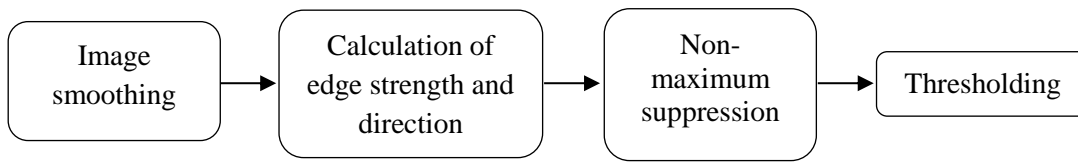


**Figure 1.12:** steps of canny edge detector

### 1) Image smoothing

The initial stage for canny detector is the smoothing of image. This stage is applied to reduce or remove the noise from images by de-blurring. In order to have a predefined image, pixel values of the input image can be convolved with predefined operators. This operation is used either for de-noising or for producing a minimal pixelated images. The best method to reduce the noise that cause false edge detection is to convolve the original image with Gaussian filter [40]. Gaussian filter, therefore, is used in order to achieve smooth results via de-noising.

A Gaussian filter is a discrete version of the 2-dimensional function given by:

$$G_{\sigma}(x, y) = \frac{1}{2\pi\sigma^2} \exp\left(-\frac{(x^2 + y^2)}{2\sigma^2}\right) \quad (1.1)$$

### 2) Finding the Gradient

In an image, Canny detector is dedicated for best detection of all edges with gray level alteration. The areas containing all those edges can be determined using gradients of that image. After that, the results of image smoothing stage is convolved with 3x3- size Sobel operator. Such operator (as discrete differential operator) is used to produces a gradient image. The edge strength of each pixel obtained from the above equation is used in the next non-maximum suppression stage. Edge orientations can be calculated at four corners; like (0, 45, 90, 135) degrees before moving to the non-maximum suppression step [13].

### 3) Non-maximum suppression

The Non-maximum suppression stage is carried out with the magnitude edge images to find out a local edge point with maximum strength in direction of gradient [41]. It is the process of converting

the blurred edges in an image of the gradient magnitudes to have sharp edges. Basically this is accomplished by preserving all local maxima in the gradient image while deleting everything else. The algorithm for each pixel in the gradient image is applied as follows:

1. Rounding of the gradient direction  $\theta$  to nearest coordinate. An 8-connected neighborhood is used.
2. Comparing the current edge strength of the pixel with the edge strength of both pixels in the positive and negative gradient direction.
3. If the edge strength of the current pixel is largest; then the value of the edge strength is preserved. Otherwise, the value is suppressed [40].

#### **4) Double thresholding**

The edge-pixels remaining after the previous stage are marked with their strength pixel-by-pixel. Some of these pixels are correct edges, but some others may appear due to noise effect or color variations. Double thresholding is the best method to differentiate these two sets of pixels. The edge pixels are classified into three sets depending on the threshold (high and low) values; edge pixels that are stronger than the high threshold are marked as strong, those which are weaker than the low threshold are concealed and finally, edge pixels between the two thresholds are marked as weak [33]. In another words, double thresholding is used to distinguish between two edge sets; maintaining the strong true edges while omitting the false [41].

#### **Applying Circular Hough transform to find iris.**

Hough transform is an algorithm presented by Paul Hough in 1962 to detect lines or circles contained in a particular shape in digital images [42]. The classical Hough transform is a standard algorithm used to detect lines and circles. Its application is spread over many computer vision problems as most images contain boundaries which can be altered to regular curves. It can be used after applying the Canny edge detection technique on the images. This algorithm is very efficient for finding the iris from an image because it works even with the presence of noise and performs well even when a large amount of the circle is hidden [43]. The main advantages of Hough transform technique are that it can fill the gaps in the boundary edge pixels resulting from an edge detector and unlike edge detectors, it is relatively a noise-immune operation [30]. In iris

recognition, the circular Hough transform turns to be dominant for determining both radius and center coordinates of pupil and iris regions [44].

Hough transform technique works on the basis of parametric equations. An iris detection strategy based on circular Hough transform and linear Hough transform methods is to be described. First, the inner and outer boundaries of the pupil in iris image are detected. Then, a linear Hough transform can be applied for de-noising, i.e., removing eyelids and eyelashes in the iris image. The equation of the circle is given by

$$(x-a)^2 + (y-b)^2 = r^2 \tag{1.2}$$

As it can be seen the circle to get three parameter  $r$ ,  $a$  &  $b$ , where  $a$  &  $b$  are the center of the circle in the direction  $x$  &  $y$ , respectively and  $r$  is the radius.

The parametric representation of the circle is

$$x = a + r \cos \theta \tag{1.3}$$

$$y = b + r \sin \theta \tag{1.4}$$

Also, the equation of the line is

$$r = x \cos \theta + y \sin \theta \tag{1.5}$$

where,  $r$  = distance between the line and the origin,  $\theta$  = angle of that distance vector. Figure 1.13 shows the result of the application of Hough Transform on an iris image after using Canny edge detector [45, 46].



**Figure 1.13:** (a) Upper and Lower Search Regions of the Iris Image. (b) Upper and Lower Eyelids Detection

### Localizing and removing the pupil:

As shown in Figure 1.13, unimportant parts such as eyelids, pupil and others in the original image must firstly be removed. Then, only the iris image itself is localized in black rectangle while all

images is resized into a single predefined size in order to decrease the distortion due to variance of the pupil and to obtain an approximate scale invariance [42].

### **Removing the other noises (eyelids and light speculation):**

There are two major of noise effects in iris images (eyelashes and eyelids). These kinds of noise have ability to change the accuracy of recognition of iris system. The application of Hough transform operation may be extended to the detection the circular noise regions and the linear noise areas in iris image. All those detected noise areas in Figure 1.14 can be removed to achieve that in Figure 1.15 [47].

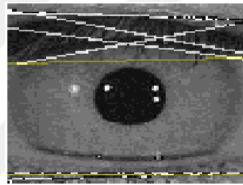


**Figure 1.14:** Detecting the noise in the original image

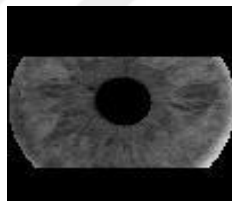


**Figure 1.15:** Iris image after removing the noise

There are many kinds of noise which must be removed from iris images. Eyelids are one factors that can be observe relevant parts especially in top and down regions [48]. Another source of noise is the eyelashes. They appear either isolated or multiple. If isolated, it appears as a very thin dark line in the iris region. The existence of multiple eyelashes in the iris regions generates uniform darker lines. Also, strong reflection regions have a high density that affects directly the iris image causing illuminated pixels in the iris image. In addition, the weak reflection regions with a low density can affect some parts of the iris image. But this kind of reflection has lower intensity values than the previous ones and can correspond to a wide range of objects that the user is surrounded by [42]. Finally, in non-cooperative iris recognition, most of errors to take an iris images are to

belong to the user if have no experience to capture iris images [49]. In a consequence, most of iris images have an error for capturing that caused some noise of images [34].

**Second Step: Normalization:** The second stage after segmentation, which transform the iris area to fixed area in order to make a comparison among all iris images. After the segmentation step, the dimensional variances between iris images results are not equal.

This process is transforming all iris images to rectangular by using these equations: Equation (1.6) and (1.7)

$$X1 = x + r * \cos (F) \tag{1.6}$$

$$Y1 = y + r * \sin (F) \tag{1.7}$$

Where, (x, y) are the coordinates of centre of the circle.

(x1 , y1) are the coordinates of pixel of rectangular image, r is a radius of iris circle that varies from inner to outer boundary of iris image and F is an angle of that varies from 0 to 360 [50] Normalization step converts from Cartesian to Polar coordinate for each pixel in the iris image. The polar is represented the normalization to a constant measurement quadrangular shape. Shows Figure 1.16 and 1.17 [51].

Due to the illumination varying and changing of the camera-to-eye distance that caused the iris, images are taken from several persons in a different size or the same person.

Normalization is produced a 2D array by the horizontal dimension of angular measurement and vertical dimension. [52]



**Figure 1.16:** Shows the original image and normalize the iris image



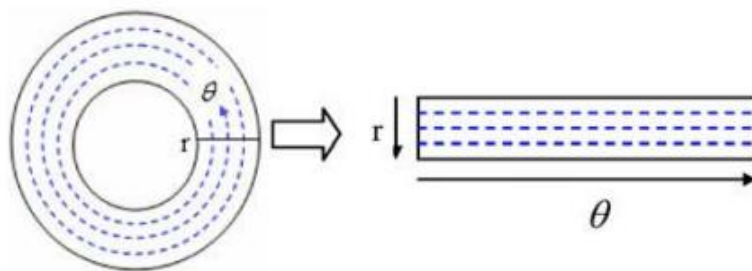


**Figure 1.17:** Shows convert the original image to normalizing image

**Third Step: Feature extraction and Encoding:** Each iris has an individual texture and represents uniquely for each person. In feature extraction techniques, it extracts the unique characteristics that existing in the iris images. Features supply the local and global datum for the iris images, which detects and quantifies the essential characteristics for each iris. There are several techniques to extract features from iris images. The most feature extraction processes collected the signal processing techniques with statistical processing programs. [53].

### Daugman's Method

Extracting the characteristics after the normalization step, Daugman method utilized a couple of dimensional texture filter named Gabor filter to an image of the iris (regarding the iris image) and extracted an impersonation of the texture, named the iris image code. The iris image codes are a group of bits, each one of which shows whether a provided bandpass texture filter (Gabor filter in Daugman technique) implemented by a given spot on the iris images has a negative or non-negative result.

### Wildes' Method

Wildes method employed a Laplacian of Gaussian filter by various scales to design a template and measure the normalized correlation as a similarity ratio after normalizing the segmented iris. He applied an image registration method to repay the scaling and rotation then an isotropic bandpass decomposition is suggested, derived from the applying of Laplacian of Gaussian filters into the iris image data. In this comparison step, a function based on the normalizing correlation within both iris image signs is applied.

### **Forth Step: Matching**

Matching step is performed after all the prior steps, which is the enrolment from the coding iris template. By selecting the binary structure regarding the encrypted bits model, XOR operation is utilized for matching both iris-code bits.

$$HD = N_i \oplus N_{j=1} \quad (1.8)$$

$$HD = N_i \oplus N_{j=0} \quad (1.9)$$

Where  $\oplus$  is the logical XOR operation. N represents the total number of the bits per bit pattern. The Hamming distance gives a measure of how many bits are the same between two-bit patterns. Using the Hamming distance of two-bit patterns, a decision can be made as to whether the two patterns were generated from different irises or from the same one.

Example 1

IrisCode1: 1 1 0 1 0 0 1 1 1 0 1 0 1 0 1 1

IrisCode2: 1 0 1 0 1 1 1 0 0 0 1 0 1 0 1 0 0

The Hamming distance of above two Iris Codes is  $HD = 0.9375$

HD schemes to compute the similarity and dissimilarity between two iris codes. If the matching result is 0, indicates the excellent matching, however, if the matching result is 1 indicates full no matching among the iris images [54].

The matching step is calculated to find the similarity among the input testing images (Acquisition) and the train images within the dataset (Enrolment). Each feature vector is analysed within various threshold methods by hamming distance for comparing the input of iris images with output images. If  $(HD) \leq \text{Threshold}$  then matching pair. Else If  $(HD) > \text{Threshold}$  then not matching pair. The purpose the technique is calculated False Accept Rate (FAR) and False Reject Rate (FRR) for finding the result of these methods [55].

For matching two-iris code templates Daugman uses Hamming distance rule as the likeness measurement:

$$HD(A, B) = \frac{1}{N} * \sum_{i=1}^N (a_i \oplus b_i) \quad (1.10)$$

Consequently, if two code iris totally equal (have the same sign) the rate of the Hamming distance rule will be zero. In totally unequal signatures, the rate of the Hamming distance rule will be 1[56].

### **Unconstrained Iris Recognition**

Constrained iris images are taken by including Near Infrared NIR camera. This can help in detecting the iris texture easily. In addition, a constant closing space for all images between the camera and iris is considered. Recently, the unconstrained iris is proposed by adding some improvements to deal with iris images in un-ideal environments. In the unconstrained iris recognition systems, we can pick the human iris image from different positions using normal camera devices. Unideal iris images use the visible wavelength lighting origin instead of the NIR lighting. In unconstrained environments, we can obtain iris images from a mobile or digital camera since we are using the visible wavelength lighting conditions [24].

Recently, researchers interesting have concentrated on iris recognition system that has conditional images like off-axis images, blur mages, lighting variations, occlusion image, and noise images. If the iris images are taking in a limited cooperative at either a distance position or taking image while person moving then the iris becomes very challenging to recognize. Furthermore, there are various effects on the iris image, like brightness difference, inadequate focus, putting lenses and putting glass that becomes very common [26].

Iris images that capture in the ideal case is easy to detect rather than that taking in non-ideal cases. Hence, unconstrained increase and supply the dataset high quality for iris images that make the researches more powerful to solve the problems [27].

### **1.9 IRIS IMAGE DATABASES**

Recently, researchers are more concentrating on the work of iris recognition; this is because of the uniqueness of human iris and the efficiency of the iris recognition. The iris recognition techniques have been achieving very good results in identifying persons for verification and identification purposes. Therefore, many universities adopted the collecting of several types of databases to help

(support) the researchers that work in biometric recognition field. In this section, we summarize and explain the common databases for iris images. There are many available databases (free downloads) on the internet like UBIRIS and CASIA. We will describe six types of databases and give characteristics for each of them regarding their use in iris biometric system. For example how many images presented in all datasets with information for each dataset.

### **1.9.1 CASIA Database**

CASIA characters mean (Chinese Academy of Sciences' Institution of Automation) for researches station that deals with biometrics and security. This dataset was published to help researchers that work in the iris recognition research field, and it can be downloaded from the Internet [57]. There are four different versions of CASIA dataset V1, V2, V3 and V4. Below, we will describe the details of each version and make a comparison among them.

#### **1.9.1.1 CASIA version 1**

This group contains 756 iris images for 108 eyes per persons. It contains seven classes for each eye image where it is divided into two groups, the first one includes three images for training while the other has four

iris images for testing. The format for iris images in this version of the database is BMP file format. It was stored and captured by using a standard camera [24]. All iris images were taken by including extremely restrained moderate features [58]. The real pupil area for iris images are corrected by CASIA, as a result the pupil area in all images is marked by dark intensity rate (black color) as shown in the figure bellow. This process is applied on iris images to increase the precision of the segmentation and estimation of iris regions [59]. Figure 1.18 shows some sample images for CASIA v1 data set.

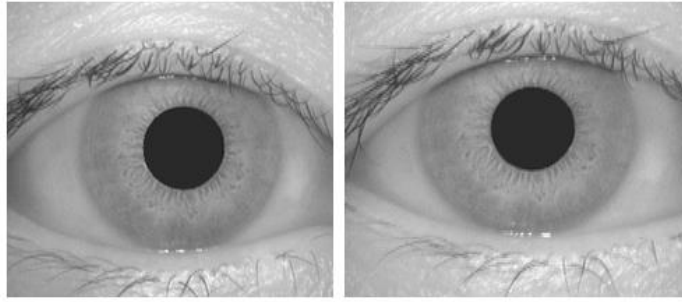


**Figure 1.18:** Two samples images form CASIA V1 database [57]

### 1.9.1.2 CASIA version 2

The CASIA database version v2 was picked using two device sensors [60]:

Device1: this dataset includes 1200 iris images, collected from 60 person. Iris images have 480x640 pixel dimension which taken by OKI Irispass-h camera.

Device2: also includes 1200 iris images that taken by OKI Irispass-h but the iris Images signified including a restrictive machine generated without changing the sizes [61], [62]. All iris images have BMP format. Figure 1.19 displays three iris examples from device1 while figure 1.20 shows three iris samples from device2.



**Figure 1.19:** Three samples iris images from CASIA V2 Device1 [57]



**Figure 1.20:** Three samples iris images from CASIA V2 Device2 [57]

### 1.9.1.3 CASIA version 3

CASIA V3 dataset constitutes from three different sets Iris-Lamp, Iris-Twins and Iris-Interval. It was obtained from 700 human persons to gather 22,034 images. The images of this database were gained from Chinese persons, but some of iris images for Iris-Interval are not Chinese because iris images gathered in various times [63]. All iris images are stored using JPEG file format and include 8 bits grey scale intensity. The Peculiarity of Iris-Interval gives in more details the texture characteristics to the CASIA V3 dataset when the pictures picked from different distances, but the Iris-Lamp gives a non-liberality for iris normalization with robust iris characteristic representation and Iris-Twins exposes the dissimilarity and similarity among Iris twins' images [64].

CASIA Version 3 images were picked using OKI camera as in Version 1, Version 2 databases. Figure 1.21 shows the used OKI sensor that can be used by hand to collect images of CASIA V1, V2 and V3. On the other hand, when captured the LAMP dataset, the lamp has (been) changed off or on to insert extra intra-class variance as shown in Figure 1.22. In Iris-Twins data set, the images collected from 100 twins [65]. Figure 1.23 presents four images from Iris-Twins dataset. (Another sentence) In Figure 1.24 shows samples of the Iris-Interval iris images.



**Figure 1.21:** OKI Device that used to pick CASIA V1, V2, V3 [63]



**Figure 1.22:** CASIA IRIS LAMP [63]

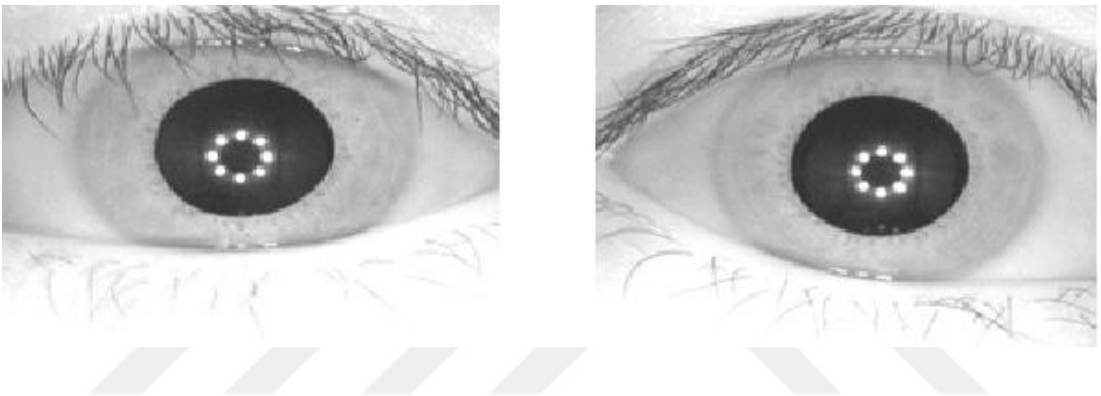


**Figure 1.23:** CASIA IRIS INTERVAL [63]

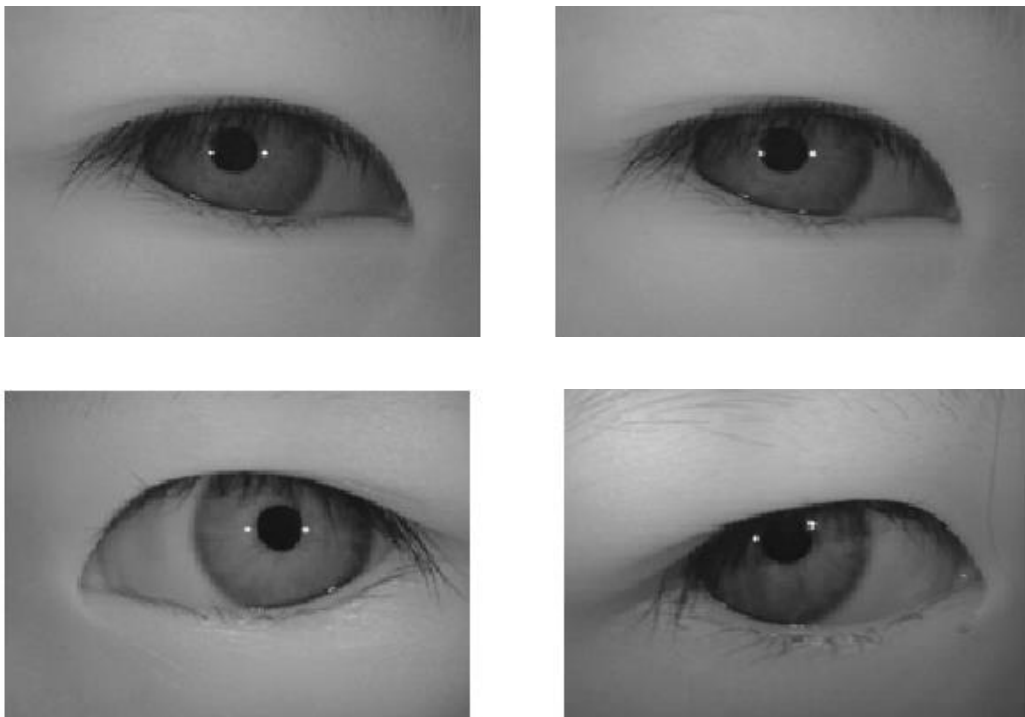


**Figure 1.24:** CASIA IRIS TWINS [63]

#### 1.9.1.4 CASIA version 4

Version 4 of CASIA Dataset involves 54601 images from different persons which some of them had real (1800 iris images) but (1000) iris images were virtual objects. The whole dataset was 8-bit grayscale with JPEG format, which got supporting with near infrared lightning [66]. CASIA V4 combines from five sets:-

- The first set is CASIA-Iris-Interval (the short name is intv) that was captured by size  $320 \times 280$  with using the sensor (CASIA close-up iris camera). Figure 1.25 shows a sample of this kind.



**Figure 1.25:** CASIA-Iris-Interval image sample [66]

- The second set called CASIA-Iris-Lamp (the short name is lamp) which was taken by OKI IRISPASS-h camera and all iris images have dimension of  $(640 \times 480)$ . Figure 1.26 displays an example from this dataset.



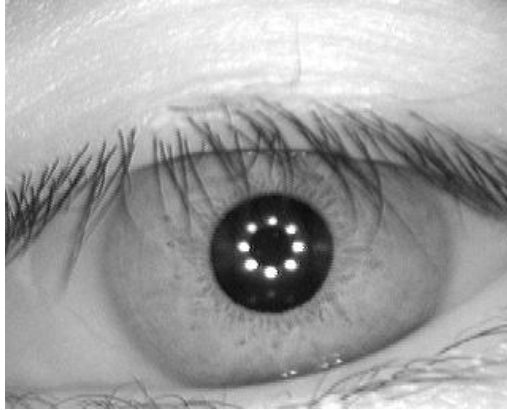


**Figure 1.26:** CASIA -Iris-Lamp image sample [66]

- The third set called CASIA-Iris-Twins (twin) which was captured by OKI IRISPASS-h with resolution  $(640 \times 480)$ . Figure 1.27 shows one sample for this kind of dataset.



**Figure 1.27:** CASIA-Iris-Twins image sample [66]

- The fourth set is CASIA-Iris-Distance (dist). It was taken by CASIA long-range iris camera with size  $(2352 \times 1728)$ . Figure 1.28 shows one sample from this database.

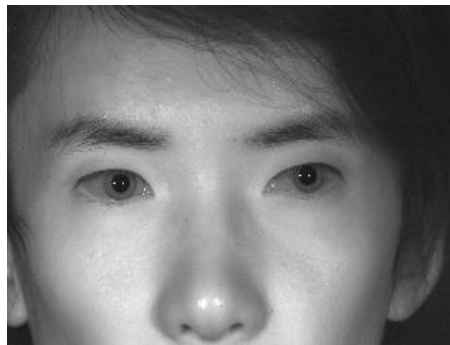


**Figure 1.28:** CASIA-Iris- Distance image sample [66]

- The fifth set is CASIA-Iris-Thousand (thou), where the Irisking IKEMB-100 camera was used to take images of this dataset with size  $640 \times 480$  for all data set images. Figure 1.29 displays one sample of this kind [67]

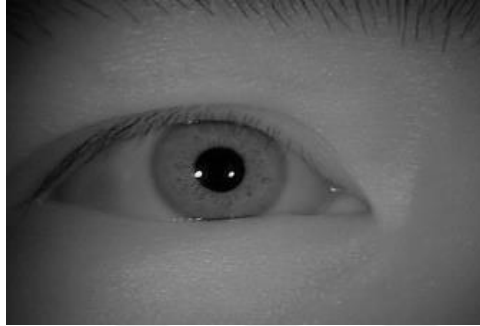


**Figure 1.29:** CASIA-Iris-Thousand image sample [67]

### 1.9.2 UBIRIS Database

The major purpose of the UBIRIS dataset [68] is to study the capabilities of applying the iris recognition systems on un-constrained environments, which can minimize the demand of user collaboration when taking the biometric template of persons automatically. By utilizing and working on iris images that are taken at-a-distance and in un-constrained conditions, the requirements for cooperation are minimized [69]. The UBIRIS has many conditions and noise operators that need effective recognition methods to be able to solve such these problems in the iris images in this dataset. It adds various kinds of noise and taking the iris images with minimum collaboration in order to force researchers to develop new efficient methods that help to develop the iris recognition methodology [31]. The UBIRIS dataset has two versions V1 and V2, and each version includes two sessions.

**UBIRIS V1:** The UBIRIS V1 includes 1877 iris images obtained from 241 persons in 2004 by making two separated sessions. This database contains iris images with various noise factors to become unconstrained iris images. UBIRIS V1 allows evaluating of the robustness of iris identification systems. The first session, took iris images in a darkness place and put some of the conditions like reflection, contrast and luminous. The second session of UBIRIS V2 captured iris images in another place and added real luminance and some unusual difficulties. The Nikon E5700 device was used to take this dataset, and the images were represented with RGB colors, and stored

with JPEG file format. This dataset can be downloaded from Internet by sending email to authors and asking them to give access to download [70]. Figure 1.30 show some examples for UBIRIS V1 Sessao\_1 iris images while Figure 1.31 displaying examples for UBIRIS V1 Sessao\_2.

**UBIRIS V2:** Iris images in this dataset were captured under noise conditions that needs a lot of effort to gain and demand to make it more difficult to analysis. In more details, the objective of UBIRIS V2 dataset is to supply iris images with different kinds of noise and simulated iris images that take without collaboration among subjects, see Figure 1.32 and 1.33. It is accounted as an effective resource to improve the robustness of iris dataset [31]. The UBIRIS.v2 database was build based on three basic factors:

1. To collect images for moving persons.
2. To collect images from different distances.
3. To collect images that include noise factors that come from un-constrained environments with dynamic lighting conditions.



**Figure 1.30:** Some samples of UBIRIS V1 sessao\_1[68]

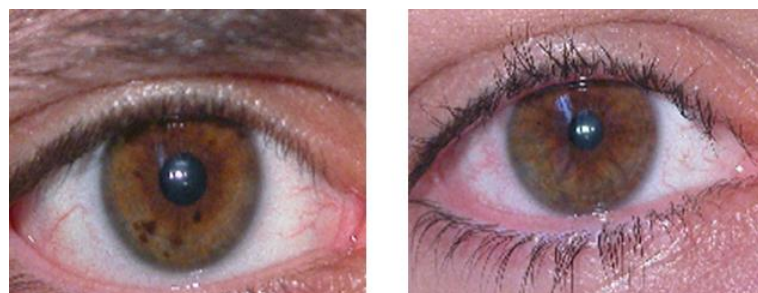


**Figure 1.31:** Some samples of UBIRIS V1 sessao\_2[68]



**Figure 1.32:** Two samples of UBIRIS V2 sessao\_1[68]

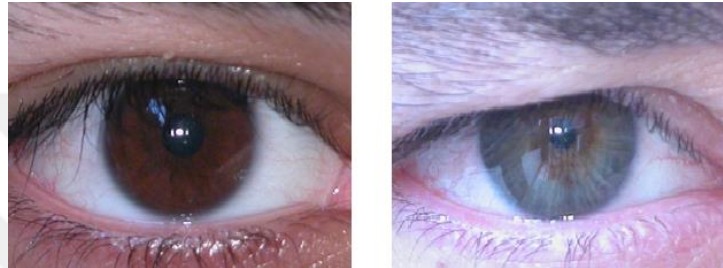


**Figure 1.33:** Two samples of UBIRIS V2 sessao\_2[68]

### 1.9.3 UPOL Database

The letters of the word "UPOL" comes from the words "University Palackeho Olomouc". It is the primary database, which applied imaging frame with a visual wavelength luminance origin. The SONY 3CCD camera was used to collect this dataset. They connected the camera to an optic device named "TOPCON". The number of persons in UPOL database are 64 people with 384 iris images. Each person has six images (3 for the right eye and 3 for the left eye) [71]. The iris images are in the file format PNG and their images size are 576\*768 pixels and the RGB color images have 24 bits depth. In this dataset, the segmentation step is completed because the iris was taken only from the eye by the camera. In addition to that, these data are not suitable for special research of restricted images because they are noise-free as well as they have homogeneous properties [72]. This is because the iris images are directly segmented with a black circle placed around the iris [73]. Figure 1.34 shows some samples of UPOL dataset. Some of researches were used UPOL color dataset that captured by another camera SONY DXC-950P with adding two conditions of the light not normal lighting and merging with brown color to appear in ill status [74].

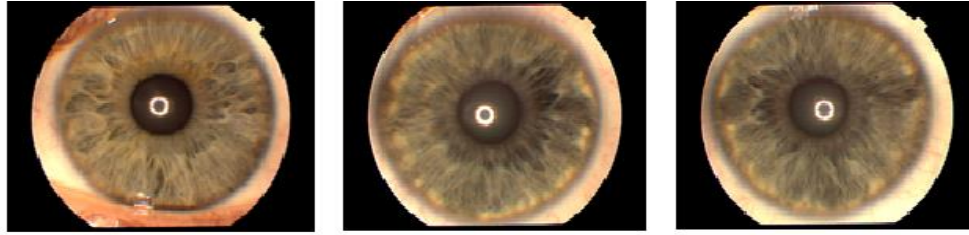


**Figure 1.34:** Samples of UPOL dataset [74]

### 1.9.4 MMU Database

MMU database is composed from two versions MMU1 and MMU2. The images of MMU1, it taken by the LG Iris Access 2200 device. The total number of MMU set is 450 iris images from 100 persons and all of them from Asian. The resolution of this dataset is 320\*280 pixels under bmp format. On the other hand, the MMU2 images were taken by Panasonic BMET100US camera. The total number of all dataset 995 images from 100 persons also all the samples from Asian, 320\*280 resolution and bmp format. In the MMU2 version, minimum noise was added [75]. MMU1 version is available on the Internet. The MMU letters mean Multimedia and the U letter means university [76]. Figure 1.35 shows some samples of MMU iris images.

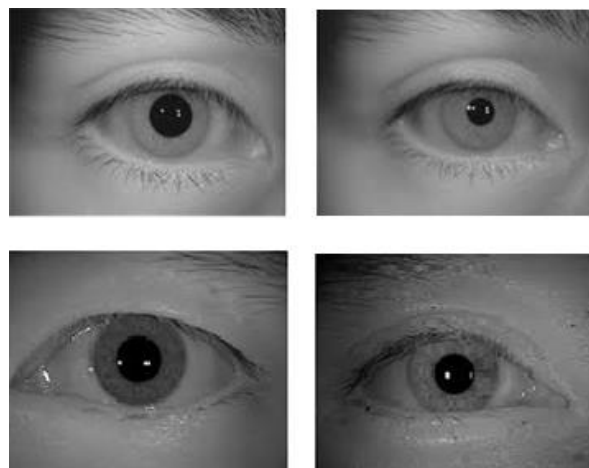


**Figure 1.35:** Some samples of MMU iris database [76]

### **1.9.5 ICE Database**

In 2005, ICE dataset released and researchers started to use this dataset by (NIST) the national institution technology. ICE (Iris Challenge Evaluation) contains 2954 iris images. It is gained in a closed space and the NIR luminance constrains, therefore the ICE database is not benefit for unconstrained iris researches. In addition, they inserted norm noise factor with bad focus iris images and closing eyelashes to the images of database [24]. ICE was prepared in order to make the measurement more precision of iris technique and this technique is divided two parts [64]:-

The first part they asked who works in iris recognition domain to participate their researches in order to improve their study about the iris recognition. The second part, ICE was given their researchers a chance to check their projects over a new iris database in order to evaluate their researches in a suitable valuation frame [59, 60]. Figure 1.36 shows some samples of images belong to ICE database.

### **1.9.6 BATH Database**

This database acquired and prepared by the University of Bath. This dataset is possessed from 800 eyesight and a total number of 16000 iris images (800 iris images for the left eye and 800 iris images for the right eye). All iris images of this dataset are obtained from staff and students that work at the Bath University. Although the high-resolution of used camera in this dataset, the images are lacked of identical properties, therefore it is not appropriate for the expression of unconstrained iris recognition. The high-quality camera includes intelligent sensors to take 1280 x 960 pixels resolution. The camera placed with the vertical position. [58, 61]. Figure 1.37 shows some samples of the Bath dataset.

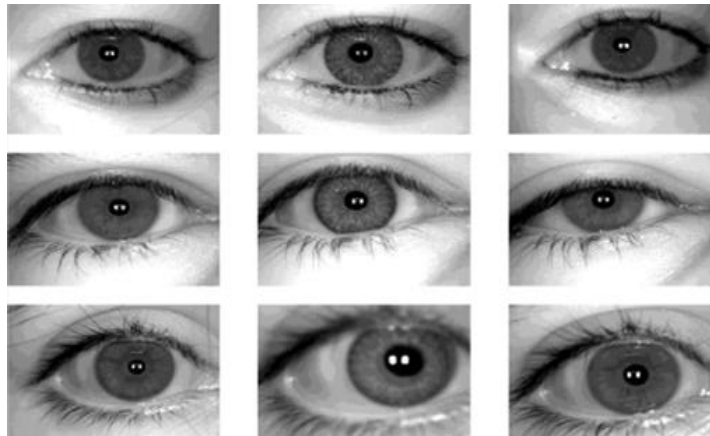


**Figure 1.36:** Samples of ICE database [24]

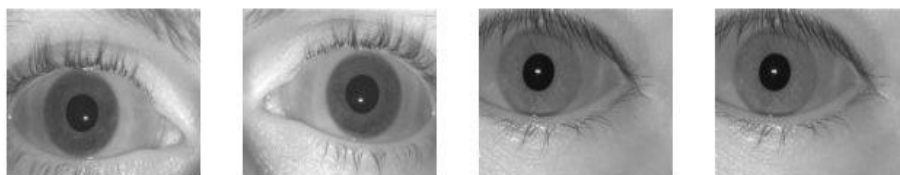


**Figure 1.37:** Some examples of BATH iris database [61]

Figure 1.38 demonstrates the process of taking iris image, and the camera agent is sitting a distance between the camera device and the eye to obtain better iris images.



**Figure 1.38:** The used camera for Bath iris database

## 2. RELATED WORK

In this chapter, we will review the most important research work that proposed recently in the domain of iris recognition. This chapter has two sections. In the first section, a review of the segmentation methods is given with more focus on non-ideal methods. In the second section, a review is presented for the whole system of iris recognition.

### 2.1 REVIEW OF THE SEGMENTATION METHODS

The iris image is considered one of the most accurate biological features because of its distinguishable and stable texture information used for personal authentication. This is why it is believed that iris recognition is the best method for biometric identification. As compared to other biometric technologies, iris recognition is prone to poor image quality. Specially, images captured from a distance which are afflicted by noise; such as blur, off axis, specular reflections and occlusions. Segmentation process plays a key role in iris recognition since the recognition rates are qualitatively dependent on the accuracy of segmented iris. The accuracy of the segmentation process used to localize the iris image structure has its impact on increasing the performance of recognition system. That is because the wrongly-segmented areas as iris regions will corrupt biometric templates causing a very poor recognition rate. Most researchers in the field of iris segmentation focus on treating the eye simply as a circular or an oval shaped structure surrounded by the eyelids which is not the case for iris images with conical shapes or those taken under unconstrained conditions. In such conditions, the parameters to facilitate the process of segmentation of those images must be included. On other hand, Classical iris segmentation algorithms can provide excellent results when iris images are captured using near infrared cameras under ideal imaging conditions. Nevertheless, when the iris images are taken in visible wavelength under non-ideal imaging conditions, the accuracy of these algorithms may significantly decrease. Inaccurate segmentations algorithms were reported due to non-circular geometry of the iris and other noise factors introduced by non-cooperative conditions. That's why non-classical iris segmentation algorithms must be used for non-ideal imaging conditions.

In system hardware implementations, general purpose sequential processing systems, such as (CPUs) are usually used. In 2009, Rakvic et al, proposed an equivalent execution for iris recognition system operations (including segmentation step) utilizing the field-programmable gate



arrays (FPGAs), resulting in a direct and parallel processing alternative (see Figure 2.1). By such execution, an increase in operational speed was offered with a potential alter of the form factor of the resulting system. Operations that consume most of the time in modern algorithms iris recognition (such as segmentation, code vector creation, and matching) were deconstructed and parallelized directly on an FPGA kit. Compared to CPU-based implementations, speedup factors of 9.6 times for segmentation, 324 times for code vector creation, and 19 times for matching were achieved. The researchers concluded that the proposed implementation method is rapid for iris recognition that supplied us with speedy outcomes [77].

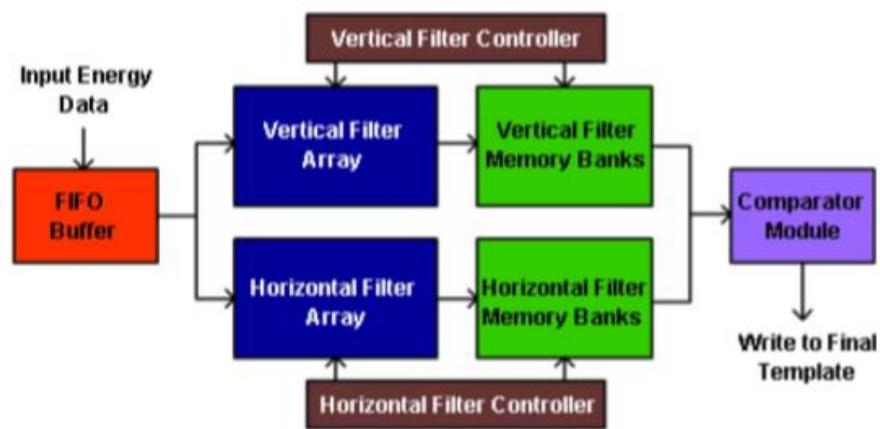


**Figure 2.1:** Template generation (VHDL) system block diagram [77]

In 2009, another version of iris segmentation that is called geodesic active contours (GACs) was presented by S. Shah and A. Ross. The scheme was employed by extracting information from all structures surrounding the eye framework. Active contours can assume any shape with segment multiple objects simultaneously. Mitigation of some of the traditional iris segmentation models was applied by suggesting an iterative method to elicit the iris. In that election, both local and global properties of the image were taken into consideration(see Figure 2.2). The researchers noted that the results obtained on the CASIA v3.0 and WVU non-ideal iris databases indicate the superiority of the segmentation method [78].

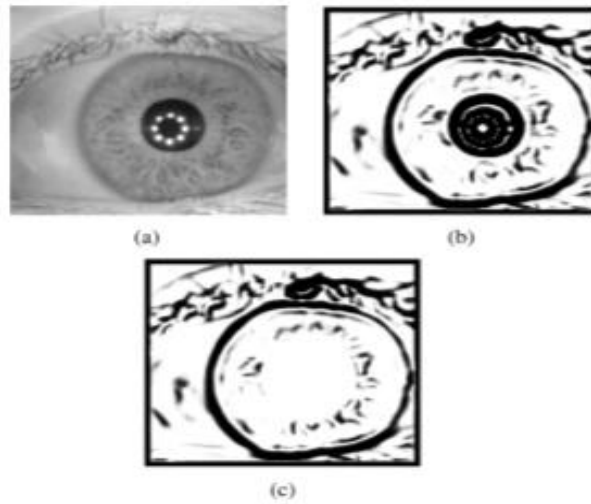


**Figure 2.2:** Stopping function for the GACs [78]. (a) Original iris image  
(b) Stopping function (c) Modified stopping function

The reliability performance of the iris biometric is highly dependent on the ideality of the iris image data. Reliable and precise segmentation is one of the most important steps in processing of a non-ideal iris pattern from remaining background. It should be noted that non-ideal iris patterns result from non-ideal imagery are simultaneously affected with some factors, such as specular reflection, blur, lighting variation, occlusion, and off-angle images(see Figure 2.3). In 2010, Zuo and Schmid presented a methodology for iris segmentation of non-ideal iris images. During the proposed segmentation methodology, compensation of various non-idealities was accomplished. Researchers confirmed the strength of their segmentation methodology via both ideal and non-ideal dataset in Chinese Sciences academic. As a result, a considerable improvement was achieved in segmentation performance over Camus-Wildes's and Masek's algorithms [79].

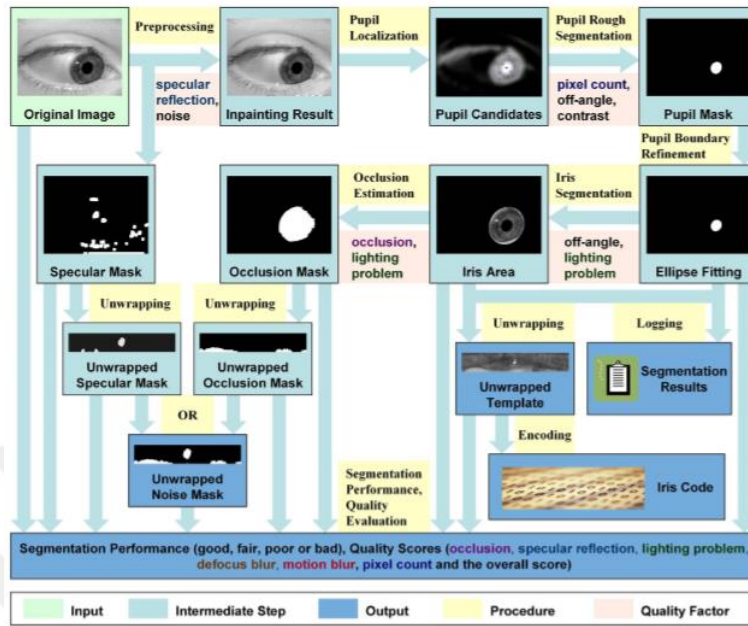


**Figure 2.3:** Block diagram of the iris segmentation procedure [79]

In 2010 also, Proenca, H., suggested a method for segmentation step to deal with iris images that were taken with less constrained cases. By this suggestion, three contributions were achieved. The first one, the sclera was the easiest part of the eye can be found in restricted images. The second, they a novel form was proposed for features, representing the ratio of sclera in all orientations, which were essential for the segmentation step (see Figure 2.4). Finally, the third one was that the procedure was implemented and made suitable for real-time applications by running the whole procedure in linear time deterministically with respect to the size of the image [80].

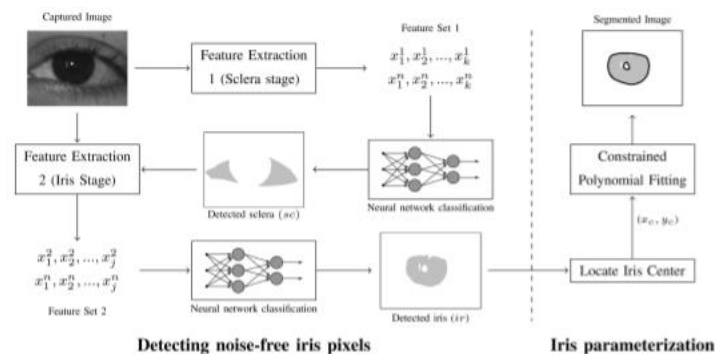


**Figure 2.4:** Block diagram of iris segmentation method [80]

Unconstrained conditions iris images have increased the quality of datasets in iris biometrics by providing us the ability to test the algorithms in difficult environments. Both moving situations and large distances are significant properties utilized visible wavelengths in the iris research to provide more difficult real-world scenarios. Proença, in 2010 [81] proposed an algorithm to evaluate the quality of visible wavelength iris examples that taken in unconstrained situations (see Figure 2.5), by adding some factors like focus, moving, and occlusions. The result pointed out the algorithm improvement by using unconstrained iris recognition and avoiding the poor quality examples in the iris recognition methods.

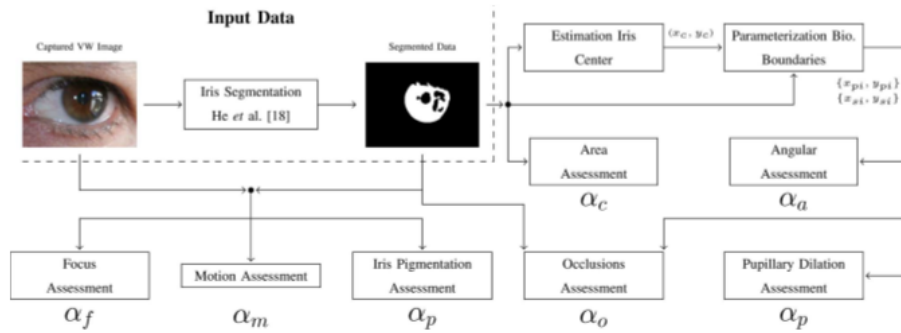


**Figure 2.5:** The proposed quality assessment method [81]

Best segmentation method for iris texture from an input iris image is an important task for robust reorganization of iris pattern. In addition, localization and capturing of available texture regions from non-ideal iris images are still difficult tasks in non-cooperative situations. Such situations may include lighting variations, on-the-move and off-angle view. In 2011, Chen et al. presented fast algorithm for accurate iris segmentation. The rough position of the iris center was found by applying an adaptive mean shift procedure. During the iris localization phase and as an initial step for achieving a real-like iris contour, a circle is set. The statistical texture modelled as Markov random field was then combined, establishing an initial active merged contour model in terms of level set theory. In order to obtain the real iris boundaries, iteration was applied to the initial contour. Eyelids, eyelashes, shadows and reflections were simultaneously detected during the curve evolving process concurrently with labeling them in iris regions (see Figure 2.6). Experimental results of various non-ideal iris images show that that the proposed iris segmentation method was

effective, accurate and could perform with low computational complexity for wide promising applications recognition systems [82].

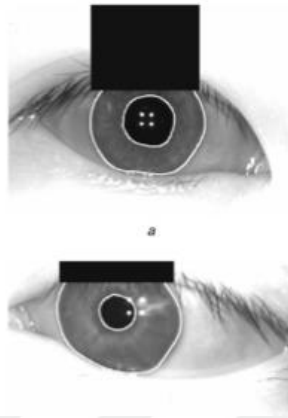


**Figure 2.6:** Segmentation results [82] a) iris image with pupil deformation. b) Iris image with off-axes view

In 2011, Yingzi Du et al., proposed a remote iris acquisition system for noncooperative iris image segmentation scheme based on video environment. The scheme incorporated a quality filter used for 1) a quick elimination of iris from an eye image, 2) employing a coarse-to-fine approach to improve segmentation efficiency, 3) modelling the deformed pupil and limbic boundaries used for fitting ellipses in a direct least squares method, and finally, 4) developing a gradient-based windowing method for iris noise removal in the detected region. The accuracy of the segmentation results was evaluated quantitatively by applying an objective method (see Table 2.1). The effectiveness of the proposed method was demonstrated via experimental results, highlighting the surveillance possibility of non-cooperative iris recognition [83].

**Table 2.1:** Upui remote database frontal look eyes matching results [83]

Algorithm	#Images	EER	GAR at FAR .1%	GAR at FAR .01%
2-D Gabor	610	0.0179	0.9297	0.8856
1-D Log Gabor	610	0.0295	0.9235	0.8980

In 2012 [84], a group of researchers proposed a new way for image segmentation, which treats the limbic iris borders and the pupillary borders. This research contained an energy minimizing

method, including a multi-label one-direction diagram, a pattern fitting method and a physiological prior. Precise segmentation is achieved even the iris has confusion, lens, glass, motion blurring, and different illumination. This main contribution of this research are developing a quick precise and reliable way to localize the iris borders in unconstrained conditions using a new dataset of iris segmentation that includes challenging iris images (It has been publicly released to the researches community service). This paper presented a comparison among three different datasets and proved that the proposed algorithm has a good performance (see Table 2.2).

**Table 2.2:** Comparative results [84]

		[3]	[13]	MC	MC+S	MC+P	MC+S+P
MMU1	OA	93.4 %	91.9 %	<b>97.5 %</b>	97.6 %	97.6%	<b>97.6 %</b>
	SA	53.0 %	34.8 %	<b>83.3 %</b>	84.1 %	84.0 %	<b>88.5 %</b>
	Time	449 ms	196 ms	<b>362 ms</b>	558 ms	379 ms	<b>557 ms</b>
IREX	OA	95.5 %	96.0 %	<b>96.2 %</b>	96.2 %	96.2 %	<b>96.3 %</b>
	SA	77.9 %	72.8 %	<b>79.5 %</b>	79.7 %	79.5 %	<b>80.8 %</b>
	Time	1044 ms	816 ms	<b>471 ms</b>	667 ms	471 ms	<b>669 ms</b>
HID	OA	95.0 %	96.1 %	<b>97.7 %</b>	98.4 %	94.1 %	<b>98.7 %</b>
	SA	76.6 %	78.3 %	<b>87.2 %</b>	90.9 %	88.3 %	<b>92.3 %</b>
	Time	1132 ms	500 ms	<b>397 ms</b>	602 ms	385 ms	<b>630 ms</b>

Iris biometrics that working in remote human description owns significant interests in large civilian and monitoring applications. In [85], the researchers proposed a novel framework for iris segmentation that can robustly segment the iris images and handles both of the near infrared and bright illumination. The presented method utilized various higher quantity local pixels to analyze and detect the eye and face area pixels (see Figure 2.7) then employing the iris segmentation step to recognize the iris. They developed a robust post processing method to reduce the noise pixels that may increase the misclassifications. They applied their proposed algorithm on UBIRIS V2, CASIA V4, and FRGC datasets and the results show competing performance.

In 2013, Sahmoud, S. A., and Abuhaiba, I. S., [34], proposed an algorithm to segment the iris image that captured under non-ideal conditions. The proposed algorithm applied the K-means clustering algorithm to determine the expected region of the iris. In order to estimate the iris radius and center, the Circular Hough Transform (CHT) was then employed. Detecting and isolating the upper eyelids were accomplished by developing an efficient algorithm. The non-iris regions were also removed. Application of the proposed algorithm on UBIRIS iris image databases demonstrated that the segmentation accuracy and operating time were both improved [34].

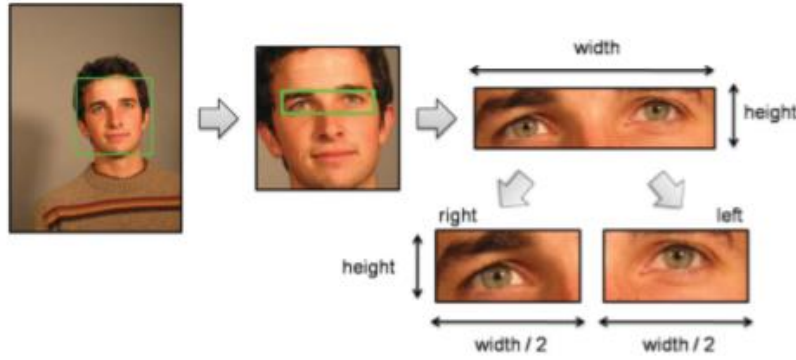


**Figure 2.7:** Hierarchical face-eye detection [85]

In another research [86], the iris images are taken from videos that captured from different distances with motion and contained noise conditions. A video-based iris segmentation method is proposed to process iris images captured in unconstrained conditions. The first step takes the frame adjustment regarding human face videos by performing a procedure to extract the eye areas from Near-Infrared facial videos (see Figure 2.8). In the second step, a novel iris segmentation way is applied to face images that taken in challenging conditions. They proposed a method to segment the iris region by detecting the eyelid and eyelashes then removing them. Results on the MBGC database show that the presented work gains higher efficiency than other recent cases in video-based iris segmentation methods.

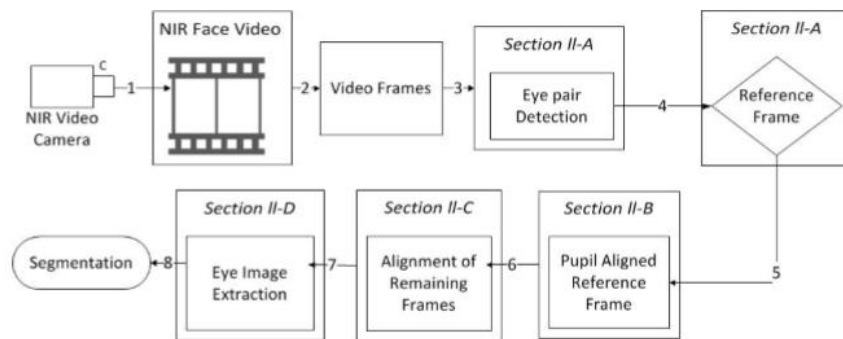


**Figure 2.8:** Stages of eye image extraction in NIR face videos [86]

There are many other methods for best segmentation of iris from an eye image. In 2016, [87], a fast Daugman's method was used to obtain both pupil and iris boundaries for Iris images on CASIA database. The iris and pupil boundary were detected. The iris boundaries were then segmented out. It was pointed that the computational time of segmentation by Daughman's method was excellent

as it needed a very small time to segment the iris and pupillary boundaries of eye image and to give the appropriate recognition rate (see Table 2.3) [87].

**Table 2.3:** Performance between LCV and BLCV on NICE.II [87]

Method	Performance Evaluation				
	Total segmentation time (sec)	DICE	PSNR	$E_1$	$E_2$
LCV (40x40)	3.97	0.821	16.50	0.0249	0.1284
LCV (60x60)	7.44	0.811	16.02	0.0282	0.1669
BLCV	6.11	0.868	18.17	0.0180	0.0723

In 2016 and based on local region treatment, Chai et al., proposed an active contour model for segmenting non-circular iris shape from noisy and inhomogeneous visible wavelength images. A bi-local neighborhood approach was employed without the need of separate image processing phases. That is to allow contour evolution using some terms based on local region with a simultaneous occlusions avoidance. To ensure simple, accurate and efficient segmentation algorithm, a b-spline formulation in the approach was followed. The limitations of active contour based methods was also overcome in terms of computational power. Good segmentation accuracies (on NICE.I and NICE.II databases) were demonstrated while applying this model [88].

In 2016, Hofbauer et al., showed also some experimental analysis presenting the iris segmentation influence on the overall iris-biometric recognition performance. They examined experimentally whether the segmentation accuracy could serve as a predictor for the overall performance of the iris recognition. Systematically speaking, they evaluated the influence of all segmentation parameters on the rest of the iris recognition chain. Such parameters included pupillary, limbic boundary and normalization center of rubbersheet model. The authors also investigated if accurately of these parameters was important and how robustness (which indicated the exact region extraction of the iris during segmentation process) influences the overall performance (see Figure 2.9). They also reported that the segmentation accuracy could improve the overall recognition performance? [89].



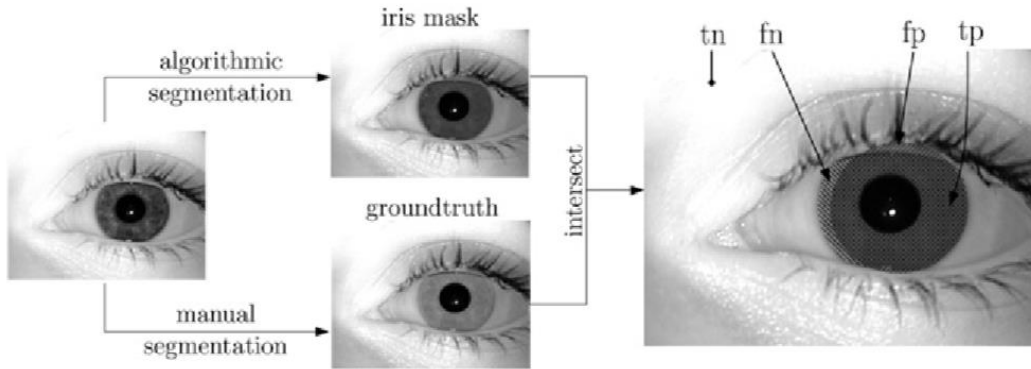


**Figure 2.9:** Example of the split between tp, fp, tn and fn for an iris image segmentation [89]

In 2017, Jalilian, E., Uhl, A., & Kwitt, R., suggested recently two methods based on pixel-level domain adaptation. A training model for convolutional neural network (CNN) based iris segmentation was introduced. Throughout experiments, it appeared that the two suggested methods transferred effectively the domains of original databases to those of the targets, thus adapted databases was produced. The adapted databases were then used for CNN training to be utilized in segmenting iris texture. The authors indicated that optimal segmentation scores could be maintained by training a specific CNN for an iris segmentation task while using a very low number of training samples (see Table 2.4) [90].

**Table 2.4:** Segmentation results for decreased number of training samples [90]

Database	Casia5a			Casia4i			IITD		
	nice1	nice2	f1	nice1	nice2	f1	nice1	nice2	f1
15 pcs	0.075	0.082	0.875	0.205	0.263	0.502	0.089	0.097	0.856
25 pcs	0.064	0.077	0.896	0.099	0.115	0.814	0.077	0.083	0.879
50 pcs	0.050	0.070	0.909	0.078	0.068	0.841	0.063	0.070	0.889
100 pcs	0.021	0.040	0.921	0.038	0.039	0.926	0.035	0.037	0.941

In 2017, Pandey, P., & Karthik, A., presented a scheme for iris segmentation. In order to segment iris from the eye in that scheme, they made use of circular geometry of the pupil and iris. The simulation results highlighted both fast speed and accuracy properties of the proposed scheme when compared to some existing others in the literature (see Table 2.5) [91].

**Table 2.5:** Simulation results [91]

Method	Total Images	Detected Correctly	Percentage	Execution Time(s)
<i>Daugman</i>	2639	2552	96.7	.009
<i>Wildes et al</i>	2639	2486	94.2	.01
<i>Proposed</i>	2639	2595	98.3	.004

In the same year 2017, Sinha et al., introduced an approach that used deep neural network to eliminate the unwanted patches influencing the performance of whole system of iris recognition. In the proposed model, a memory efficient representation in the form of up-sampled indices were used at the decoder (see Figure 2.10). Ubiiris V.2 database was applied to perform the experimental analysis [92].

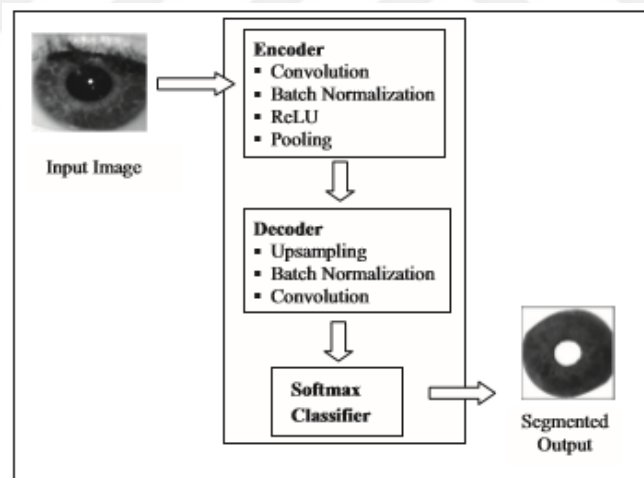


**Figure 2.10:** The proposed system for iris segmentation [92]

More recently, In (2018), Proença, H., and Neves, J. C., presented a disruptive hypothesis algorithm for periocular biometrics in visible-light data. An optimized recognition performance was achieved by simply discarding the components of both iris and the sclera, resulting in an exclusively based recognition on the surroundings information of the eye. A processing chain was described based on convolutional neural networks (CNNs). CNNs were used to define the regions-of-interest in the input iris data without masking out any areas in both learning mode samples and test mode samples. An exclusively ocular segmentation algorithm was used in the learning data

for separating the ocular from the periocular parts. A large set of “multi-class” artificial samples were produced by interchanging the periocular and ocular parts from different subjects. For data augmentation purposes, the resulting samples were used and fed to the learning mode of the CNN taking into consideration labeling the ID of the periocular part. By this approach, the CNN received multiple samples of different ocular classes for every periocular region. That forced to conclude that such regions should not be considered in CNN’s response. During the test mode, samples were provided without any segmentation mask. Disregarding of the ocular components was done naturally by the CNN, contributing performance improvements. Two known data sets (UBIRIS.v2 and FRGC) were employed in the experiments. The results showed that the proposed algorithm (see Table 2.6) could reduce the EERs in almost 82% for (UBIRIS.v2) and 85% for (FRGC) while improvements were gained in the Rank-1 of more than 41% for (UBIRIS.v2) and 12% for (FRGC) [93].

**Table 2.6:** Comparison between the performances obtained by the method proposed in this paper with respect to three state-of-art strategies [93]

Method	AUC	Rank-1	EER
<b>UBIRIS.v2</b>			
Proposed ( <i>Periocular CNN</i> )	$0.998 \pm 4e^{-4}$	$0.88 \pm 0.02$	$0.019 \pm 6e^{-4}$
Proposed ( <i>All CNN</i> )	$0.994 \pm 4e^{-4}$	$0.84 \pm 0.02$	$0.039 \pm 8e^{-4}$
Zhao and Kumar [27]	$0.984 \pm 5e^{-4}$	$0.62 \pm 0.02$	$0.109 \pm 2e^{-3}$
Tan and Kumar [24]	$0.913 \pm 3e^{-3}$	$0.44 \pm 0.02$	$0.153 \pm 3e^{-3}$
Proença [19]	$0.965 \pm 1e^{-3}$	$0.58 \pm 0.03$	$0.114 \pm 3e^{-3}$
<b>FRGC</b>			
Proposed ( <i>Periocular CNN</i> )	$0.999 \pm 4e^{-4}$	$0.92 \pm 0.01$	$0.011 \pm 3e^{-4}$
Proposed ( <i>All CNN</i> )	$0.996 \pm 4e^{-4}$	$0.89 \pm 0.02$	$0.028 \pm 3e^{-4}$
Zhao and Kumar [27]	$0.995 \pm 4e^{-4}$	$0.82 \pm 0.03$	$0.040 \pm 1e^{-3}$
Tan and Kumar [24]	$0.971 \pm 3e^{-3}$	$0.69 \pm 0.02$	$0.062 \pm 2e^{-3}$
Proença [19]	$0.979 \pm 2e^{-3}$	$0.70 \pm 0.03$	$0.058 \pm 3e^{-3}$

In 2018 also, Bazrafkan, S., and Corcoran, P., presented an appropriate augmentation method as a solution to the problem of the iris segmentation task in handheld devices. This was accomplished with the development of a deep learning scheme. During experiments, pre designed challenging image datasets were employed to emulate the quality of images obtained from a handheld device.

Comparisons with the previous iris segmentation algorithms (see Table 2.7) showed some significant improvements in performance of the proposed method [94].

**Table 2.7:** Segmentation accuracy of Bazrafkan, S., and Corcoran, P algorithm [94]

Method/Database	UBIRIS	MobBio
Proposed method	<b>99.3%</b>	<b>97.07%</b>
MFCN [8]	99.1%	--
HCNN [8]	98.89%	--
[9]	98.79%	--
[10]	98.69%	--
[11]	98.28%	--
[12]	98.13%	--
[13]	98.1%	--
IFFP [14]	44.38%	50.58%
GST [15]	42.59%	42.21%
WAHET [16]	27.4%	44.27%
Osiris [17]	26.46%	20.08%
CAHT [18]	18.02%	28.37%

Recently, in 2019 [95] a new scheme is proposed in iris segmentation that deals with neural networks to recognize and robust the iris images. This paper consists of three parts, the first part is a convolution neural network that constructed and combined to handle dense sections in the iris segmentation step. It related to dense-fully convolution networks and adopted some traditional optimizer techniques like batching normalization (see Figure 2.11). The second part labels the known ground-truth mask areas for the CASIA V4 and IITD iris datasets that block the iris areas by employing the (Labelme software) packaging. The third step is encouraging outcomes of operations on (UBIRIS V2, CASIA V4.0 (Interval) and IITD) iris image datasets to obtain by many conditions detect that the iris segmentation networks. CNNs are used in this paper to examine the performance, robust and reflect of the proposed algorithm against the other algorithms.

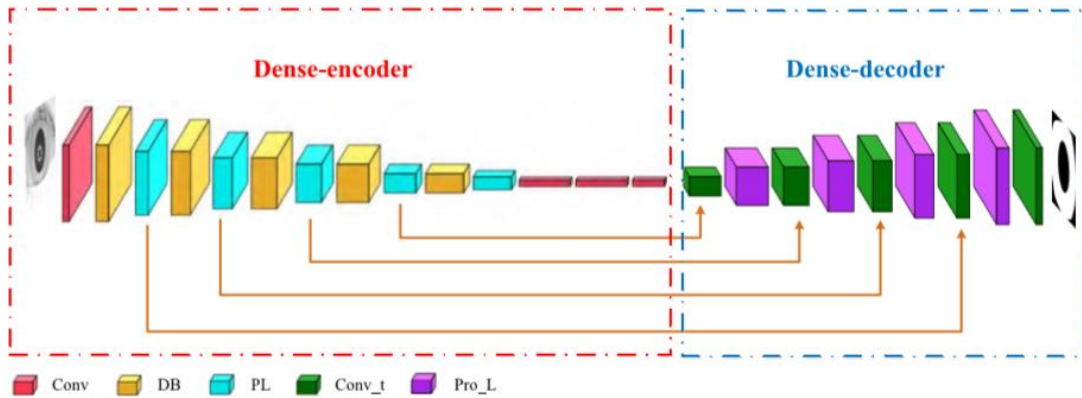


**Figure 2.11:** The DFCN architecture [95]

## 2.2 REVIEW OF THE IRIS RECOGNITION SYSTEMS

Recently, many researchers that developed several algorithms have studied the iris recognition system. Most of those researchers were assumed that the iris images are frontal and have high-quality conditions. Daugman's approach is considered one of the most common algorithm in this domain, and it is still used in many commercialized biometric systems [96]. In the Daugman method, he transformed the segmented iris image into log-polar coordinates. He first located the boundaries of iris by using a differential operator that is a little time consuming. After that, to extract the features from the iris image the convolution of complex Gabor filters is computed. After that, the complex map of phasors is generated and a 2048-bit iris code is computed. In order to compare the iris code of current image with other iris codes, the Hamming distance criteria is used. The Gabor filter-based method has a high accuracy and gives good results, but it requires a long computational time [97], which recognized as the main disadvantage of this method. Wildes analyzes the iris textures by using four-level Laplacian Pyramid method [98]. Firstly, he uses the circular Hough transform and gradient criterion to localize the iris borders. After that, the Laplacian operator is applied to extract the features of iris image in four accuracy levels (see Table 2.8).

Z. Sun et al. applied a fundamental iris image method [99] that called BOIs (blocks of interest) for segmenting the iris by using zero-crossing wavelet transformation after the normalization steps. In this study, using the statistical and structural classifiers are cascaded for getting the best iris recognition results. The efficiency of the iris recognition was significantly enhanced by using the

inexpensive cost that paid during the computation steps. However, applying additional classifier requires additional time to perform the work (see Figure 2.12).

**Table 2.8:** Results of algorithm given from [97] by tested it on CASIA database

database	Number of users	Number of images	Accuracy of locating method (%)	Average of implementation time(sec)
CASIA1	108	754	99.73	0.221
CASIA3-right eyes	165	965	98.24	0.246
CASIA3-left eyes	185	1318	97.04	0.246
MMU1-left eyes	42	211	99.05	0.233
MMU1-right eyes	45	222	99.55	0.233

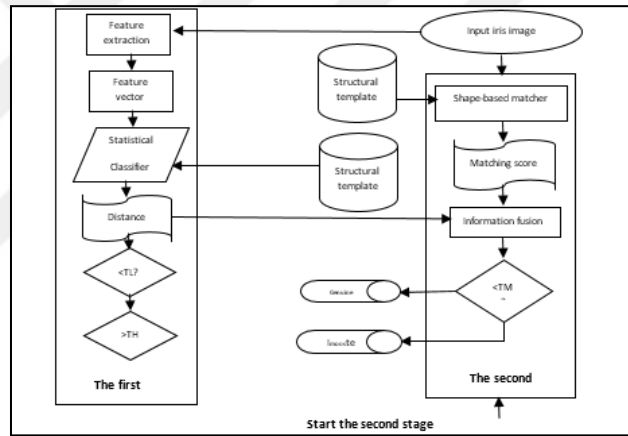


**Figure 2.12:** Overview of proposed algorithm [99]

Sudha et al. [100], [101]; presented another efficient technique using maps of edges to extract iris codes using Hausdorff-distance for the evaluation of code matching. Although, edge maps in terms of low storage space have some advantages, and in fast transmission, fast processing and hardware compatibility, the high recognition rates cannot be achieved unless different values of parameters such as partialness and block size are studied and processed (see Figure 2.13). The experimental outcomes on UPOL iris dataset present a high performance values comparing with other state-of-the-art algorithms.

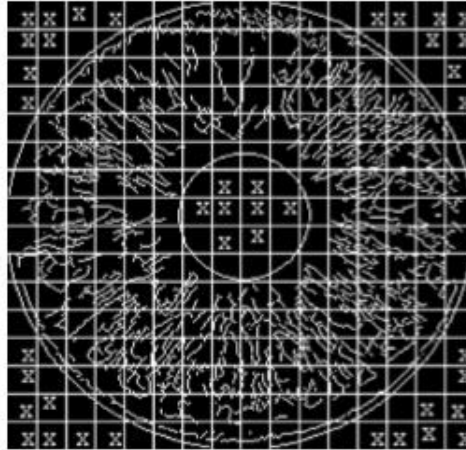


**Figure 2.13:** Division of an iris edge image into non-overlapping blocks [100], [101]

Du et al. proposed with his supervisor a non-ideal iris recognition method, where a Gabor descriptor is applied on the iris image to extract the features [102]. The presented algorithm can work even with iris images that have off-angle and less resolution properties. The Gabor wavelet filter is merged with Scale Invariant Feature Transformation (SIFT) to get more good features extraction ability. To describe the feature points locally, both magnitude and phase of the Gabor wavelet outputs are used in this method. Double feature region maps are designed to globally and locally to choose the feature points. For each map, a sub-area is locally adjusted by using the contraction, dilation, and deformation (see Figure 2.14). This proposed algorithm showed better performance for both the frontal and off-angle iris images, but the computation complexity is increased significantly.

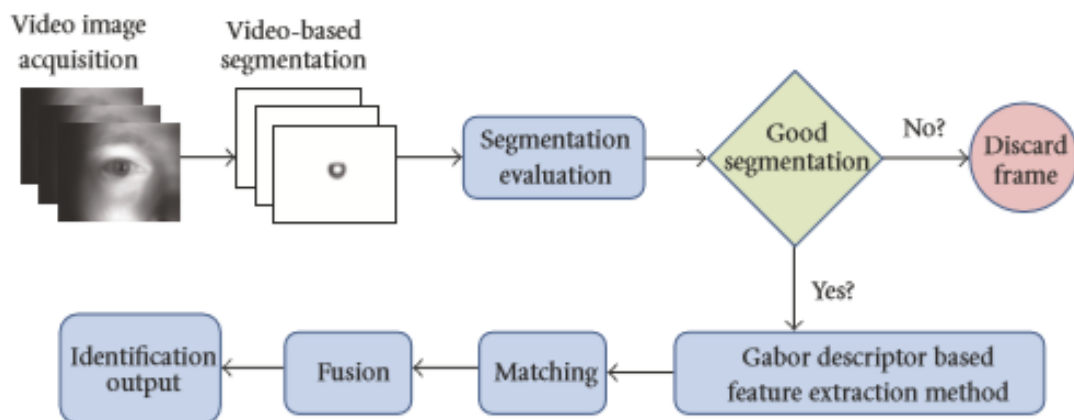


**Figure 2.14:** The Proposed video-based non cooperative iris recognition system [102]

In 2011, M. Abdullah [103] presented a method to integrate iris recognition into smart card. This is important to develop a high security access system using iris recognition system. An ordinary Haar-wavelet filter was utilized to extract the features that stored in a smart card to be compared with other stored cards information for authentication purposes. In addition, the proposed system performance can be enhanced using other types of wavelet filters. They presented the CRR algorithm with 236 bits of iris template size (see Figure 2.15). The test results show a feature vector carrying concatenation of five sets (LH4, HL4, LH5, HL5 and HH5) supplies the valid results.

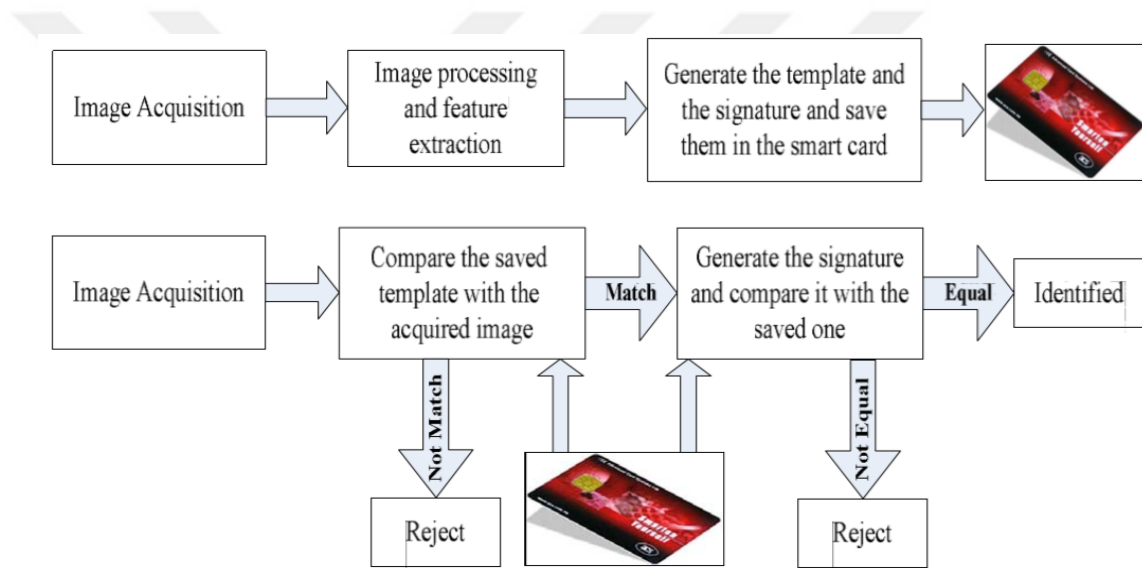


**Figure 2.15:** The block diagram of the designed system [103]

Again in 2011, another algorithm focused on rapid and accurate iris identification is presented even if the images are occlude [104]. It also focused on robust iris recognition, even with gazing-away eyes or narrowed eyelids which can serve the security related problems. In the feature extraction step, only the fourth and fifth vertical and diagonal Haar wavelet coefficients were taken to express the characteristic patterns in the iris mapped image. Here also, the performance of the proposed system can be improved using other types of wavelet filters. In addition of the property of wavelets of lacking the orientation information.

The main steps of iris feature extracting mechanism in [104]:

- Applying 2DDWT algorithm with 5-levels Haar up.



- Applying 4-levels, decomposition details to construct the feature vector.
- Binarizing the details of the feature vector from previous step.

In 2012, B. Jain et al. developed an efficient and novel iris recognition algorithm by using a Fast Fourier Transform mechanism and the calculation of possible moments sets [105]. Matching step was achieved in this algorithm by using Euclidean Distance. The recognition results are generated using preferred conditions, which reflects the dependency on different illumination circumstances (see Table 2.9).

**Table 2.9:** Comparison of available Iris Recognition Algorithms [105]

<b>Serial No.(a)</b>	<b>Method (b)</b>	<b>Recognition Rate% (c)</b>	<b>Equal Error Rate% (d)</b>
1.	Boles [5]	92.64%	8.13%
2.	Daugman [3]	100%	0.08%
3.	Tan [19]	99.19%	0.57%
4.	Moment method (present work)	100%	0.0032%&0.58%
5.	Characterizing key local variables[4]	100%	0.07%

In 2012 also, J. M. Abdul-Jabbar and Z. N. Abdulkader [106] introduced a non-traditional step for feature extraction by applying a new bank of two-dimensional (2-D) elliptical-support wavelet Haar filter bank to capture the iris characteristics. A five-level 2-D elliptical-support wavelet decomposition was needed to form a reduced fixed length quantized feature vector with improved performance. As a final step for iris matching, Hamming distance was applied. Experimental results showed that the method is reliable with rapid recognition, since it achieves good recognition rate with reduced number of feature vectors. However, the method needs a complex 2-D filter back decomposition.

More recently, in 2013, K. N. Thanh in his Ph. D. dissertation [107] has presented human identification at a distance using iris and face. In that dissertation, three major challenges in human identification at a distance was addressed; namely, input image resolution, input data quality variation and unavailability of a part of biometric modalities. Super-resolution techniques were adopted to enhance the lack of resolution, resulting in some improvements in recognition performance of the biometric system. However, estimating the statistics of prior probabilities of

the features and noise requires the statistics of noise and the prior probability of high resolution features to be estimated beforehand. This may need prerequisite estimation performed on a training set (see Figure 2.16).

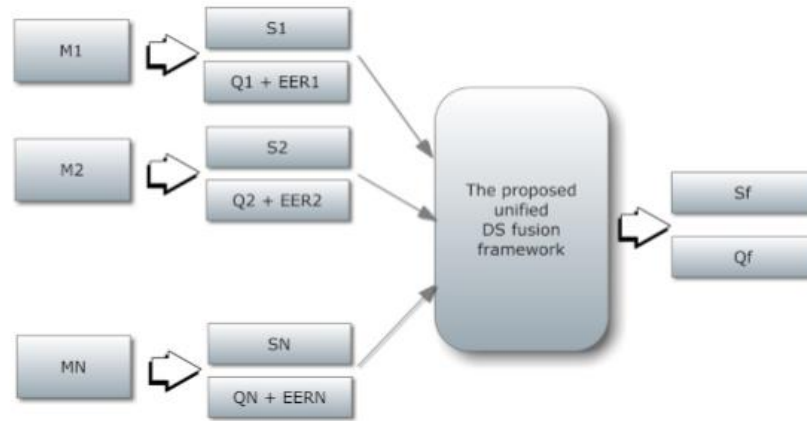


**Figure 2.16:** Combining multiple sources of evidence using DS theory [107]

This means that the method is a set-dependent. Again in 2013, M. S. Khalili and H. Sadjedi [97] presented a method by applying a mask to the iris image to remove the unexpected factors affecting the location of the iris. Then Canny edge detector was used to locate the exact location of the iris. Distinctive features were extracted via 2-D discrete stationary wavelet transform with Symlet 4 filters. The features obtained from the application of the wavelet were investigated with the implementation of a similarity criteria for feature selection procedure. Semi-correlation criterion was finally used to perform the iris matching. Although good accuracy values were achieved, but that was accomplished on behalf of the time-consuming process of finding similar features. Ideal image acquisition conditions are assumed in most above mentioned iris recognition systems. These conditions may include a near infrared (NIR) light source for clear iris texture and iris look retrieval. In addition, these conditions may also include stare constraints and close distance from the capturing device. However, when these constraints are relaxed, the recognition accuracy in most systems decreases. Recently, different processing methods for iris images captured in unconstrained environments were proposed.

In 2012, an effective method was proposed by M. Mahlouji and A. Noruzi [108] for localization of iris inner and outer boundaries, presenting an iris recognition system in unconstrained environments. In such method, circular Hough transform was used for segmentation and

localization of boundaries between upper and lower eyelids occluding iris was performed via application of linear Hough transform. When compared with other popular iris segmentation methods, a relatively higher precision was obtained for this method with less processing time. A high accuracy rate of 97.50% was achieved while testing the results on CASIA database images. However, processing time can further be reduced without using the normalization (see Table 2.10).

**Table 2.10:** Efficiency comparison on CASIA database for popular algorithms [108]

<i>Algorithm</i>	<i>FAR (%)</i>	<i>FRR (%)</i>	<i>Overall system accuracy (%)</i>
Yahya [11]	2.08	0.03	97.89
Daugman [2]	0.09	0.01	99.90
Ma [6]	8.79	0.84	89.37
Proposed method	0.50	2	97.50

J. M. Colores *et al.*, in (2012) [25], they proposed a method that deals with video iris recognition schemes with a non-ideal environment presented in this work. This technique includes two levels the iris quality evaluation to recognize significant rate enhancement by Daugman method utilization. Although the similar error rate (EER) amount obtained that reduce about (12.2) percentage, the traditional recognition technique of Daugman received the high processes time. They assumed that the obtained eye image frames include various noises with distortion like frames and motion blurring. This influence the segmentation operation and consequently affects the recognition scale. Due to a bad situation to take iris frames, got a high quality to evaluate and segment steps (see Figure 2.17).

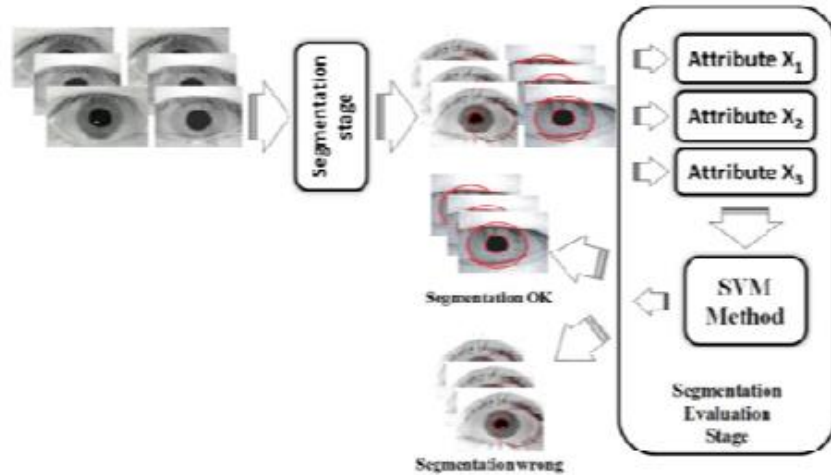


**Figure 2.17:** Block diagram to evaluate the quality of iris segmentation [25]

Iris images captured in the constrained environment can reflect sufficient information to discriminate them individually. In noisy environment, any iris recognition system of these types may show good recognition rate but with degrades performance.

P. M. Patil proposed in 2013 [109] a research of improved iris recognition system in low constrained environments with diverse challenges. Various iris recognition techniques have studied and provided in a certain platform for the future improvements in the iris recognition system by adding limited constrained conditions. The iris images are taken in the ideal conditions, then added some noise to distinguish an individual of another.

The noisy iris images can markedly degrading recognition accuracy by increasing the intra-individual variations. To overcome these problems, R. Gupta and A. Kumar [110] in 2013 also, proposed a segmentation technique to handle iris images captured with less constrained conditions. The technique investigated different types of noise, such as iris obstructions and specular reflection with some error percentage reductions. K-means clustering algorithm and circular Hough transform were used to localize iris boundary. Then the noisy regions were detected and isolated. In 2014, N. Kaur and M. Juneja [16] proposed an approach for iris recognition in unconstrained environment with a fuzzy C-mean clustering based technique applied as a pre-processing stage for iris segmentation. Classical edge maps detection (canny edge detector and circular Hough transform) was used with some initially added enhancement stage for more accuracy.

Nevertheless, in this approach, the addition of the two stages of clustering and enhancement increased the complexity of computations.

This method was used to localize the iris edges and to establish three main performance criteria:

- High detection ratio.
- High segmentation performance.
- Decrease false edges.

Again in 2014, Y. Chen *et al.* [111] proposed an improved iris recognition system using three feature selection strategies (orientation probability distribution function, magnitude probability distribution function and a compounded strategy combining the two methods for further selection of optimal sub-feature). A matching method based on weighted sub-region matching fusion was applied utilizing particle swarm optimization to accelerate weight determination of different sub-regions and to match their scores and generate the final decision (see Figure 2.18). Databases of the types CASIA-V3 Interval, Lamp, and MMU-V1 were tested resulting in high recognition rate. However, the process of generating the final decision may need some additional computation complexity.

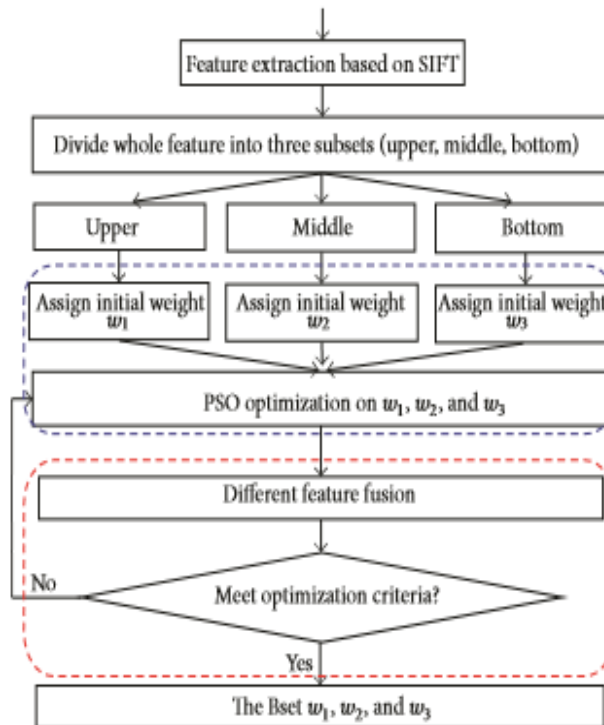


**Figure 2.18:** Block diagram for the process of weights assign with PSO [111]

By Al-Rifae, several methods were proposed in (2014) [24] for processing the iris images taken in unideal environments. The efficiency of iris recognition methods is developed. Although, they still own some difficulties in the steps of segmentation and feature extraction steps, results in a high false rejection rate (FRR) and false acceptance rate (FAR) are failures. This thesis is contained four stages:

- The first stage: he presented a new method to detect the pupil borders of individual iris and limbus with high property evaluation rules.
- The second stage: he classified the quality results from the first stage within seven various classes based on the RGB color intensity.
- The third stage: he binarized the results that detect the iris part in the first stage, and take a threshold from the second stage.
- The fourth stage: he segmented the pupil region using the (HSV) color to find the smallest pixels since the pupil includes the darkest pixels in the eye.

In 2016, Y. Fei et al. [112] proposed a performance-improvement method of unconstrained iris recognition in different environments based on domain adaptation metric learning solved by kernel matrix calculation. The optimization learning constraints in the process of iris recognition were performed using the intra-class/inter-class Hamming distance. The distance between two iris samples was redefined after computing an optimal Mahalanobis matrix for certain cross-environment system. The results indicated that this method increased the accuracy of the unconstrained iris recognition in different circumstances, highlighting improvement in the classification ability of iris recognition system (see Figure 2.19).

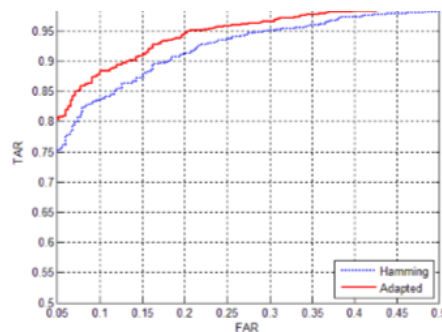


**Figure 2.19:** ROC Curve of DAML Optimized [112]

Also in 2016, M. A. M. Abdullah *et al.* [113] proposed a segmentation method for non-ideal iris images. Two algorithms were proposed for pupil segmentation in iris images captured under unconstrained condition. In addition, a fusion of an expanding and a shrinking active contour was developed for iris segmentation by integrating some pressure force to the active contour model. Such segmentation method adopted a noncircular iris normalization scheme to effectively unwrap the segmented iris. A method for closed eye detection was also given. The whole introduced recognition scheme was proved to be robust in finding the exact iris boundary and in isolating the eyelids of the iris images. Experimental results were carried out on CASIA V4.0, MMU2, UBIRIS V1 and UBIRIS V2 iris databases (see Table 2.11), indicating a high value for segmentation accuracy. Moreover, the comparative study with the current iris segmentation algorithms indicated some considerable improved accuracy with more efficient computations.

**Table 2.11:** Visual Segmentation Results of the Images in the CASIA V4, MMU2, and UBIRIS V1 Databases [113]

<b>Database</b>	<b>Correct</b>	<b>Fair</b>	<b>Bad</b>
CASIA-IrisV4-Lamp	95.1%	2.9%	2%
UBIRIS V1 Session 1	96.5%	2.2%	1.3%
UBIRIS V1 Session 2	94.4%	3.3%	2.3%
MMU2	93.7%	4.1%	2.2%

### **3. PUPIL-BASED IRIS SEGMENTATION ALGORITHM FOR VISIBLE WAVELENGTH IMAGES**

Recently, the research on iris recognition systems has been receiving increasing attention, especially in unconstrained environments. In the literature, there are many published papers aim to develop new algorithms that can segment and recognize human iris templates in visible wavelength environments. In less constrained environments, the sources of noise in eye images are significantly increased, leading to severe degradation in the iris image. As a result, the iris segmentation process has become a major issue in iris recognition, since most of the traditional iris segmentation techniques fail under such challenging conditions. In this chapter, a new segmentation algorithm is proposed to handle iris images acquired in visible wavelength environments. The proposed segmentation algorithm decreases the degradation and noise by starting to search from the most easily distinguishable region of the iris, which is the pupil. After that, the iris is localized accurately using a fast circular Hough transform. In addition, the methods which are most convenient are used to isolate the upper and lower eyelids and eyelashes from the iris region.

#### **3.1 INTRODUCTION**

Biometrics is the automated recognition of individuals by collecting features from the physical and biological characteristics of an individual. There are two features that make biometric techniques very important in our life: first, human components obtain the actual outcomes from behavioral features; and second, the human elements do not alter over time. There are many human components which are suitable for use to extract biometrics, such as the face, iris, fingers, hands, etc. [114]. The technological usage of biometrical systems is becoming stronger and stronger at the moment, and most ministry institutions, banks, airports and hospitals use biometrics in a very acceptable and effective way [115].

Among the many biometrics traits, the iris is considered as one of the most important and accurate traits that used to identify persons [116]. Our human eyes consist of five parts, as shown in figure 3.1. The iris is the object surrounded by the sclera and between the upper and lower eyelids [117], [118]. The iris biometric means the measurements that are obtained from the chromatic area of



each eye for the confirmation or identification of humans. It is very accurate since it is unique for every person, and no person has the same iris as anyone else, even in twins [119]. Another advantage of the iris is that it can be extracted only by capturing the iris image of a person from a distance [108]. Most researchers consider the extraction of the iris biometric not only from images but also through video imaging that performs the identification [120]. Furthermore, iris recognition systems are considered as the safest biometric among all biometric methods. Therefore, it is used in many public places, such as in airports, where it is employed instead of passports [121], [122].

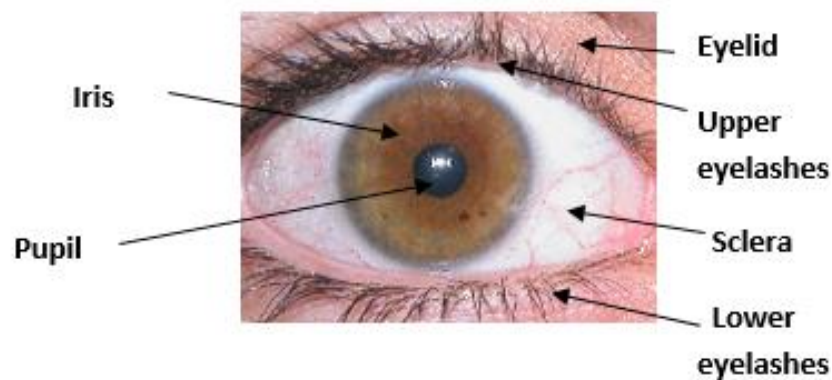


**Figure 3.1:** Parts of the human iris [29]

A classical iris recognition method usually consists of four steps: segmentation, normalization, feature extraction (encoding), and finally, matching.

In iris segmentation, the main task of the recognition system is to locate the valid and correct part of the iris, including detecting the pupil and limbic boundaries of the iris, localizing its upper and lower eyelids, and detecting and excluding any superimposed occlusions of eyelashes. The most common approach used in iris segmentation is that created by Daugman [48] and Wildes [123]. Daugman uses a sophisticated integral differential method for detecting the pupil and the iris borders. On the other hand, Wildes suggested pair levels for segmenting the iris, using Hough transformation, which is applied to verify the internal and external iris borders [124]. The segmentation step is significant for all iris recognition steps, because all the later levels depend on the segmentation stage. If any error occurs in this stage, the results will be not correct for the rest of the steps [113]. The second step in the iris recognition system is the normalization, which is

important to transform the circular shape of the segmented iris into a simpler shape. Iris recognition requires the normalization step to represent the template in a more general way and with an identical size. To normalize the iris region, we need to delete noise regions and change the iris pixels to a polar style.

The third step is the feature extraction, which is an operation of converting the normalized iris image into arithmetic values for easy handling and matching. Each iris includes unique attributes such as circles, winding collarette, etc. Many methods can be used to extract the features from an iris image, such as the Gabor filter [53], wavelet transformation [125], [126] and the two-dimensional DCT model to analyze iris texture [127]. The last step of iris recognition is the checking of the template bits that are obtained from the previous stage to decide if two iris images belong to the same person or not. The Hamming distance (HD) is a standard utilized method to check if the iris images belong to the same person or not by comparing the code bits of each image.

### **3.2 BACKGROUND ON IRIS SEGMENTATION**

The iris image is considered as one of the most accurate biological features because of its distinguishable and stable texture information, which is used for personal authentication, and therefore it is believed that iris recognition is the best method for biometric identification. As compared to other biometric technologies, iris recognition is prone to poor image quality, especially for images captured from a distance, which are afflicted by noise such as blur, off-axis, specular reflections and occlusions. The segmentation process plays a key role in iris recognition since the recognition rates are qualitatively dependent on the accuracy of the segmented iris. The accuracy of the segmentation process used to localize the iris image structure has an impact on increasing the performance of recognition systems. This is because the wrongly segmented areas in iris regions will corrupt biometric templates, causing a very poor recognition rate. Most researchers in the field of iris segmentation focus on treating the eye simply as a circular or an oval-shaped structure surrounded by the eyelids, which is not the case for iris images with conical shapes or those taken under unconstrained conditions. Under such conditions, the parameters to facilitate the process of segmentation of those images must be included. On the other hand, classical iris segmentation algorithms can provide excellent results when iris images are captured using near-infrared cameras under ideal imaging conditions. Nevertheless, when the iris images

are taken in the visible wavelength under non-ideal imaging conditions, the accuracy of these algorithms may significantly decrease. Inaccurate segmentation algorithms were reported due to the non-circular geometry of the iris and other noise factors introduced by non-cooperative conditions. That is why non-classical iris segmentation algorithms must be used for non-ideal imaging conditions.

One of the first research works on iris recognition was undertaken by Rakvic et al. He proposed an efficient iris recognition system using different steps (including a segmentation step) by utilizing field-programmable gate arrays (FPGAs), resulting in a direct and parallel processing alternative. By this execution, an increase in operational speed was offered with a potential alteration of the form factor of the resulting system. Compared to CPU-based implementations, speedup factors of 9.6 times for segmentation, 324 times for code vector creation and 19 times for matching were achieved. The researchers concluded that the proposed implementation method was rapid for iris recognition, supplying us with speedy outcomes [77].

The reliability performance of the iris biometric is highly dependent on how ideal the iris image data are. Reliable and precise segmentation is one of the most important steps in processing non-ideal iris patterns. It should be noted that non-ideal iris patterns resulting from non-ideal imagery are simultaneously affected by some factors, such as specular reflection, blur, lighting variation, occlusion and off-angle images. To handle such situations, Zuo and Schmid presented a methodology for the iris segmentation of non-ideal iris images. They confirmed the strength of their segmentation methodology via both ideal and non-ideal datasets. As a result, a considerable improvement was achieved in segmentation performance over the Camus–Wildes and Masek algorithms [79].

Proenca, H., suggested another segmentation method to deal with iris images that were taken with less constrained cases. Firstly, the sclera was handled and localized since it is considered as the easiest part of the eye. Secondly, they proposed a novel method to extract the features that represent the region of the sclera in all orientations, which were essential for the segmentation step. Finally, the procedures were implemented and made suitable for real-time applications by running the whole procedure in linear time deterministically with respect to the size of the image [80].

In 2011, Chen et al., presented a fast algorithm for accurate iris segmentation. The rough position of the iris center was found by applying an adaptive mean shift procedure. The statistical texture of the iris is modeled as a Markov random field, and then combined to establish an initial active merged contour model. Eyelids, eyelashes, shadows and reflections were simultaneously detected during the curve evolving process by labeling them in iris regions. Experimental results of various non-ideal iris images show that that the proposed iris segmentation method was effective, accurate and has low computational complexity for widely promising applications of recognition systems [82].

In 2013, Sahmoud, S. A., and Abuhaiba, I. S. proposed an adaptive algorithm to segment an iris image that was captured under non-ideal conditions. The proposed algorithm applied the K-means clustering algorithm to determine the expected region of the iris. In order to estimate the iris radius and center, the CHT (circular Hough transform) was employed. Detecting and isolating the upper eyelids was accomplished by developing a new efficient algorithm. The application of the proposed algorithm to UBIRIS iris image databases demonstrated that the segmentation accuracy and operating time were both improved [34].

In , the authors presented a scheme for iris segmentation using the circular geometry of the pupil and iris. The simulation results highlighted both the fast speed and accuracy properties of the proposed scheme when compared to other existing methods in the literature [91]. In , deep-learning schemes were employed to segment the iris region accurately. Comparisons with the previous iris segmentation algorithms showed some significant improvements over the performance of existing segmentation methods [94].

### **3.3 OUR PROPOSED SEGMENTATION ALGORITHM**

In order to simplify the iris localization process and avoid the problems of the previous iris segmentation methods, in the first step, our proposed algorithm concentrates on the darkest part of the iris, which is the pupil. Compared to the iris region, the pupil region has almost the same color (i.e., same intensity level in gray scale images) and it is usually the darkest region of the eye. After that, the exact boundaries of the pupil are determined using a simple and fast circular Hough transform. Based on the detected pupil center and radius information, the iris is localized using the circular Hough transform again. Determining the iris and pupil regions is not enough for the next

iris segmentation steps (normalization and encoding) because of the existence of different noise types in non-ideal environments, such as eyelashes, eyebrow, and luminance. To remove the noise parts from the iris region, our proposed algorithm uses two different methods for the upper and lower eyelashes and eyelids.

The overall steps of the proposed iris segmentation algorithm are described in figure 3.2. It can be seen that different morphological operations, adaptive thresholding, edge detection operators, Hough transform techniques and adaptive noise removing algorithms are applied to correctly extract the clean region of the iris. Each step is explained in more detail in the next subsections.

### 3.3.1 Determining the Candidate Pupil Region

One of the most important questions in iris segmentation algorithms is the selection of the object that will be searched first. As reviewed in Chapter 2, there are different approaches regarding the object that will be localized first in the eye image, and among them, starting to search directly for the iris region or its boundaries is a common approach. Conversely, the proposed algorithm selects the pupil of the iris to be the first object that will be localized. Our algorithm is based on the detection of the pupil region because it always has a black or dark color. On the other hand, the iris color or intensity is very unstable and widely changes between different persons, which makes it difficult to be detected.

In order to detect the pupil region, a simple adaptive image segmentation algorithm is used. The steps of this algorithm can be summarized as follows:

Compute the average intensity of the eye image (gray scale image) using the following equation:

$$I_{avg} = \frac{1}{m * n} \sum_i \sum_j P_{ij} \quad V = I.R \quad (3.1)$$

where m and n are the number of rows and columns in the eye image, respectively, while  $P_{ij}$  is the (i, j)th pixel of the eye image;

Compute the threshold that will be used to segment the eye image:

$$C_{thr} = \frac{I_{avg}}{2} - S \quad (3.2)$$

where  $S$  is a constant value that is fixed for each environment or iris database and is less than 10;

Loop over all pixels in the image and generate a binary image using the threshold computed from the previous step.

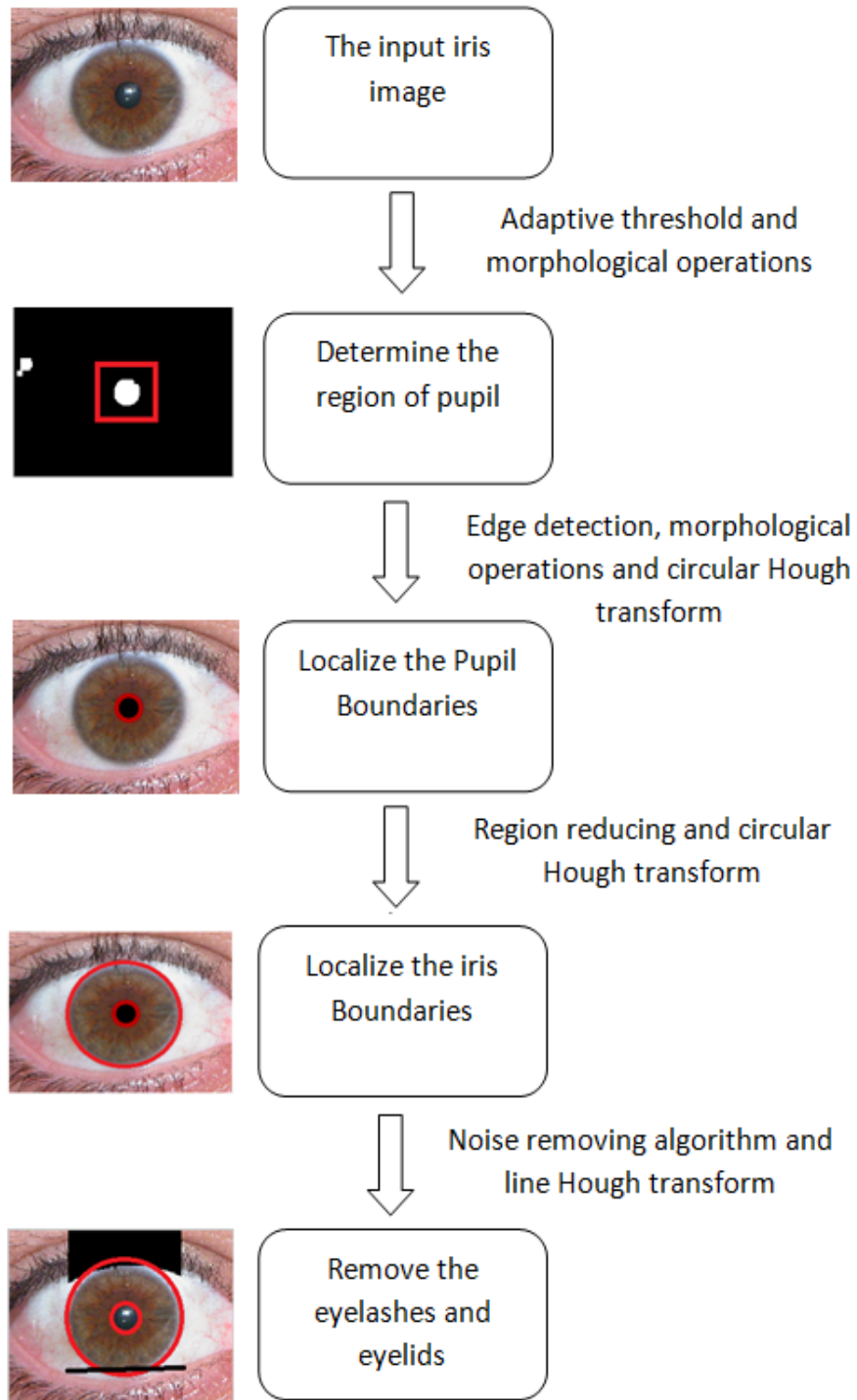


**Figure 3.2:** The main steps of the proposed iris segmentation algorithm

After applying this simple adaptive segmentation algorithm, a binary image that represents the dark regions in the eye image will be obtained. Note that the segmentation threshold is adaptively selected for each eye image based on their pixel intensities, which is much better than using a fixed value threshold that may not be suitable for all eye images in the tested image database. Figure 3.3 shows sample images from the UBIRIS v1 database after applying the adaptive segmentation algorithm on them. It can easily be noted from figure 3.3 that the sources of the dark regions on the eye image can be one of three objects, which are the pupil, the eyelashes and the eyelids. In the next step, we will explain how to handle this binary image by using different filters and operators to extract only the pupil region.

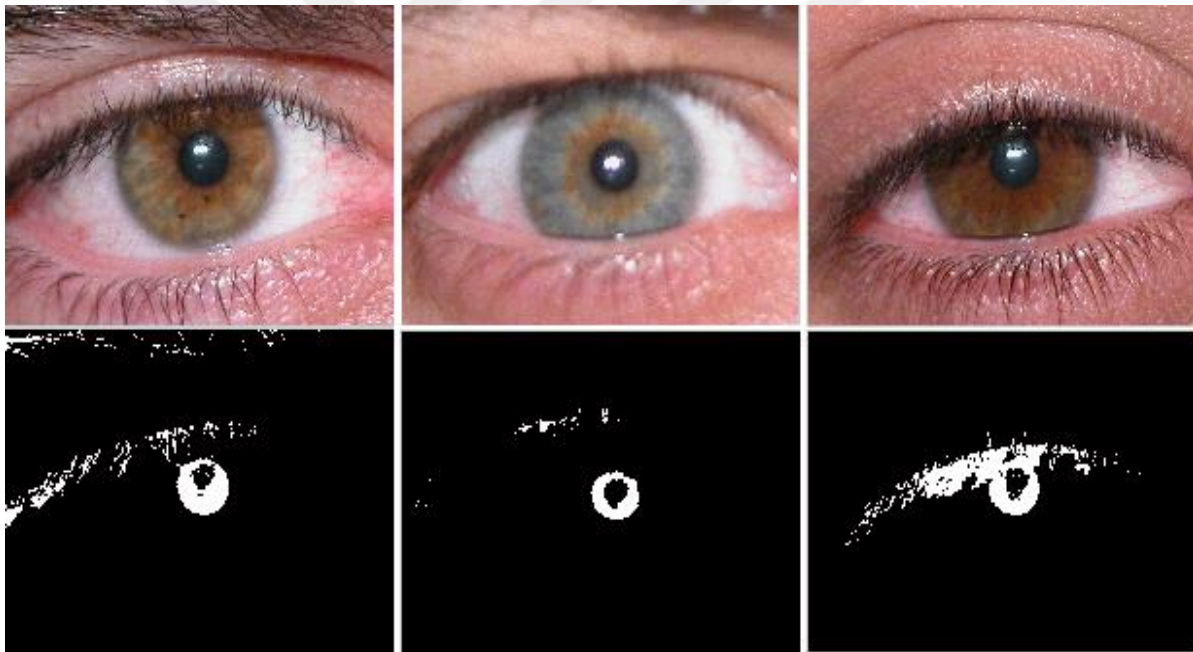


**Figure 3.3:** The main steps of the proposed iris segmentation algorithm



### 3.3.2 Localizing the Pupil Boundaries

As described before, the binary image that results from the previous step needs to be handled by many filters to extract the pupil image only. The following operations will be applied to reduce the candidate pupil region as much as possible without losing important information:

1. Delete all small blocks that have an area less than a fixed value  $A_m$ . The value of  $A_m$  can be determined according to the tested iris database, and it represents the minimum area that can be part of the pupil;
2. Fill the holes inside the remaining blocks;
3. Apply some morphological operations to smooth the remaining blocks by using erosion and dilation operations;
4. Delete the large blocks located on the boundaries of the eye image.

Figure 3.4 shows the resultant binary images before and after applying these steps. It is clear that the pupil region is detected accurately and the other dark regions on the eye image can be eliminated. After eliminating the non-pupil regions from the binary image, we obtain the candidate region of the pupil, which in some cases may include other objects as in the third image of figure 3.4. Therefore, our proposed algorithm does not depend directly on the localized region, and a Canny edge detection followed by a circular Hough transform are applied to accurately detect the boundaries of the pupil. Note that the Canny edge detection and the circular Hough transform are applied on the extracted pupil region only and not on all edges of the eye image, which significantly reduces the required processing time and decreases the error percentage.

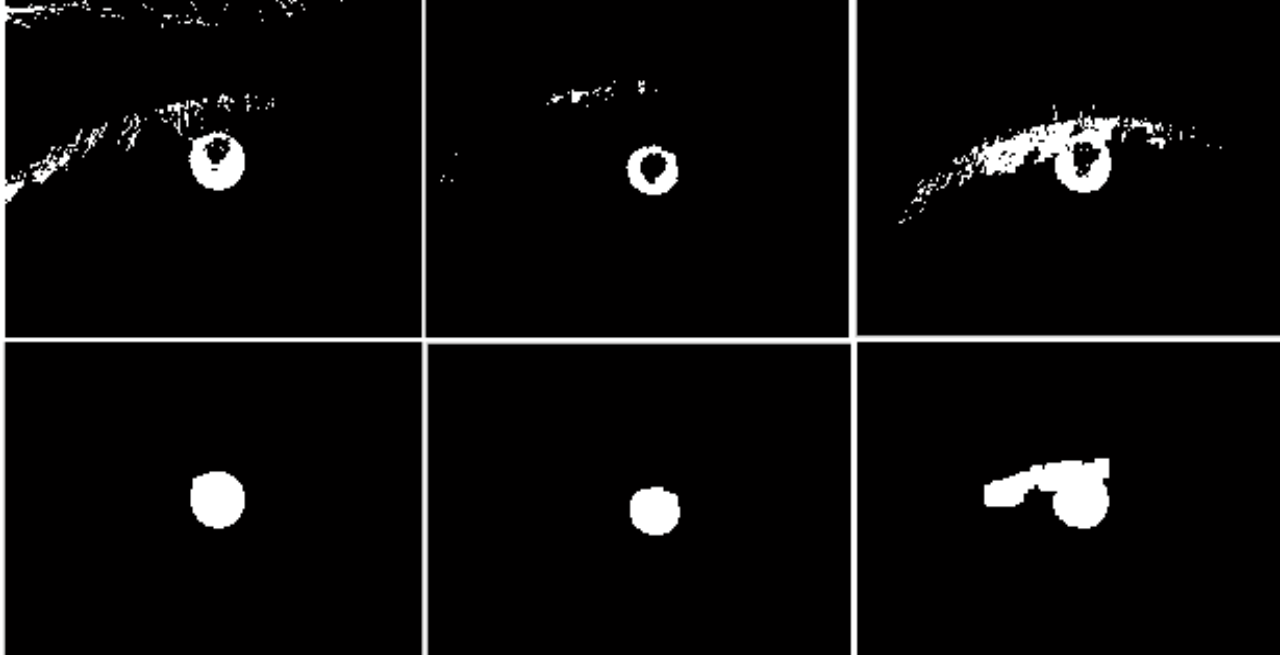


**Figure 3.4:** Eliminating the non-pupil dark regions in the proposed iris segmentation algorithm

### 3.3.3 Localizing the Iris Boundaries

In the previous step, the region of the pupil of the eye, which is located at the center of the iris region, is determined. Therefore, the localization of the iris region becomes simpler since the center of the pupil is usually very close to the iris center, or it may be identical to it. In order to reduce the search area and eliminate most of the error sources in the eye image, we reduce the searching process of the iris region on a square with a center which is the same as the pupil center and has a diameter slightly bigger than the maximum iris diameter of the testing dataset. The first row of figure 3.5 shows the selected area to be handled for the iris localization of three sample images. As shown in figure 3.5, the iris search area of our segmentation algorithm excludes many other noisy objects and regions which are the main cause of many segmentation errors in the other segmentation algorithms. To accurately localize the iris boundaries on the selected iris region, the following steps are applied:

1. Remove the upper part of the square, which usually includes the eyelid regions;

2. Apply a vertical Canny edge detection to the remaining area only;
3. Remove the small and unconnected pixels from the edge image;
4. Apply the circular Hough transform on the resulting edge image;
5. Find the best fit circle and mark it as the iris boundary.

Figure 3.5 shows the results of applying these steps on three sample eye images. It is clear that our proposed segmentation method concentrates on the relevant edge points only, as shown in the third row of figure 3.5. As a result, the proposed algorithm can work very quickly with an accurate localization of the iris edges, as shown in the last row of figure 3.5.

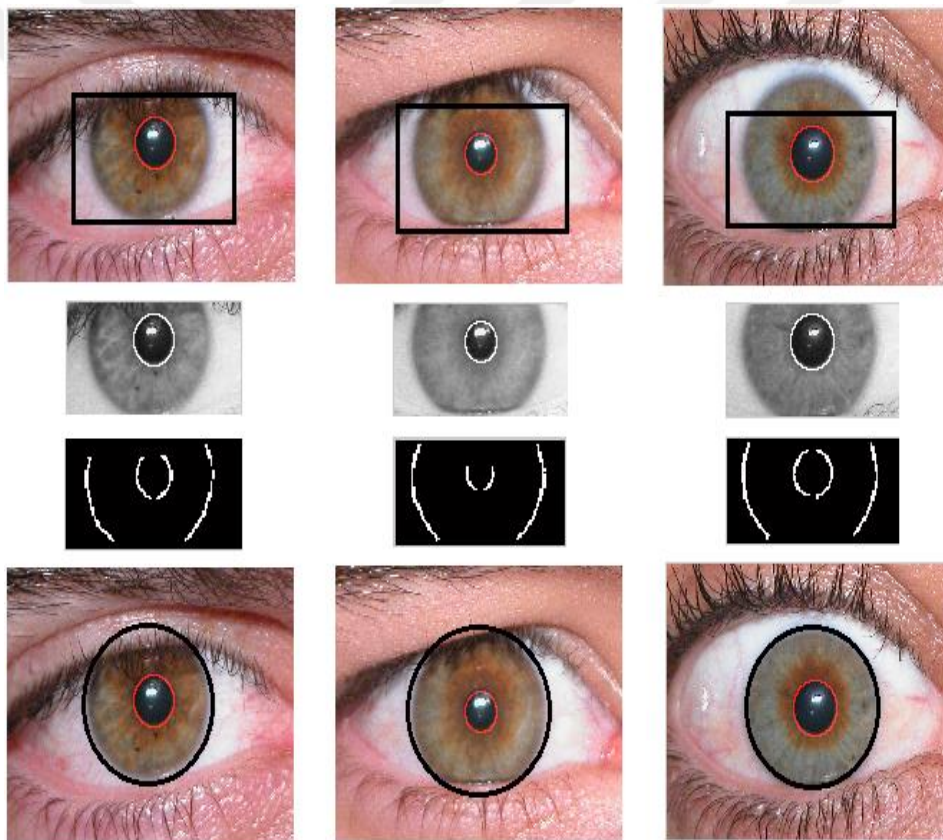


**Figure 3.5:** Iris localization steps of three selected images from the UBIRIS v1 database

### 3.3.4 Removing the Upper and Lower eyelashes and eyelids

In the unconstrained environments, many other noisy objects such as eyelids and eyelashes often cover the iris region. Passing the segmented iris to the next steps (normalization and encoding) without removing the non-iris or noisy regions causes mis-classifications in the verification or

identification tasks. Therefore, it is very important to search for all non-iris regions and isolate them from the iris region. The percentage of iris occlusion differs from image to image, but if it covers more than 50 percent of the iris region, it may degrade the biometric template and cause errors in the classification and verifications tasks even if we correctly remove all noise regions. In this research, we will not deal with the problem of degrading the biometric template because of the high occlusion parts, and we will concentrate on accurately removing the non-iris regions from the iris region.

### **3.3.5 Removing the Upper eyelashes and eyelids**

The upper eyelashes and eyelids are usually the biggest cause of iris occlusions. Furthermore, the isolation of the eyelashes and eyelids is considered one of the most difficult tasks in iris segmentation algorithms, especially when dealing with unconstrained environments. In our proposed segmentation algorithm, we use a method similar to the mechanism presented in [87]. This is because this method is very effective in dealing with unconstrained environments where most of the traditional methods do not work perfectly. The steps of the upper eyelash and eyelid removal can be summarized as follows:

1. Isolate two small rectangle images from the two sides of the localized iris circle;
2. Apply horizontal Canny edge detection to the two isolated images, and enhance the resulted binary image by morphological operations;
3. Determine the noisiest point in each side and draw an arc between them to isolate the upper eyelid. The radius and the center of the arc are determined exactly as explained in [87].

### **3.3.6 Removing the Lower eyelashes and eyelids**

The isolating of the lower eyelid of the iris is much easier than the upper eyelid. In this research work, we use the line Hough transform because the lower eyelid is usually small and in the shape of line. Firstly, an edge detection algorithm is applied on a reduced-size image that includes only the lower half of the iris. After that, the line Hough transform is applied on the edge image to search for the best line that represents the occlusion of the lower eyelid. If the maximum vote is less than a certain value, then we consider that no occlusion exists in the lower part of the iris

image. Figure 3.6 shows the results of removing the upper and lower eyelids and eyelashes from some sample iris images.

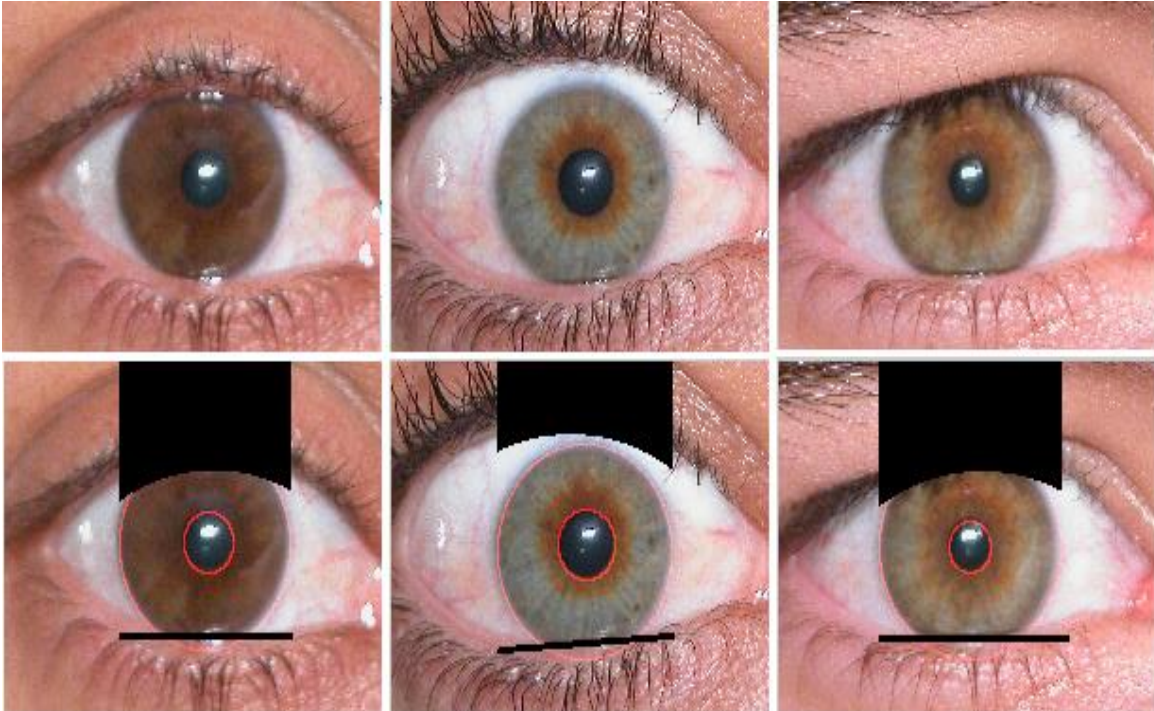


**Figure 3.6:** Removing the upper and lower eyelids and eyelashes from the iris region using images from the UBIRIS v1 database

### 3.4 RESULTS AND DISCUSSION

To investigate the performance of the proposed segmentation algorithm, it is implemented using MATLAB R2013 software. After that, the UBIRIS v1 (Session 1) [31] iris database is used to evaluate the performance of our segmentation algorithm. The UBIRIS v1 database is public and is one of the most famous databases used to test iris recognition and segmentation algorithms. The database has 1877 iris images which were collected from 241 different eyes. These were especially collected to simulate unconstrained imaging conditions. The proposed algorithm is compared with another five iris segmentation algorithms (namely, Daugman [123], Martin–Roche [87], Fourier spectral [92], Camus–Wildes [128] and Wildes [91]). The experiments were conducted on an HP

Pavilion computer with the Windows 10 operating system. The processor of the PC is core i5 with 4 GB RAM. Figure 3.7 shows some true segmented images with different iris occlusion situations. As seen in the figure, the proposed algorithm can accurately localize the pupil in the first step, and then the iris boundaries are searched for in the reduced iris candidate area, as explained in the previous section. In addition, the results show that the non-iris regions are deleted from the iris regions perfectly without affecting the important parts of the iris.

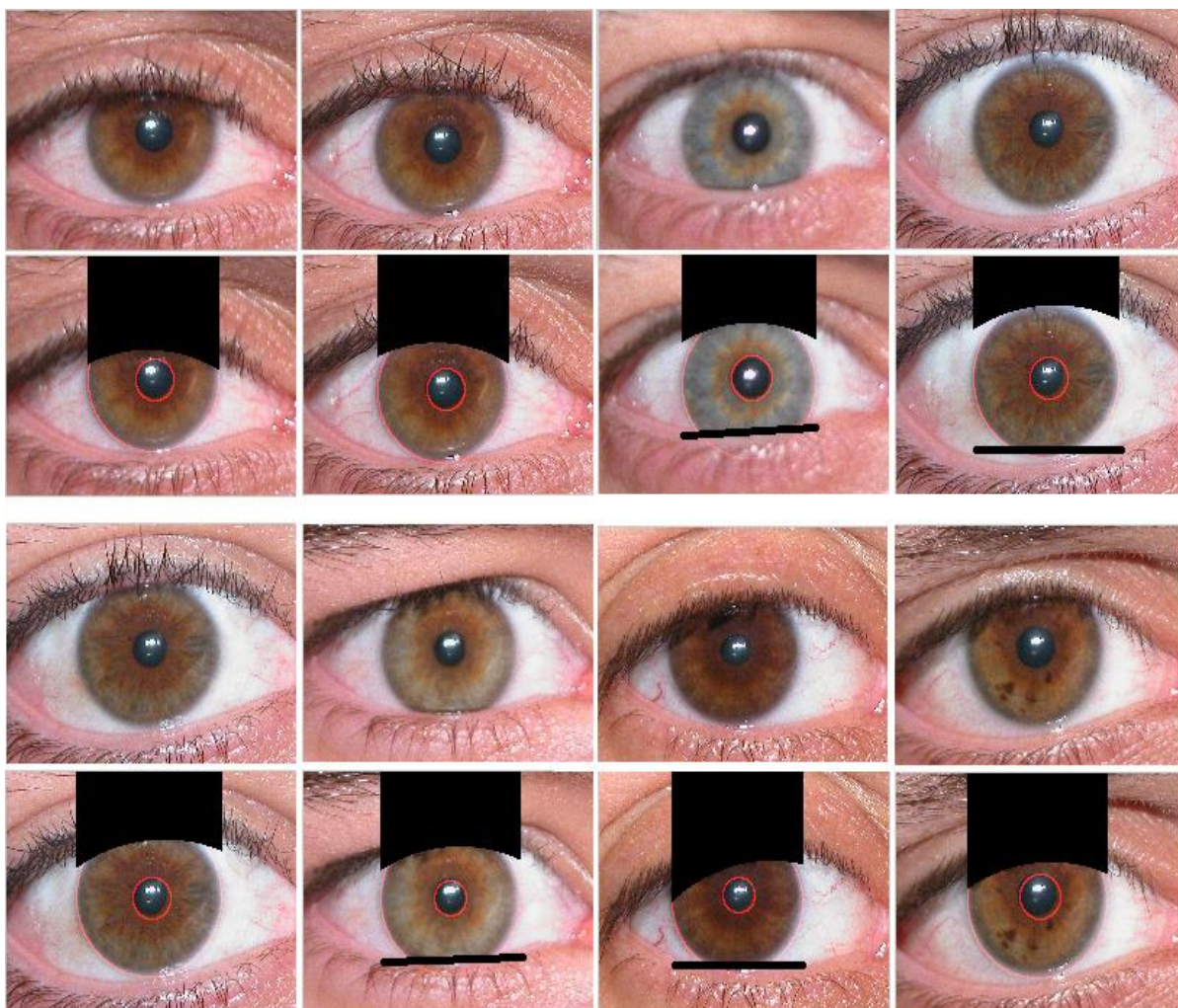


**Figure 3.7:** Sample selected images before and after applying the proposed segmentation algorithm from the UBIRIS v1 database [31]

Figure 3.8, shows some original iris images chosen from Ubiiris1 database are shown in the first row while the second row shows the same images after using CHT (Canny-Hough Transform) and reflecting correct results. The third row shows the same iris images after removing non-iris reign like the eyelids, eyelashes, reflections and pupil noises. Canny edge detection and Hough transform gives better results. Using the CHT method, most of the noise and other affects (such as light and camera movement in the iris image) can be removed.

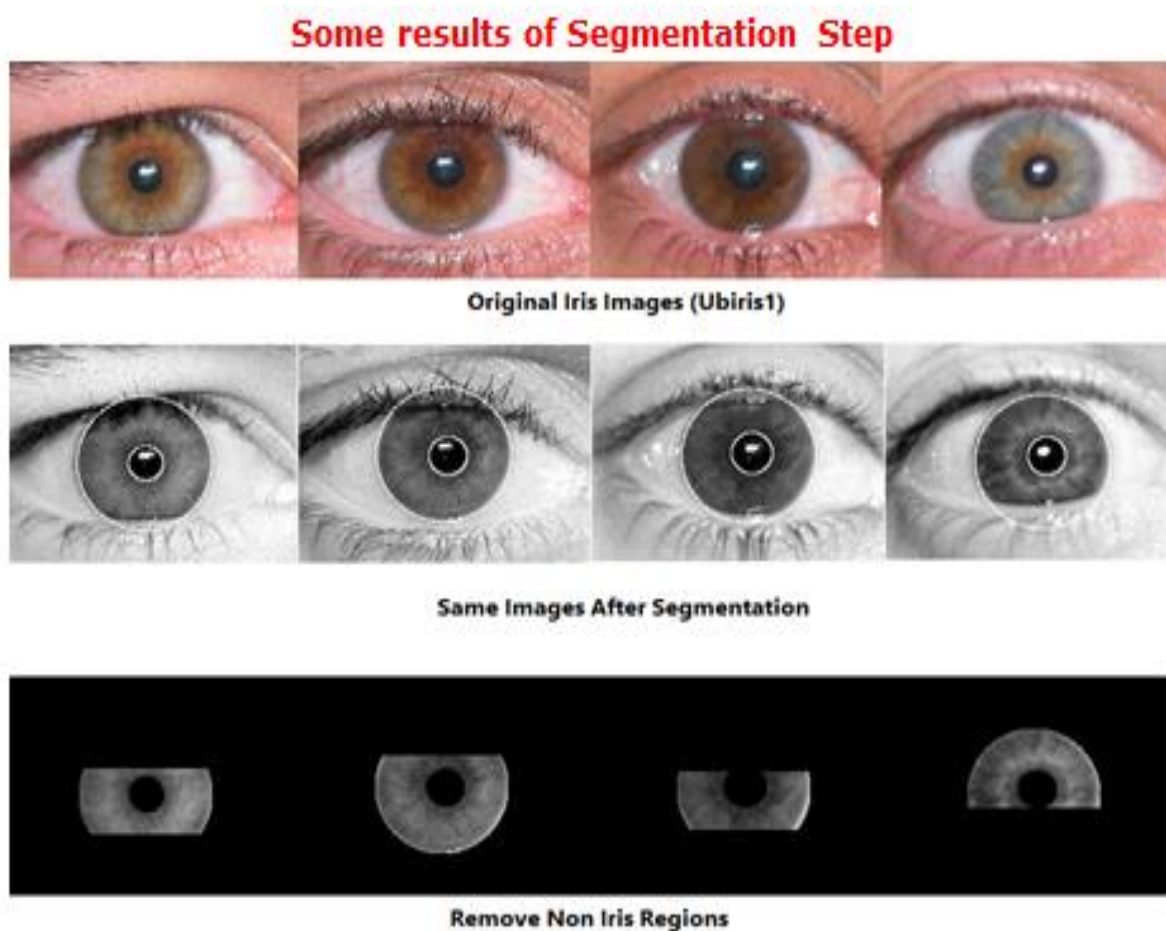


**Figure 3.8:** Sample images before and after applying the proposed segmentation algorithm steps

Table 3.1 shows a comparison between our proposed pupil-based segmentation algorithm and the other five state-of-the-art iris segmentation algorithms. The segmentation of each iris is considered to be correct if the following two conditions are satisfied: firstly, the iris and the pupil should be localized correctly by detecting the two circles that fall exactly into the iris and the pupil borders; secondly, the upper and the lower eyelid regions should be correctly determined to be eliminated from the iris image. The segmentation is considered to be wrong if one of these two conditions is not satisfied. The results show that our proposed algorithm can significantly outperform a number of segmentation algorithms and is competitive with other algorithms. Specifically, our algorithm outperforms the well-known segmentation algorithm of Daugman, since it is designed for near-infrared iris images which can more simply be segmented. The Daugman algorithm faces many difficulties when dealing with unconstrained images such as those from the UBIRIS v1 database. On the other hand, the performances of our proposed segmentation algorithm and Wildes algorithm are very close, since both of them use mechanisms that can deal with noisy eye images such as the circular Hough transform.

**Table 3.1:** Performance comparison between the proposed iris segmentation algorithm and the other five algorithms

<b>Segmentation Algorithm</b>	<b>Accuracy</b>
Daugman	95.22%
Martin–Roche	77.18%
Fourier spectral	94.47%
Camus–Wildes	96.78%
Wildes	98.68%
Proposed	98.75%

The proposed pupil-based iris segmentation algorithm cannot deal with small cases when segmenting noisy images. One such case is when eyelids or eyelashes cover a large part of the iris region. We noted that when the upper eyelid covers more than 50% of the iris region, our proposed algorithm might fail to accurately segment iris. Another case is when the lower or the upper eyelids of the eye cover parts of the pupil; this is because our segmentation algorithm mainly depends on



the pupil region to segment the iris. Figure 3.9 shows some examples of iris images that our segmentation algorithm fails to segment because one of the previous causes.

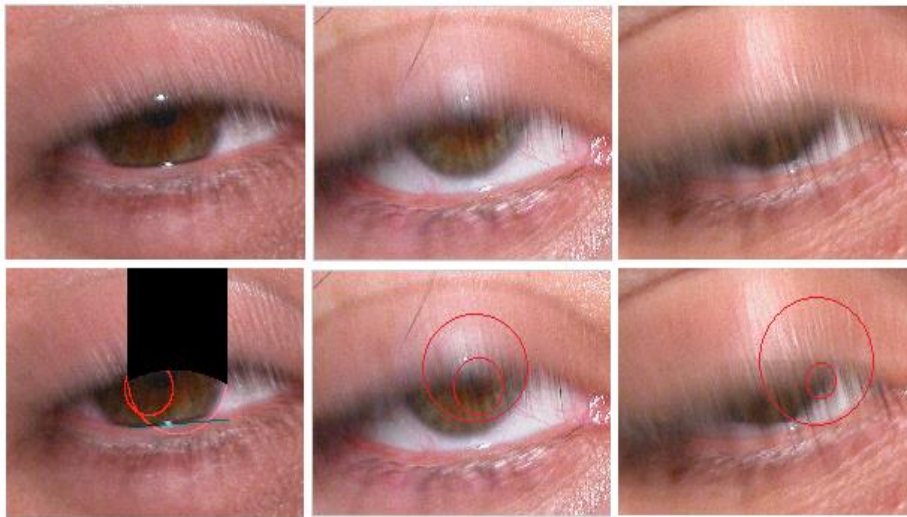


**Figure 3.9:** Sample images from falsely segmented iris images after applying the proposed segmentation algorithm

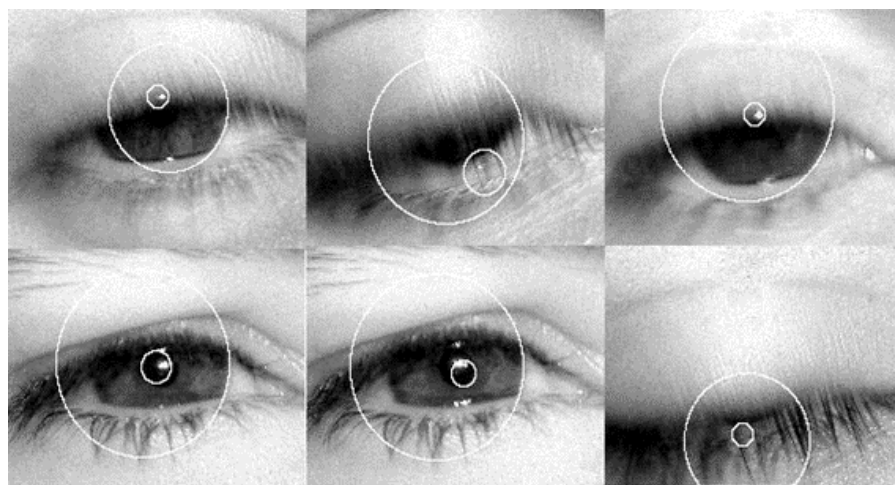


**Figure 3.10:** Sample images from falsely segmented iris images after applying the proposed segmentation algorithm

Figure 3.11 shows the rest images (11 images) with incorrect segmentation. These images have the correct detection of outer circles while all inner circles are incorrect. The total of incorrect segmented images are only 17 out of 1205 images, thus the error rate is only 1.4%.

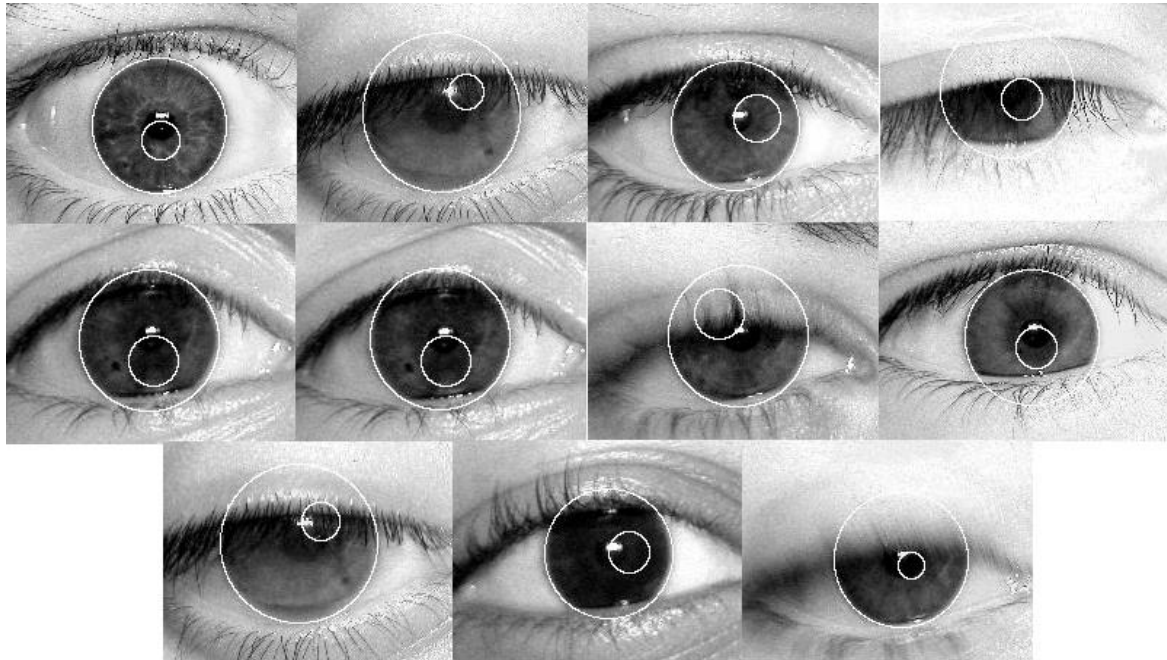


**Figure 3.11:** Sample images from falsely segmented iris images after applying the proposed segmentation algorithm

### 3.5 REVIEW OF THE CHAPTER

In less constrained environments, the sources of noise in eye images are significantly increased, which leads to the severe degradation of iris images. As a result, the iris segmentation step becomes a major issue, since most of the traditional iris segmentation techniques fail in such challenging conditions. In this chapter, a new segmentation algorithm has been proposed for handling iris images acquired in visible wavelength environments. It has been shown that the proposed segmentation algorithm can decrease the degradation and noise sources by starting to search from

the pupil, which is the most easily distinguishable region of the iris. The iris has been localized accurately using a fast circular Hough transform. In addition, other convenient methods have been used to isolate the upper and lower eyelids and eyelashes from the iris region. The proposed algorithm has been compared with a number of state-of-the-art segmentation algorithms using the UBIRIS database, and the results validate the effectiveness of the proposed algorithm against the others.



## **4. THE NEW PROPOSED IRIS RECOGNITION SYSTEM BASED ON CCT-LIKE MASK FILTER BANK**

Recently, several methods have been developed for iris recognition. Most of those methods were designed for frontal and high-quality iris images. Among them, the most widely known is Daugman's approach, which is still used in most commercialized iris recognition systems [96]. After the work of Daugman, many other research papers are presented to deal with many challenges of the iris recognition systems. In this chapter, a new personal identification method based on unconstrained iris recognition is presented. We apply a nontraditional step for feature extraction where a new circular contourlet filter bank is used to capture the iris characteristics. This idea is adopted from a new geometrical image transform called the circular contourlet transform (CCT). The CCT transform provides both multiscale and multi-oriented analysis of iris features. In the proposed recognition system, only five out of seven elements of the gray level co-occurrence matrix are required in the creation of the feature vector, which leads to a further reduction in computations. In addition, the highly discriminative frequency regions due to the use of circular-support decompositions can result in highly accurate feature vectors, reflecting good recognition rates for the proposed system. The proposed system has encouraging performance in terms of high recognition rates and a reduced number of elements of the feature vector. This reflects reliable and rapid recognition properties. In addition, some promising characteristics of the system are apparent since it can efficiently be realized with lower computation complexity. The proposed iris recognition method is a modified version of the classical iris recognition method, which usually consists of four steps: segmentation, normalization, feature extraction and coding, and matching. A new identification method is achieved by applying a nontraditional step for feature extraction (where a new filter bank of CCT filters is used to capture the iris characteristics). It is known that 2D filters are widely used for various types of image processing and analysis. Although the classical 2D discrete wavelet transform(2DDWT)is known to be a powerful tool in many image processing applications such as compression, noise removal, image edge enhancement, and feature extraction, 2D DWT is not optimal for capturing the 2D singularities found in images and often required in many segmentation and compression applications. In particular, natural images consist of edges that are smooth curves, which cannot be captured efficiently by the classical 2D wavelet transform. Thus, more effective methods for 2D singularity-

capturing transforms have been developed. One of the most recent transformation methods is the 2D elliptical-support wavelet transform (2DESWT), which was efficiently used as the main feature extractor in a recent method for iris recognition [106]. Another attempt at a geometrical image transform is the 2D circular-support wavelet transform (2D CSWT) [129] which can efficiently represent images using circular split 2D spectral schemes (circularly decomposed frequency subspaces). The designed 2D filters using circular-support schemes can function as a 2D wavelet filter bank. One of the main benefits of circular-support schemes is that they can possess better performance than rectangular-support schemes when it is desired to extract as much low-frequency information as possible in a 2D low-pass filtering channel (or as much high-frequency information as possible in a 2D high-pass filtering channel) [130]. It was shown in [129] that the 2D circular-support decomposition scheme can effectively improve the operation of extracting both approximation and detail coefficients from original images using 2D circular filters instead of using the traditional two-stage 1D filter decomposition in the classical 2D discrete wavelet transform. Therefore, it is believed that a new type of multiscale decomposition can be achieved in this thesis using 2D circular support frequency decomposition regions, which can serve as highly discriminated regions, while the iris features will accurately represent all iris image contents at the right scale. The filters of the 2D circular-support wavelet transform can be simply realized by frequency-masking filters with shapes just like the 2D circular-support regions in different scales. This reflects simplicity in realizing the processing system in addition to its accuracy. Nevertheless, wavelets may not be the best choice for representing natural images (such as those of the iris). This is due to the fact that wavelets are blind to the smoothness along the edges commonly found in images and always lack texture orientation information. Hence, the use of the contourlet transform [131, 132] is preferred in this paper to identify iris features as it offers both the important properties of anisotropy scaling and directionality. The contourlet transform is often used in image processing (such as image denoising, compression, etc.) [133–31]. In the classical contourlet transform (CT), a double-stage filter bank structure is usually considered: a stage of subband decomposition followed by a directional transform. A Laplacian pyramid (LP) is employed for the first stage, while directional filter banks (DFBs) are used in the second stage of angular decomposition. A comparison between the contourlet shows the improved edge contours due to both the multiscale and multi orientation decompositions of the latter [132].

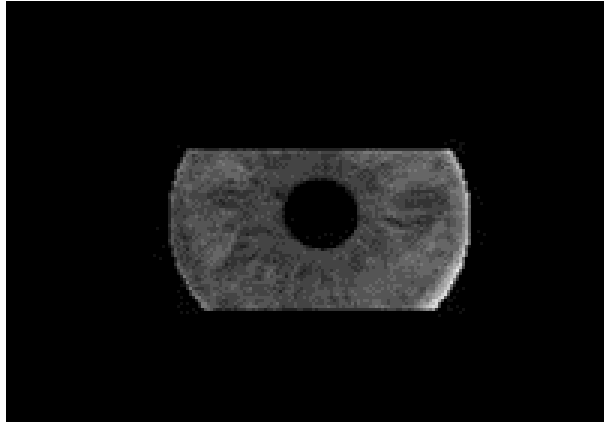


**Figure 4.1:** Iris image after segmentation step

#### **4.1 FEATURE VECTOR EXTRACTION AND CODING STEP**

As mentioned before, the CCT is applied in the feature extraction stage of this iris recognition system. A simple frequency-masking filter bank can be used to realize the CCT with circular contourlet-like shapes simulating the CCT's two filtering stages of multiscale and multidirectional decompositions. This reflects the simplicity of realization of the processing system. In addition, the new type of multiscale decomposition can be achieved by the use of circular-support decomposition regions, which can serve as highly discriminative frequency regions, giving some accurate features of the iris image by the correct representation of all its contents at the right scale and the right orientation. This can result in high accuracy values for the proposed less-complex iris recognition system.

In the previous section, iris segmentation with de-noising and normalization stages was detailed. By performing de-noising, the unimportant black pixels of the segmented image were deleted in order to reduce the number of processed pixels, thus increase the processing speed. In this section, feature extraction and coding is discussed. A 2-D FFT is applied on the normalized image. A block diagram of the proposed system is shown in Figure 4.2. The time-frequency conversion in Figure 4.2 is accomplished by using a 2-D FFT after the normalization step. Before that, in the normalization step itself, the well-known rubber sheet model was applied to convert the isolated radial area into a rectangular area.

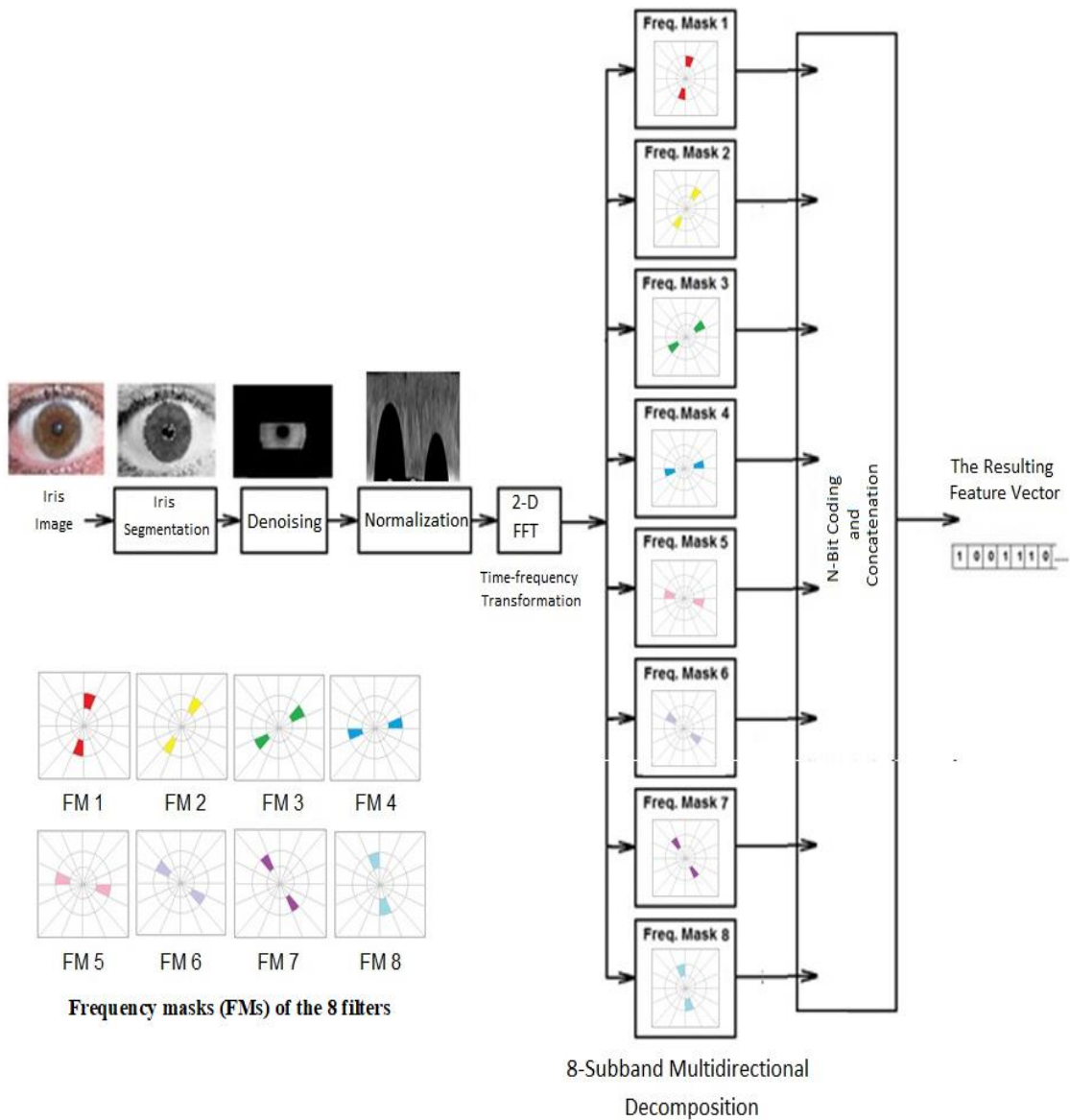


**Figure 4.2:** Block diagram of the proposed system

As shown in Figure 2, eight filters with frequency masks (FM 1–FM 8) were multiplied with the 2-D FFT of the image; thus, eight resulting components were obtained. For each component, seven features were calculated by using the following formulas of the GLCM [136].

$$Energy = \sum_i \sum_j P(i, j)^2 \quad (4.1)$$

$$Contrast = \sum_{n=0}^{N_g-1} n^2 \left[ \sum_{i=1}^{N_g} \sum_{j=1}^{N_g} P(i, j) \|i - j\| = n \right] \quad (4.2)$$

$$Correlation = \frac{\sum_i \sum_j (ij) P(i, j) - \mu_x \mu_y}{\sigma_x \sigma_y} \quad (4.3)$$

$$Homogeneity = \sum_i \sum_j \frac{1}{1+(i-j)^2} P(i, j) \quad (4.4)$$

$$Autocorrelation = \sum_i \sum_j (ij) P(i, j) \quad (4.5)$$

$$Dissimilarity = \sum_i \sum_j |i - j| P(i, j) \quad (4.6)$$

$$Inertia = \sum_i \sum_j (i - j)^2 P(i, j) \quad (4.7)$$

The physical values in the formulas (4.1)–(4.7) are usually calculated for each of the eight outputs of all circular multiscale and multi-orientation mask filters. Instead, in this research, the following algorithms represent both processes of the iris image feature extraction and bit-coding of features.

A) Algorithm for constructing features from an iris image:

- 1- Read image after completing the segmentation step.
- 2- Remove the boundary around the iris.
- 3- Convert iris from polar coordinates to rectangular coordinates.
- 4- Perform the 2-D Fast Fourier transform (FFT).
- 5- Perform the FFT shift to center all the frequencies on the 2-D spectrum sheet.
- 6- Convert filter masks into binary.
- 7- Multiply (pixel-based) the 2-D spectrum sheet of the iris image by the filter mask.



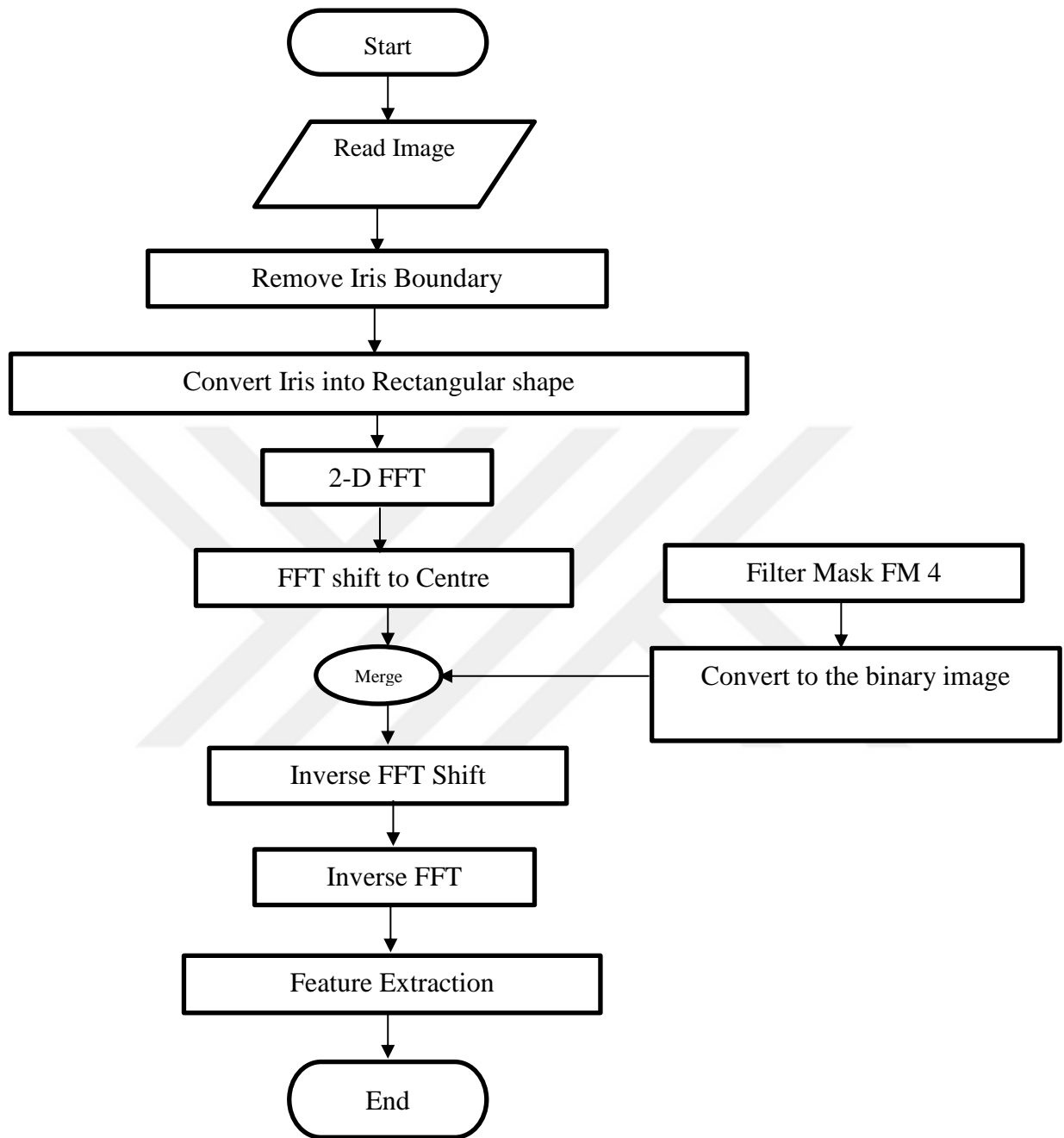
- 8- Apply the inverse FFT shift.
- 9- Perform the inverse Fourier transform.
- 10- Execute a feature extraction step.

Figure 4.3 shows the flow chart for constructing features from iris images. Many tests were performed in order to choose a good combination (concatenation) of useful outputs of different filter masks among the group of eight filter masks shown in Figure 2. Fortunately, filter mask FM 4 is the only one that displayed the best feature characteristics. Figure 4.4 shows the block diagram of a reduced-complexity system using the single filter mask FM 4, resulting in a single component with only five required elements, rather than all seven elements of the GLCM, described by Equations (1)–(7). These elements are energy, autocorrelation, dissymmetry, inertia, and contrast, as shown in Figure 4.4. The five outputs from these elements are coded and concatenated to form the final feature vector representing the input iris image characteristics.

B) Algorithm for binary-bit coding and feature vector creation:

- 1- Read all elements.
- 2- Normalize all element values to match 10-bit codes.
- 3- Remove the least significant bit (LSB) from all coded features to form reduced-length features.
- 4- Concatenate the reduced-length feature bits resulting from using five out of the seven elements of the calculated GLCM matrix. The elements are
  - Energy (repeated twice)
  - Autocorrelation (repeated twice)
  - Dissymmetry
  - Inertia
  - Contrast (repeated twice)
- 5- Generate a final feature vector with code length  $(9*5) + (9*3) = 72$  bits.

Figure 4.5 shows the flow chart for binary-bit coding and feature vector creation with reduced length.



**Figure 4.3:** Flow chart for constructing features from iris images

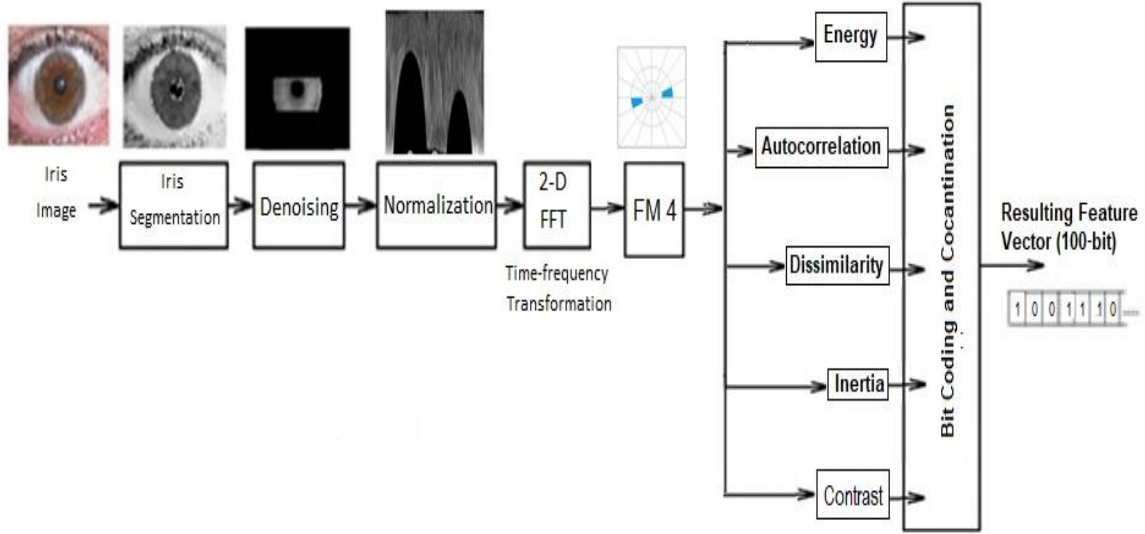


**Figure 4.4:** Block diagram of a reduced system

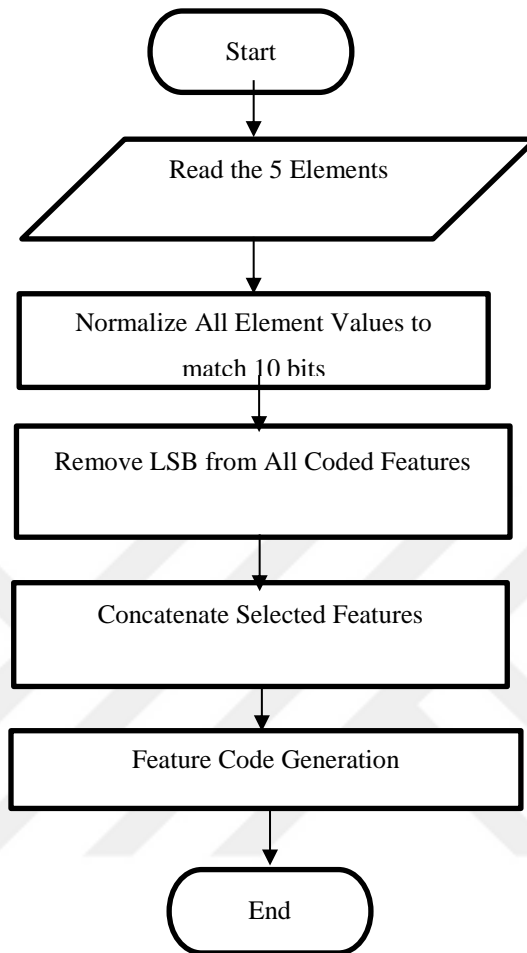


**Figure 4.5:** Flow chart for reduced-length bit-coding and feature vector creation

Over many experiments, what code number is better for greater accuracy was tested while keeping the vector length as short as possible. To accomplish this, tests were performed on the iris images of the UBIRIS V1 dataset [32]. Some samples of results before the standard normalization of values are shown in Table (4.1), while Table (4.2) shows the same results after the standard normalization of all values. Table (4.3) shows the decimal values corresponding to 10-bit implementation (from 0 to 1023) of the normalized values from Table (4.2).

**Table 4.1:** Some samples of UBIRIS V1 images before standard normalization

<b>BIRIS V1 images</b>	<b>Energy</b>	<b>Autocorrelation</b>	<b>Dissimilarity</b>	<b>Inertia</b>	<b>Contrast</b>
<b>1c1</b>	<b>0.00018</b>	<b>4022660</b>	<b>41399.09</b>	<b>2077427</b>	<b>1585.313</b>
<b>2c1</b>	<b>0.000189</b>	<b>2643074</b>	<b>32358.39</b>	<b>1515701</b>	<b>1475.183</b>
<b>3c1</b>	<b>0.000214</b>	<b>5746313</b>	<b>62089.54</b>	<b>3150226</b>	<b>1779.461</b>
<b>4c1</b>	<b>0.000247</b>	<b>6678443</b>	<b>64931.67</b>	<b>3204912</b>	<b>1625.245</b>
<b>5c1</b>	<b>0.000212</b>	<b>4750258</b>	<b>42900.11</b>	<b>2069054</b>	<b>1387.804</b>

**Table 4.2:** Some samples of UBIRIS V1 images after standard normalization

<b>UBIRIS V1 images</b>	<b>Energy</b>	<b>Autocorrelation</b>	<b>Dissimilarity</b>	<b>Inertia</b>	<b>Contrast</b>
<b>1c1</b>	<b>0.483013</b>	<b>0.623229</b>	<b>0.275148</b>	<b>0.276718</b>	<b>0.392763</b>
<b>2c1</b>	<b>0.301924</b>	<b>0.342782</b>	<b>0.158636</b>	<b>0.135048</b>	<b>0.259907</b>
<b>3c1</b>	<b>0.226875</b>	<b>0.270072</b>	<b>0.541797</b>	<b>0.547284</b>	<b>0.626975</b>
<b>4c1</b>	<b>0.495109</b>	<b>0.346534</b>	<b>0.578425</b>	<b>0.561076</b>	<b>0.440935</b>
<b>5c1</b>	<b>0.758223</b>	<b>0.80929</b>	<b>0.294493</b>	<b>0.274607</b>	<b>0.154496</b>

**Table 4.3:** Decimal values corresponding to 10-bit implementation of the normalized values

<b>UBIRIS V1 images</b>	<b>Energy</b>	<b>Autocorrelation</b>	<b>Dissimilarity</b>	<b>Inertia</b>	<b>Contrast</b>
<b>1c1</b>	<b>483</b>	<b>623</b>	<b>404.4</b>	<b>406</b>	<b>393</b>
<b>2c1</b>	<b>302</b>	<b>343</b>	<b>194.1</b>	<b>173.8</b>	<b>260</b>
<b>3c1</b>	<b>227</b>	<b>270</b>	<b>401.3</b>	<b>394.4</b>	<b>627</b>
<b>4c1</b>	<b>495</b>	<b>347</b>	<b>640</b>	<b>677.2</b>	<b>441</b>
<b>5c1</b>	<b>758</b>	<b>809</b>	<b>692.7</b>	<b>753.4</b>	<b>154</b>

From Table (4.3), it appears better to repeat the bits of energy twice, autocorrelation, and contrast, resulting in a final 72-bit-length feature vector. Table (4.4) shows the 72-bit codes resulting from concatenating individual codes representing the decimal values of energy (repeated twice), autocorrelation (repeated twice), dissimilarity, inertia, and contrast (repeated twice) for each sample of UBIRIS V1 images in Table (4.3).

**Table 4.4:** Final 72-bit-length feature vectors of UBIRIS V1 images of Table (4.3)

UBIRIS V1 images	Final 72-bit-length feature vector
1c1	0110001000110001000010101000010101000010100101010001001010001010010001010010001010
2c1	0100000100100000100011101000011101000011101000010001001001111001000011001000011
3c1	100111001100111001011001111101100111100011101100001111100010001100010001
4c1	0110111000110111001010010011010010011010111101001000011000110001000100011000
5c1	0010011010010011010110010000110010000110011000010010011010001001010001001010001001

The Hamming distance (HD) matching algorithm was used to simulate the iris feature vector matching. This matching algorithm is shown by the flow chart in Figure 4.6.

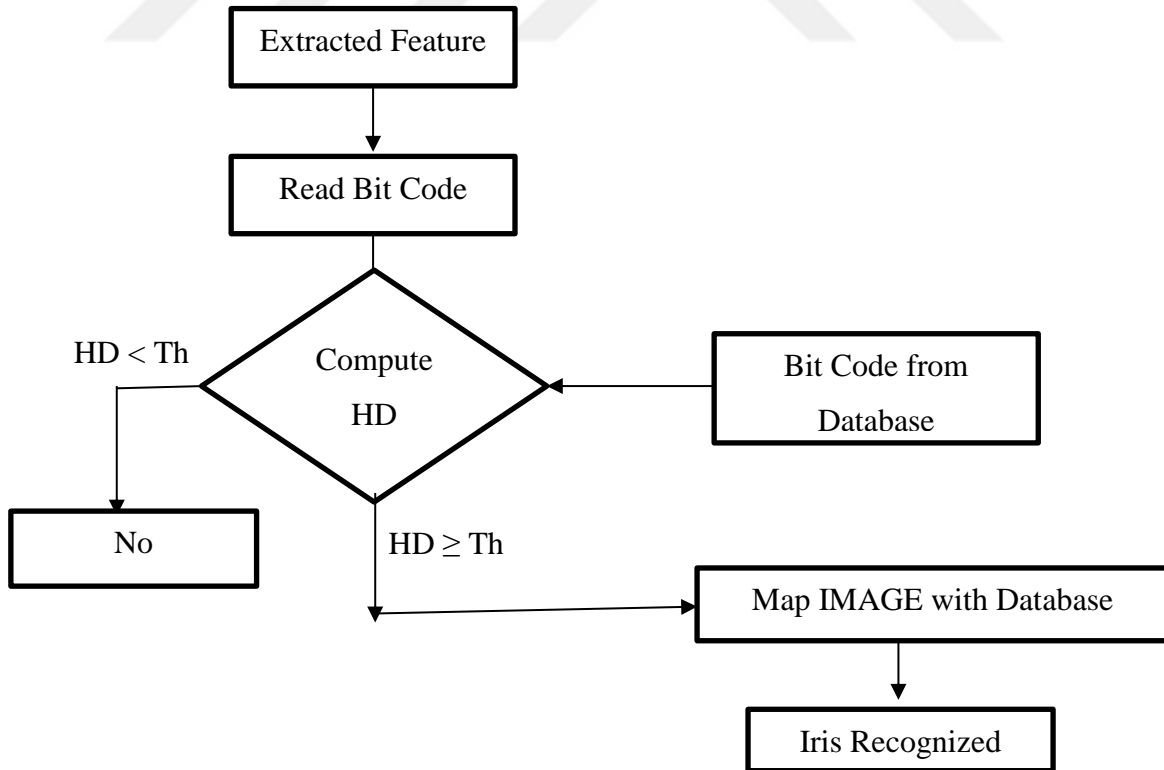
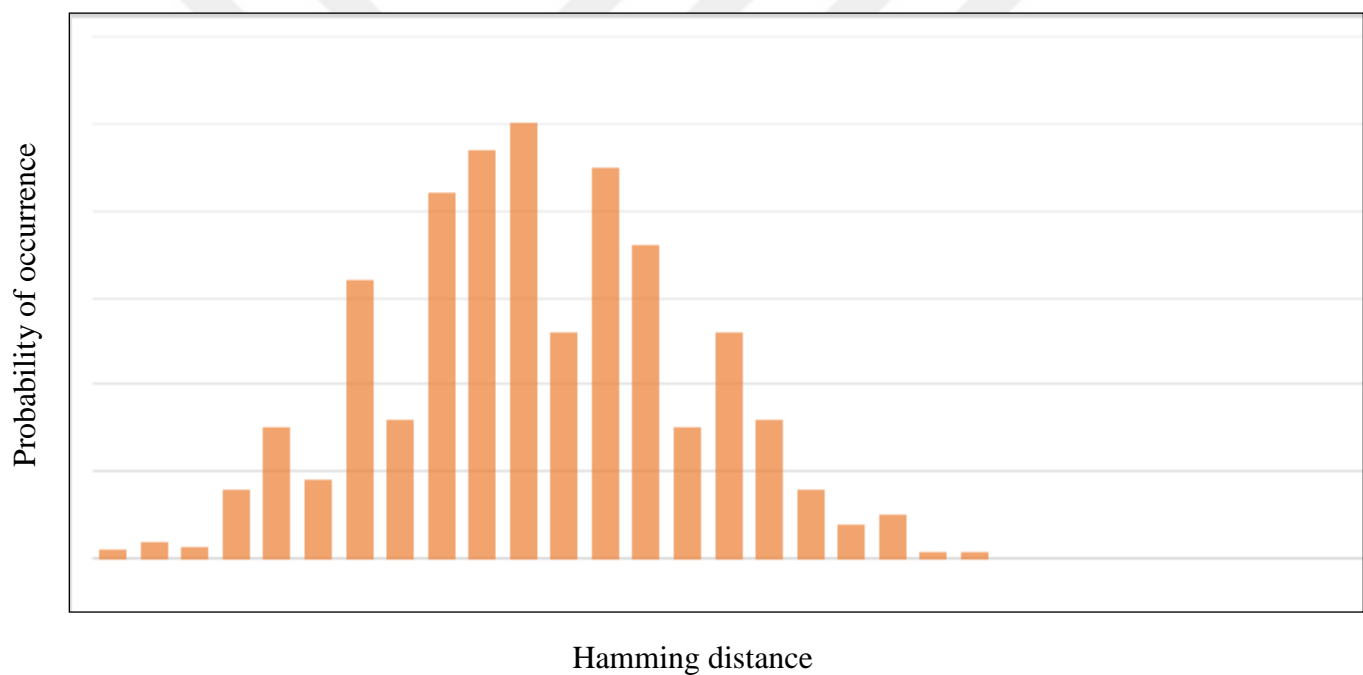


**Figure 4.6:** Flow chart of the HD matching algorithm

In Figure 4.6, the inter- and intra-class Hamming distances (HDs) were computed between the feature vectors of the input irises and the feature vectors of the database irises for 2000 iris images. Figure 4.7 shows both the inter-class and intra-class distributions, appearing with a threshold  $Th = 0.46$ . For the recognition phase, the following rules were applied:

*If  $HD \geq Th$ , then the iris is recognized and image is mapped to the database;*

*If  $HD < Th$ , then the iris is not recognized.*



**(a) Inter-class distribution.**



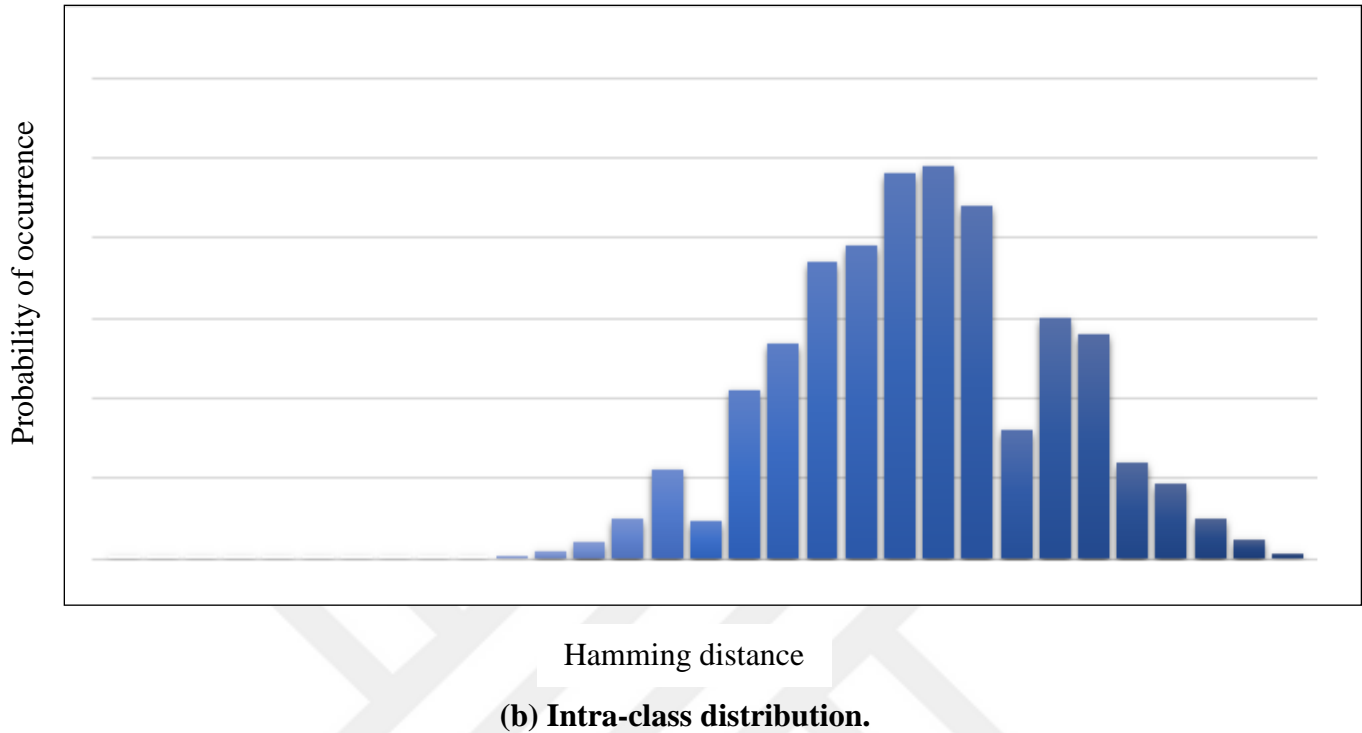


**Figure 4.7:** inter-class and intra-class distributions

## 4.2 RESULTS AND DISCUSSION

A comparative study between different methods of iris recognition is summarized in Table (4.5). This comparison is based on the kind of utilized dataset, the applied method for feature extraction, the resulting feature vector length (in bits), the type of matching algorithm, and the achieved percentage rate of accuracy.

From Table (4.5), it can be seen that the resulting recognition rate of the proposed method is of the same order compared to those of the other illustrated methods, whereas the system is superior in the sense of the feature vector length (72 bits), reflecting a rapid recognition process. In addition, a single sub-band out of eight is needed in constructing the CCT, while five out of seven elements of the GLCM are sufficient for feature vector creation. Both reductions imply a less complex recognition system with fewer computations. In addition, an important thing to remember is that the tested UBIRIS V1 dataset is of the type containing iris images captured in an unconstrained

environment, which means that the proposed system is an efficient unconstrained iris recognition system.

**Table 4.5:** Comparison of the proposed methods with some known methods

Method	Dataset	Feature Extraction Method	Feature Vector Length (Bits)	Matching Algorithm	Rate of Accuracy %
Daugman [96]	UBIRIS v1	Gabor wavelets	2048	HD	95.2
Martin-Roche[138]	UBIRIS v1	Gabor wavelets	2048	HD	77.81
[137]	CASIA v1	NSCT with GLCM	490	SVM	96.3
Our proposed	UBIRIS v1	CCT (using Single Sub-band) with GLCM (with 5 out of 7 Elements)	72	HD	96.2

### 4.3 CHAPTER CONCLUSIONS

An efficient unconstrained iris recognition system has been proposed in this thesis using the circular contourlet transform (CCT) to extract 2-D anisotropic oriented features from degraded iris templates rather than using classical methods based on textural analysis wavelet transform or even the classical contourlet transform (CT). Multiscale characteristics are usually noticed in iris images due to the improper alignment of eyes in front of cameras, while multiphase characteristics are noticed from the differently oriented curves in iris images. CCT sub-band decomposition has been proposed because of the multiscale and multidirectional properties of the iris feature vectors. CCT decomposition has been applied to UBIRIS V1 iris images (the iris image is treated as a pattern that is rich with multiphase and multiscale characteristics). While performing matching, the

resulting feature vectors has been proved to give a comparable recognition rate with rapid recognition, since only a reduced feature vector length of 72 bits has been required. In the phase of constructing the CCT filter bank, a single sub-band out of eight has been considered enough to cover most feature characteristics of iris images, while only five out of seven elements of the GLCM have been required for feature vector creation. Both reductions result in a less complex recognition system with fewer computations. This reflects a reduced-complexity implementation of the whole recognition system. Also, the required CCT sub-band filter has been easily realized by masks, again highlighting a greater reduction in the realization requirements of the whole recognition system. Finally, in the process of simplifying the whole system, it has been noticed that due to the multiscale characteristics of the CCT, no highly accurate segmentation process is needed.

## 5. CONCLUSION

In this thesis, we focused on enhancing the iris recognition systems by considering the problems of the unconstrained iris recognition problems. These problems cause that high error rate due to increasing number of noise sources in eye images, which leads to a degradation in the segmentation and feature extraction processes. As a result, the iris segmentation and feature extraction steps have become major issues in unconstrained iris recognition systems, since most of the traditional iris segmentation techniques fail under such challenging conditions. Firstly, a new segmentation algorithm has been proposed for handling iris images acquired in visible wavelength environments. It has been shown that the proposed segmentation algorithm can decrease the degradation and noise sources by starting to search from the pupil, which is the most easily distinguishable region of the iris. The iris has been localized accurately using a fast circular Hough transform. In addition, other convenient methods have been used to isolate the upper and lower eyelids and eyelashes from the iris region. The proposed algorithm has been compared with a number of state-of-the-art segmentation algorithms using the UBIRIS database, and the results validate the effectiveness of the proposed algorithm against the others.

Secondly, an efficient unconstrained iris recognition system has been proposed in this thesis using the circular contourlet transform (CCT). Its main idea is to extract 2-D anisotropic oriented features from degraded iris templates rather than using classical methods based on textural analysis wavelet transform or even the classical contourlet transform (CT). CCT decomposition has been applied to UBIRIS V1 iris images (the iris image is treated as a pattern that is rich with multiphase and multiscale characteristics). While performing matching, the resulting feature vectors have been proved to give a comparable recognition rate with rapid recognition, since only a reduced feature vector length of 72 bits has been required. Finally, in the process of simplifying the whole system, it has been noticed that due to the multiscale characteristics of the CCT, no highly accurate segmentation process is needed.

In future work, we are planning to apply our proposed segmentation and feature extraction methods on more databases. Moreover, enhancing the proposed algorithms to be able to deal with more unconstrained scenarios is another open research topic [139]. Recently, there are many new biometric based recognition systems proposed such as [140], [141], [142], and [143], we are planning to use them to enhance our recognition system.

## REFERENCES

- [1] <https://www.nap.edu/read/12720/chapter/2> (6-5-2019)
- [2] Biometrics: a guide Government office of science (6-5-2019)
- [3] <http://chillelife.com/biometric-security-system/> (13-5-2019)
- [4] A. Jain, L. Hong and S. Pankanti, "Biometric Identification," Communications of the ACM, Vol. 43, No. 2, 2000, pp. 90-98. <http://dx.doi.org/10.1145/328236.328110>
- [5] A. Babich, (2012). "Biometric Authentication. Types of biometric identifiers". Bachelor's Thesis. University of Applied Science. 2012.
- [6] <https://www.techopedia.com/definition/10239/biometrics/> (13-5-2019)
- [7] <https://biometrictoday.com/10-advantages-disadvantages-biometrics-technology/> (13-5-2019)
- [8] <https://www.iritech.com/blog/biometric-accuracy-evaluation/> (13-5-2019)
- [9] <https://www.information-age.com/are-biometrics-scalable-275496/> (13-5-2019)
- [10] <https://www.planetbiometrics.com/article-details/i/5257/desc/flexenable-to-reveal-smartcard-with-500-dpi-flexible-fingerprint-sensor/> (15-5-2019)
- [11] <https://www.veridin.com/blog/5-advantages-of-biometric-security-systems/> (7-5-2019)
- [12] <https://biometrictoday.com/types-of-biometrics/> (7-5-2019)
- [13] Charfi, N. (Doctoral dissertation, Ecole nationale supérieure Mines-Télécom Atlantique). "Biometric recognition based on hand shape and palmprint modalities", (2017).
- [14] <http://www.youreyescenter.com/EyeAnatomy.html> (19-5-2019)
- [15] <https://www.brailleinstitute.org/event/the-aging-eye> (17-5-2019)
- [16] Kaur, N., & Juneja, M. "A novel approach for iris recognition in unconstrained environment". Journal of Emerging Technologies in Web Intelligence, (2014), 6(2), 243-246.

- [17] Source (eye image): Dr. Jan Drewes. [www.jandrewes.de](http://www.jandrewes.de)
- [18] Chen, Yu, et al. "A new unconstrained iris image analysis and segmentation method in biometrics", 2009 IEEE International Symposium on Biomedical Imaging: From Nano to Macro. IEEE, 2009.
- [19] Raghavendra, Ramachandra, et al. "Combining iris and periocular recognition using light field camera", 2013 2nd IAPR Asian Conference on Pattern Recognition. IEEE, 2013.
- [20] Kaur, N., & Juneja, M. "A review on iris recognition". In 2014 Recent Advances in Engineering and Computational Sciences (RAECS), (2014, March). (pp. 1-5). IEEE.
- [21] Sun, Z., & Tan, T. "Ordinal measures for iris recognition". IEEE Transactions on pattern analysis and machine intelligence, (2008), 31(12), 2211-2226.
- [22] Ross, A. Iris recognition: The path forward. Computer, (2010), 43(2), 30-35.
- [23] Ng, T. W., Tay, T. L., & Khor, S. W. (2010, July). Iris recognition using rapid Haar wavelet decomposition. In 2010 2nd International Conference on Signal Processing Systems (Vol. 1, pp. V1-820). IEEE.
- [24] M. AlRifae, "Unconstrained Iris Recognition", Improving Unconstrained Iris Recognition t, De Montfort University, UK, Sept. 2014.
- [25] Colores-Vargas, J., García-Vázquez, M., Nakano-Miyatake, M., & Perez-Meana, H. (2012). Iris recognition system based on video for unconstrained environments. Scientific Research and Essays, 7(35), 3114-3127.
- [26] Parikh, Y., Chaskar, U., & Khakole, H. (2014, February). Effective approach for iris localization in nonideal imaging conditions. In Proceedings of the 2014 IEEE Students' Technology Symposium(pp. 239-246). IEEE.
- [27] Dong, W., Sun, Z., Tan, T., & Wei, Z. (2009, November). Quality-based dynamic threshold for iris matching. In 2009 16th IEEE International Conference on Image Processing (ICIP) (pp. 1949-1952). IEEE.

- [28] <https://courses.cs.washington.edu/courses/cse576/book/ch10.pdf> (11-5-2019)
- [29] <http://www.cs.toronto.edu/~jepson/csc2503/segmentation.pdf> (11-5-2019)
- [30] C. Houston and Rochester Institute of Technology "Iris Segmentation and Recognition Using Circular Hough Transform and Wavelet Features ".
- [31] H. Proenc, a, and L. A. Alexandre, "UBIRIS: A noisy iris image database", In Proceedings of the 13th International Conference on Image Analysis and Processing (ICIAP2005), pages 970–977, Calgary, September 2005.
- [32] Shaikh. I. J , Shaikh .A .H.A.R "Iris Localization Using Segmentation & Hough Transform Method" International Journal of Scientific & Engineering Research, Volume 5, Issue 2, February-2014 79 ISSN 2229-5518.
- [33] S. Singh, S Singh "Iris Segmentation Along with Noise Detection using Hough Transform", International Journal of Engineering and Technical Research (IJETR) ISSN: 2321-0869, Volume-3, Issue-5, May 2015.
- [34] Shaaban A. Sahnoud, Ibrahim S. Abuhaiba "Efficient iris segmentation method in unconstrained environments", PatternRecognition46(2013)3174–3185.
- [35] Li Ma, Tieniu Tan, Fellow, IEEE, Yunhong Wang, Member, IEEE, and Dexin Zhang "Efficient Iris Recognition by Characterizing Key Local Variation,IEEE TRANSACTIONS ON IMAGE PROCESSING, VOL. 13, NO. 6, JUNE 2004.
- [36] Naveen Singh, Dilip Gandhi, Krishna Pal Singh "Iris recognition system using a canny edge detection and a circular Hough transform", International Journal of Advances in Engineering & Technology, May 2011.
- [37] U T Tania, S M A Motakabber, M I Ibrahimy "Edge detection techniques for iris recognition system" 5th International Conference on Mechatronics (ICOM'13) IOP Conf.Series:Materials Science and Engineering 53 (2013) 012041.

- [38] Amit Bendale, Aditya Nigam, Surya Prakash, Phalguni Gupta "Iris Segmentation Using Improved Hough Transform", ICIC 2012, pp 408-415.
- [39] [http://shodhganga.inflibnet.ac.in/bitstream/10603/44989/11/11\\_chapter\\_03.pdf](http://shodhganga.inflibnet.ac.in/bitstream/10603/44989/11/11_chapter_03.pdf) (10-5-2019)
- [40] Research Article, Survey Paper, Case Stud "International Journal of Advance Research in Computer Science and Management Studies" Volume 3, Issue 7, July 2015.
- [41] Sonia Sangwan , Reena Rani "Hough Transform, SURF Technique For Automatic Iris Recognition" International Journal of Innovative Research in Science,Engineering and Technology (An ISO 3297: 2007 Certified Organization) Vol. 4, Issue 9, September 2015.
- [42] VISHRUTH BG , GIRISH RAO SALANKE N.S "A Competent Noise removal method for Iris Recognition".
- [43] Prateek Verma, Maheedhar Dubey, Somak Basu, Praveen Verma "Hough Transform Method for Iris Recognition-A Biometric Approach" (ISSN: 2277-3754 ISO 9001:2008 Certified) International Journal of Engineering and Innovative Technology (IJEIT) Volume 1, Issue 6, June 2012.
- [44] Bouridane, "Recent Advances in Iris Recognition: A Multiscale Approach", Imaging for Forensics and Security, Signals and Communication Technology, DOI 10.1007/978-0-387-09532-5 4, Springer Science+Business Media, LLC 2009.
- [45] Chinni. Jayachandra, H.Venkateswara Reddy" Iris Recognition based on Pupil using Canny edge detection and K-Means Algorithm" International Journal Of Engineering And Computer Science ISSN:2319-7242 Volume 2 Issue 1 Jan 2013 Page No. 221-225.
- [46] Nouredine Cherabit, Fatma Zohra Chelali, Amar Djeradi "Circular Hough Transform for Iris localization" Science and Technology 2012, 2(5): 114-121 DOI: 10.5923/j.scit.20120205.02.



- [47] Amit Madhukar Wagh, Satish R Todmal "Eyelids, Eyelashes Detection Algorithm and Hough Transform Method for Noise Removal in Iris Recognition" International Journal of Computer Applications (0975 – 8887) Volume 112 – No. 3, February 2015.
- [48] J. Daugman, "High confidence visual recognition of persons by a test of statistical independence", IEEE Transactions on Pattern Analysis and Machine Intelligence, 1148–1161, November 1993.
- [49] H. Proenca, L. A. Alexandre, "The NICEI: Noisy Iris Challenge Evaluation—Part I", in: Proceedings of the First International Conference on Biometrics "Theory, Applications, and Systems, 2007, pp. 1–4.
- [50] James, S. S. (2015, March). Iris Recognition Process. In Proceedings of the UGC Sponsored National Conference on Advanced Networking and Applications.
- [51] Global Colloquium in Recent Advancement and Effectual Researches in Engineering, Science and Technology (RAEREST 2016)
- [52] j. Luis and Y. Eduardo (iris recognition system survey) (2014).
- [53] K K1 Fasna, P1 Athira, J S2 Remya Krishna. "A Review on Iris Feature Extraction Methods". International Journal of Engineering Research and General Science Volume 4, Issue, March-April, 2016 ISSN 2091-27302 , (2016).
- [54] Tobji, R., Di, W., Ayoub, N., & Haouassi, S. (2018). Efficient Iris Pattern Recognition Method by using Adaptive Hamming Distance and 1D Log-Gabor Filter. INTERNATIONAL JOURNAL OF ADVANCED COMPUTER SCIENCE AND APPLICATIONS, 9(11), 662-669.
- [55] Gaikwad, A. T., & Ali, M. M. (2017). Iris Feature Extraction and Matching by using Wavelet Decomposition and Hamming Distance. International Journal of Computer Applications, 158(4), 43-47.
- [56] Sahmoud, S. A. I. (2011). Enhancing iris recognition. Enhancing Iris Recognition.

- [57] <http://www.cbsr.ia.ac.cn/IrisDatabase.htm> 5-7-2018.
- [58] Parashar, R., & Joshi, S. (2012). Comparative study of iris databases and UBIRIS database for iris recognition methods for non-cooperative environment. *International Journal of Engineering Research & Technology (IJERT)*, 1(5).
- [59] Iris Images Databases and Image Acquisition Framework chapter 3
- [60] Badejo, J. A., Majekodunmi, T. O., & Atayero, A. A. (2011). Development of CUiris: A dark-skinned African iris dataset for enhancement of image analysis and robust personal recognition.
- [61] Kalka, N., Bartlow, N., Cukic, B., & Ross, A. (2015). A preliminary study on identifying sensors from iris images. In *Proceedings of the IEEE Conference on Computer Vision and Pattern Recognition Workshops* (pp. 50-56).
- [62] [https://shodhganga.inflibnet.ac.in/bitstream/10603/77607/10/10\\_chapter4.pdf](https://shodhganga.inflibnet.ac.in/bitstream/10603/77607/10/10_chapter4.pdf) Chapter – 4 Materials and Method (3-7-2018).
- [63] [http://islab.hh.se/mediawiki/Iris\\_Segmentation\\_Groundtruth](http://islab.hh.se/mediawiki/Iris_Segmentation_Groundtruth) (2-7-2018).
- [64] [https://www.researchgate.net/publication/316093004\\_A\\_Short\\_Survey\\_for\\_Iris\\_Images\\_Databases](https://www.researchgate.net/publication/316093004_A_Short_Survey_for_Iris_Images_Databases) (2-7-2018).
- [65] <http://www.cbsr.ia.ac.cn/IrisDatabase.htm> (2-7-2018).
- [66] Debiassi, L., & Uhl, A. (2015, March). Techniques for a forensic analysis of the casia-iris v4 database. In *3rd International Workshop on Biometrics and Forensics (IWBF 2015)* (pp. 1-6). IEEE.
- [67] Thesis (A Forensic Analysis of the CASIA-Iris V4 Database).
- [68] University of Beira Interior, <http://iris.di.ubi.pt/ubiris1.html>
- [69] UBIRIS Noisy Visible Wavelength Iris Image Databases <http://iris.di.ubi.pt/> cited in May 8, 2019

- [70] <http://theses.gla.ac.uk/6780/> . Thesis (A Generic Computer Platform For Efficient Iris Recognition)
- [71] Proenca, H., Filipe, S., Santos, R., Oliveira, J., & Alexandre, L. A. (2010). The ubiris. v2: A database of visible wavelength iris images captured on-the-move and at-a-distance. IEEE Transactions on Pattern Analysis and Machine Intelligence, 32(8), 1529-1535.
- [72] Alrifaae, M. M., Abdallah, M. M., & Al Okush, B. G. A Short SURVEY OF IRIS IMAGES DATABASES.
- [73] Shah, N., & Shrinath, P. (2014). Iris Recognition System—A Review. International Journal of Computer and Information Technology, 3(02).
- [74] Rhodopsin of Retina: An Effective Approach to Segment Iris from Color Image  
S. Mahdi Hosseini, Babak N. Araabi, Ahmad Poursaberi and H. Member, IEEE
- [75] <http://www.cs.princeton.edu/~andyz/irisrecognition> (1-7-2018)
- [76] Hofbauer, H., Alonso-Fernandez, F., Wild, P., Bigun, J., & Uhl, A. (2014, August). A ground truth for iris segmentation. In 2014 22nd international conference on pattern recognition (pp. 527-532). IEEE.  
[https://www.academia.edu/27920912/A\\_Ground\\_Truth\\_for\\_Iris\\_Segmentation](https://www.academia.edu/27920912/A_Ground_Truth_for_Iris_Segmentation)
- [77] R. N. Rakvic, B. J. Ullis, R. P. Broussard, R. W., & Steiner, N. “Parallelizing iris recognition”. IEEE transactions on information forensics and security, 4(4), 812-823, (2009).
- [78] S. Shah & A. Ross, “Iris segmentation using geodesic active contours”. IEEE Transactions on Information Forensics and Security, 4(4), 824-836, (2009).
- [79] J. Zuo, & N. A. Schmid, “On a methodology for robust segmentation of nonideal iris images”. IEEE Transactions on Systems, Man, and Cybernetics, Part B (Cybernetics), 40(3), 703-718, 2010.

- [80] H. Proença, Iris recognition: “On the segmentation of degraded images acquired in the visible wavelength”. *IEEE Transactions on Pattern Analysis and Machine Intelligence*, 32(8), 1502-1516.64-74,(2010).
- [81] Proença, H. (2010). Quality assessment of degraded iris images acquired in the visible wavelength. *IEEE Transactions on Information Forensics and Security*, 6(1), 82-95.
- [82] R. Chen, X. R. Lin & T. H. Ding, “Iris segmentation for non-cooperative recognition systems”. *IET image processing*, 5(5), 448-456,(2011).
- [83] Du, Y., Arslanturk, E., Zhou, Z., & Belcher, C. (2011). Video-based noncooperative iris image segmentation. *IEEE Transactions on Systems, Man and Cybernetics, Part B: Cybernetics*, 41(1), 64-74.
- [84] Fernández, C., Pérez, D., Segura, C., & Hernando, J. (2012, March). A novel method for low-constrained iris boundary localization. In *2012 5th IAPR International Conference on Biometrics (ICB)* (pp. 291-296). IEEE.
- [85] Tan, C. W., & Kumar, A. (2012). Unified framework for automated iris segmentation using distantly acquired face images. *IEEE Transactions on Image Processing*, 21(9), 4068-4079.
- [86] Mahadeo, N. K., Paplinski, A. P., & Ray, S. (2013, November). Robust video based iris segmentation system in less constrained environments. In *2013 International Conference on Digital Image Computing: Techniques and Applications (DICTA)* (pp. 1-8). IEEE.
- [87] D. A. Roy & U. S. Soni, “IRIS segmentation using Daughman's method”. In *International Conference on Electrical, Electronics, and Optimization Techniques (ICEEOT)* , 2668-2676, (March 2016).
- [88] T. Y. Chai, B. M. Goi, Y. H. Tay, K. S. Teng, & I. Yeo, “ Bi-Local Region Based Iris Segmentation Framework for Less-Constrained Visible Wavelength Images”, (2016).
- [89] Hofbauer, H., Alonso-Fernandez, F., Bigun, J., & Uhl, A. (2016). Experimental analysis regarding the influence of iris segmentation on the recognition rate. *Iet Biometrics*, 5(3), 200-211.

- [90] Jalilian, E., Uhl, A., & Kwitt, R. (2017). Domain adaptation for CNN based iris segmentation. BIOSIG 2017.
- [91] P. Pandey & A. Karthik, "Geometry based method for iris segmentation". In 2017 Fourth IEEE International Conference on Image Information Processing (ICIIP), 1-4, (2017, December).
- [92] Sinha, N., Joshi, A., Gangwar, A., Bhise, A., & Saquib, Z. (2017, April). Iris segmentation using deep neural networks. In 2017 2nd IEEE International Conference for Convergence in Technology (I2CT), 548-555.
- [93] Proença, H., & Neves, J. C. (2018). Deep-PRWIS: Periocular recognition without the iris and sclera using deep learning frameworks. IEEE Transactions on Information Forensics and Security, 13(4), 888-896.
- [94] Bazrafkan, S., & Corcoran, P. (2018, January). Enhancing iris authentication on handheld devices using deep learning derived segmentation techniques. In 2018 IEEE International Conference on Consumer
- [95] Chen, Y., Wang, W., Zeng, Z., & Wang, Y. (2019). An Adaptive CNNs Technology for Robust Iris Segmentation. IEEE Access, 7, 64517-64532.
- [96] J. Daugman, "Biometric Personal Identification System Based on Iris Analysis", U.S. Patent (5): 291 560, 1994.
- [97] M. S. Khalili<sup>1</sup> and H. Sadjedi, "A Robust Iris Recognition Method on Adverse Conditions", International Journal of Computer Science, Engineering and Information Technology (IJCSUIT), Vol.3, No.5, pp. 33-48, Oct. 2013.
- [98] R. Wildes, "Iris Recognition: An Emerging Biometric Technology," Proceeding of the IEEE, Vol. 85, No. 9, pp. 1348-1363, 1997.
- [99] Z. Sun, Y. Wand, T. Tan, and J. Cui, "Cascading Statistical and Structural Classifiers for Iris Recognition", Proceedings of ICIP, pp. 1261-1264, 2004.

- [100] N. Sudha, N. B. Puhan, H. Xia, and X. Jiang, "Iris Recognition on Edge Maps," in Proceedings of the 2007 6th International Conference on Information, Communications and Signal Processing, Singapore, 2007.
- [101] N. Sudha, N. B. Puhan, H. Xia, and X. Jiang, "Iris Recognition on Edge Maps," IET Computer Vision, Vol. 3, No. 1, pp. 1–7, 2009.
- [102] Y. Du, C. Belcher, and Z. Zhou, "Scale Invariant Gabor Descriptor-Based Non-cooperative Iris Recognition", Hindawi Publishing Corporation EURASIP Journal on Advances in Signal Processing, Article ID 936512, pp. 1-13, 2010.
- [103] M. A. Abdullah, F. Al-Dulaimi, W. Al-Nuaimy and A. Al-Ataby, " Smart Card with Iris Recognition for High Security Access Environment", Proceeding of The First Middle East Conference on Biomedical Engineering (MECBME'11), Sharjah-UAE, February 22-25, 2011.
- [104] V. Chirchi, L. M. Waghmare and E. R. Chirchi, "Iris Biometric Recognition for Person Identification in Security Systems", International Journal of Computer Applications (IJCA), Vol. 24, No. 9, pp. 1-6, June 2011.
- [105] B. Jain, M. K. Gupta and J. Y. Bharti, "Efficient Iris Recognition Algorithm Using Method of Moments", International Journal of Artificial Intelligence & Applications (IJAIA), Vol. 3, No. 5, pp. 93-105, Sept. 2012.
- [106] J. M. Abdul-Jabbar and Z. N. Abdulkader, "Iris Recognition Using 2-D Elliptical-Support Wavelet Filter Bank ", Proceedings of the 3rd International Conference on Image Processing Theory, Tools & Applications (IPTA 2012, 15-18 October, 2012, Istanbul Aydin University, Istanbul, Turkey, (IEEE Xplore Digital Library), pp. 359-363, 2012.
- [107] N. Thanh, "Human identification at a distance using iris and face", Ph.D. Thesis, submitted to Queensland University of Technology, Image and Video Research Laboratory, Science and Engineering Faculty, May 2013.

- [108] M. Mahlouji and A. Noruzi, "Human Iris Segmentation for Iris Recognition in Unconstrained Environments", *International Journal of Computer Science Issues (IJCSI)*, Vol. 9, Issue 1, No 3, pp. 149-155, Jan. 2012.
- [109] P. M. Patil, " Iris Recognition in Less Constrained Environment", *International Journal of Emerging Technology and Advanced Engineering*, Vol. 3, Issue 7, pp.196-200, July 2013.
- [110] R. Gupta and A. Kumar, " An Effective Segmentation Technique for Noisy Iris Images", *International Journal of Application or Innovation in Engineering & Management (IJAIEM)*, Vol. 2, Issue 12, pp. 118-125, Dec. 2013.
- [111] Y. Chen, Y. Liu, X. Zhu, F. He, H. Wang and N. Deng, "Efficient Iris Recognition Based on Optimal Sub-feature Selection and Weighted Sub-region Fusion", *Scientific World Journal*, Hindawi Publishing Corporation, Feb. 2014.
- [112] Y. Fei, Z. Changjiu and T. Yantao, " Improving Unconstrained Iris Recognition Performance via Domain Adaptation Metric Learning Method", *International Journal of Security and Its Applications*, Vol. 10, No. 5, pp.27-40, 2016.
- [113] M. A. Abdullah, S. S. Dlay, W. L. Woo, and J. A. Chambers," Robust Iris Segmentation Method Based on a New Active Contour Force with A Noncircular Normalization", *IEEE Transactions on Systems, Man, and Cybernetics: Systems*, Vol. 99, pp. 1-14, 2016.
- [114] X. Giné, J. Goldberg, Michigan, S. Sankaranarayanan, I. P. Sheerin, & I. D. Yang, "Use of biometric technology in developing countries", (2012).
- [115] N. Guliani., M. K Shukla, A. K Dubey, & , Z. A "Jaffery. Analysis of multimodal biometric recognition using Iris and sclera". In *Reliability, Infocom Technologies and Optimization (Trends and Future Directions)(ICRITO)*, 2017 6th International Conference on (pp. 472-475). IEEE. (2017, September).
- [116] J. Horst, Iris Recognition: "A General Overview. *Journal of Student research*", 19-23, (2006).
- [117] L. Masek, "Recognition of human iris patterns for biometric identification", (2003).

- [118] B. Thiyaneswaran & S. Padma, "SIris Recognition using Left and Right Iris Feature of the Human Eye for Biometric Security System". *International Journal of Computer Applications*, 50(12), (2012).
- [119] N. Kak, R. Gupta, & S. Mahajan, "Iris Recognition System". *International Journal of Advanced Computer Science and Applications*, 1, 34-40, (2010).
- [120] Y. Lee, P. J. Phillips & R. J. Micheals. "An automated video-based system for iris recognition". In *International Conference on Biometrics*, Springer, Berlin, Heidelberg, (2009, June). (pp. 1160-1169).
- [121] S. S. Harakannanavar & V. I. Puranikmath, "Comparative survey of iris recognition". In *Electrical, Electronics, Communication, Computer, and Optimization Techniques (ICEECCOT)*, IEEE, 2017 International Conference on, (pp. 280-283(2017, December).
- [122] M. F. F. Khan, A. Akif & M. A., "Haque, Iris recognition using machine learning from smartphone captured images in visible light". In *Telecommunications and Photonics (ICTP)*, IEEE, 2017 IEEE International Conference on (pp. 33-37), (2017, December).
- [123] R. J. Wildes, G. G. Asmuthand, H. Hsu, "A system for automated iris recognition", *Second IEEE workshop on applications of computer vision*, (2004).
- [124] B. O. Adegoke. E. O. Omidiora, S. A., Falohun & J. A. Ojo, "Iris Segmentation: a survey". *International Journal of Modern Engineering Research (IJMER)*, 3(4), 1885-1889, (2013).
- [125] B. O. Adegoke, E. O. Omidiora, J. A. Ojo, & S. A. s Falohun, "Iris feature extraction: a survey. *Computer Engineering and Intelligent Systems*", 4(9), 7-13, (2013).
- [126] C. Abikoye Oluwakemi, J. S. Sadiku, , S. Adewole Kayode, , & G. Jimoh Rasheed, "Iris feature extraction for personal identification using fast wavelet transform (FWT)", *structure*, 6(9), 2014.



- [127] A. Kumar, A., Potnis & A. Singh, "Iris recognition and feature extraction in iris recognition system by employing 2D DCT". IRJET International Research in Computer Science and Software Engineering, and Technology, 3(12), 503-510, (2016).
- [128] Hugo Proenca, "Towards non-cooperative biometric iris recognition" (PhD thesis), University of Beira Interior, October 2006.
- [129] J. M. Abdul-Jabbar and H. N. Fathee, "Design and Realization of Circular Contourlet Transform", Al-Rafidain Engineering Journal, Vol. 18, No. 4, pp. 28 - 42, Aug. 2010.
- [130] M. N. Do and M. Vetterli, "Contourlets: A Directional Multiresolution Image Representation", Proceedings of the IEEE International Conference on Image Processing, Rochester, Vol. No.1, pp. 357–360, Sept. 2002.
- [131] M. N. Do and M. Vetterli, "The Contourlet Transform: An Efficient Directional Multiresolution Image Representation", IEEE Transactions on Image Processing, Vol. 14, No. 12, pp. 2091–2016, 2005.
- [132] S. Satheesh and K. R. Prasad, "Medical Image Denoising Using Adaptive Threshold Based on Contourlet Transform", Advanced Computing: An International Journal (ACIJ), Vol. 2, No. 2, pp. 52-58, March 2011.
- [133] G. Liu, J. Liu, Q. Wang, W. He, "The Translation Invariant Wavelet-based Contourlet Transform for Image Denoising", Journal of Multimedia, Vol. 7, No. 3, pp. 254-261, June 2012.
- [134] K. Sakthivel, "Contourlet Based Image Denoising Using New Threshold Function", Proceedings of International Conference on Global Innovations In Computing Technology (ICGICT'14), Tamilnadu, India, 6-7, March 2014.
- [135] J. M. Abdul-Jabbar, A. I. Kanaan and Z. N. Abdulkader, "Contourlet-Based Method for Speckle Reduction with Adaptive Estimation of Noise Level", Al-Rafidain Engineering Journal, Vol. 22, No. 5, Dec. 2014.

- [136] A. Azizi and H. R. Pourreza, "Efficient IRIS Recognition through Improvement of Feature Extraction and subset Selection", *International Journal of Computer Science and Information Security (IJCSIS)*, Vol. 2, No.1, June 2009.
- [137] S. Khalighi, P. Tirdad, F. Pak and U. Nunes, "Shift and Rotation Invariant Iris Feature Extraction Based on Non-Subsampled Contourlet Transform and GLCM", *Proceedings of the 1st International Conference on Pattern Recognition Applications and Methods (ICPRAM 2012)*, Jan. 2012.
- [138] M. Dobes, J. Martineka, D.S.Z. Dobes, J. Pospisil, Human eye localization using the modified Hough transform, *Optik—International Journal for Light and Electron Optics* 117 (2006) 468–473.
- [139] Fathee, H. N., Ucan, O. N., Abdul-Jabbar, J. M., & Bayat, O. (2019). Efficient Unconstrained Iris Recognition System Based on CCT-Like Mask Filter Bank. *Mathematical Problems in Engineering*, 2019.
- [140] Almajmaie, LaythKamil, Osman N. Ucan, and Oguz Bayat. "Fingerprint Recognition System Based on Modified Multi-Connect Architecture (MMCA)." *Cognitive Systems Research* (2019).
- [141] Alazzawi, Abdulbasit, Osman N. Ucan, and Oguz Bayat. "Robust face recognition algorithm based on linear operators discrete wavelet transformation and simple linear regression." *Proceedings of the First International Conference on Data Science, E-learning and Information Systems*. ACM, 2018.
- [142] AlAZZAWI, Abdulbasit, Osman Nuri Uçan, and Oğus Bayat. "Face recognition based on multi features extractors." *2017 International Conference on Engineering and Technology (ICET)*. IEEE, 2017.
- [143] Sardouk, Farah, Adil Deniz Duru, and Oğuz Bayat. "Classification of Breast Cancer Using Data Mining." *American Scientific Research Journal for Engineering, Technology, and Sciences (ASRJETS)* 51.1 (2019): 38-46.